2011

Surface-initiated Polymerization as a Novel Strategy towards Preparation of Organic Semiconducting Polymer Thin Films

Euiyong Hwang
Louisiana State University and Agricultural and Mechanical College

SURFACE-INITIATED POLYMERIZATION AS A NOVEL STRATEGY TOWARDS PREPARATION OF ORGANIC SEMICONDUCTING POLYMER THIN FILMS

A Dissertation
Submitted to the Graduate Faculty of the
Louisiana State University and
Agricultural and Mechanical College
in partial fulfillment of the
requirements for the degree of
Doctor of Philosophy

in

The Department of Chemistry

by
Euiyong Hwang
B.S., Chung-Ang University, Korea, 2002
M.S., Chung-Ang University, Korea, 2004
May 2011

To

Hyunmi Kim and Brian K Hwang,

ACKNOWLEDGEMENTS

Before starting this dissertation, I would like to convey gratitude to my advisor, Professor Evegueni E. Nesterov, with all my respect. During my research at Louisiana State University, he has guided and advised me to achieve valuable experiences and knowledge about organic semiconducting materials. Furthermore, when my family was in adversity, his generous support encouraged us to overcome difficulties. He is more than an advisor to me and I appreciate God to allow me to meet such great mentor in my life. Although I will leave Louisiana State University, I will be always a student of Professor Evgueni E. Nesterov.

I also thank my committee members, Dr. Robin L. McCarley, Dr. Carol M. Taylor, Dr. Graca Vicente, and Dr. J. Gregory Stacy.

To Nesterov group members: Dr. Jiba Raj Acharya, Jinwoo Choi, Rajib Mondal, Deepa Pangeni, Brian Imsick, Sang Gil Youm, Carlos Chavez, Sourav Chatterjee, and undergraduate students: Chad A. Seevers and Corey Bretz not only for their support and encouragement to my research but also for personal help.

I acknowledge my collaborators, Dr. Jie-Ren Li, Kathie L. Lusker, and Professor Jayne C. Garno for their great contributions into this project related to surface morphology measurements with AFM and state-of-the-art nanoparticle lithography. I also appreciate Professor Bernad Kippelen and his group members at Georgia Institute of Technology for their generous support in teaching me to learn the basic knowledge about organic photovoltaic devices, and training in their fabrication.

Specially, I appreciate my previous advisor, Professor Jong Chan Lee at Chung-Ang University. Without his continuous encouragement, I could not decide to study abroad and would lose an honorable chance to be an alumni of Louisiana State University.

To my friends, Dr. Jungyoung Cho, Dr. Gyun-Tack Bae, Dr. Wonbae Lee, Dr. Jeonghoon Lee, Chang-uk Lee, Jinwoo Choi, Sang Gil Youm, and Sung-Gun Park, I really thank them for great support, encouragement, and advices to adjust to Baton Rouge and to overcome tough times.

With all of my love, I would like to show my appreciation to my wife, Hyumi Kim. Even though she was a graduate student in Department of Chemistry at Louisiana State University, she sacrificed her research for my success. I also thank my son, Brian K Hwang. His smiling face always reminds me how happy I am. Finally, I show my appreciation to my parents and to my brother and his family for their constant encouragement and support.

TABLE OF CONTENTS

LIST OF TABLES

LIST OF FIGURES

LIST OF SCHEMES

ABBREVIATIONS

AFM	- Atomic force microscopy
BHJ	- Bulk-heterojunction
COD	- Cyclooctadiene
CP	- Conducting (or conjugated) polymer
CuAAC	- Cu-catalyzed acetylene-azide click reaction
CVD	- Chemical vapor deposition
CV	- Cyclic voltammetry
DMF	- Dimethylformamide
DMSO	- Dimethyl sulfoxide
dppp	- 1,3-bis(diphenylphosphino)propane
HOMO	- Highest occupied molecular orbital
ICPE	- Incident photon-to-current conversion efficiency
ITO	- Indium tin oxide
LUMO	- Lowest unoccupied molecular orbital
M_n	- Number average molecular weight
OFET	- Organic field effect transistor
OLED	- Organic light emitting diode
OPV	- Organic photovoltaics
OTS	- Octadecyltrichlorosilane
P3HT	- Poly(3-hexylthiophene)
PDMS	- Polydimethylsiloxane
PDI	- Polydispersity index
PEDOT	- Poly(3,4-ethylenedioxythiophene)
PGMA	- Poly(glycidyl methacrylate)
PPP	- Poly(p-phenylene)
PS-Br	- Poly(4-bromostyrene)
PT	- Polythiophene
PVD	- Physical vapor deposition
TBAF	- Tetra-n-butylammonium fluoride
$TBAPF_6$	- Tetrabutylammonium hexafluorophosphate
$TBABF_4$	- Tetrabutylammonium tetrafluoroborate
THF	- Tetrahydrofuran
UV/Vis	- Ultraviolet-visible spectroscopy
XPS	- X-ray photoelectron spectroscopy

ABSTRACT

Organic semiconducting polymer thin films are core materials for organic electronics that are conventionally prepared by solution processing techniques. Despite having the advantage of easy and fast thin film manufacturing, solution techniques have intrinsic drawbacks, such as disordered and poor molecular organization in the film (often resulting in poor device performance), as well as insufficient stabilities of the films and resulting devices. To improve this situation, we designed a novel "bottom-up" fabrication of surface-immobilized organic semiconducting thin films through *in situ* polymerization. This new strategy will allow high degree of control over molecular organization which therefore results in improved free charge carrier transport efficiency. An additional benefit of this strategy will be the enhanced stability of thin films due to covalent attachment of the resulting conducting polymers to the surface.

Initially, we developed an approach towards deposition of surface-bound semiconducting polymer thin films via *in situ* electropolymerization. When the resulting thin films were used as hole transporting materials in photovoltaic devices, they demonstrated enhanced photocurrent generation quantum efficiencies and remarkable stabilities as compared to conventional spin-casted thin films.

Based on the promising results from this initial attempts, a chemical surface-initiated *in situ* polymerization based on Ni catalyst transfer living Kumada polycondensation was developed using highly efficient Ni(II) external catalytic initiator. Thin polythiophene films with improved surface morphologies were successfully grafted on substrates after systematic optimization of the experimental conditions. As an important extension of this strategy, we also prepared nanopatterned surface-immobilized polythiophene thin films as a hole transporting counterpart of the ideal heterostructures for bulk-heterojunction type organic photovoltaic devices.

In a parallel study, surface-immobilized semiconducting polymer thin films were prepared by stepwise surface-initiated *in situ* polymerization using highly efficient Cu-catalyzed alkyne-azide cycloaddition (click) reaction. In this project, we found that stepwise preparation of semiconducting polymer thin films not only promises complete control over surface morphology, thickness, and molecular composition of the resulting polymer films but also allows building complex copolymer thin films with desired photophysical properties. Taken together, those three methods represent a powerful "bottom-up" alternative to the traditional methods of preparation of semiconducting polymer thin films.

CHAPTER 1 ORGANIC ELECTRONIC MATERIALS: THIN FILMS OF CONJUGATED POLYMERS.

1.1 Organic Semiconductors: Conjugated Polymers.

Nowadays, polymers are among the most widely used materials and it is hard to imagine a life without plastics. However, before Shirakawa, Heeger, and MacDiarmid reported a first conducting polymer (**CP**), doped polyacetylene, polymers have been the general choice as insulating materials in our stereotype.[1] Indeed, even polyacetylene in its neutral, undoped form does not have high conductivity, 10^{-3} ~ 10^{-2} S/m for trans-polyacetylene and 10^{-8} ~ 10^{-7} S/m for cis-polyacetylene, almost same as conductivity of glass.[2] However, once it is oxidized with chlorine, bromine, or iodine vapor, conductivity of polyacetylene increases dramatically due to charge carrier generation. The doping of cis-polyacetylene with AsF_5 even gave conductivity as high as 10^{11} S/m.[2, 3] The extraordinary behavior of polyacetylene originates from two factors. The first one is an array of conjugated double bonds spanning along the backbone allowing for charge delocalization or transfer. Generation of charge carriers, electrons or holes (positively charged carriers), would be the second important factor for increasing conductivity. (Electron transfer from neighboring polymers or polymer backbone provides a mechanism for long range charge transfer.) Comparing with conductivity of metals which is usually more than 10^8 S/m, polyacetylene would be a great candidate as an "organic metal". Despite well-established synthetic pathways to prepare it, and its high conductivity, polyacetylene cannot be used in commercial electronics due to its air and moisture sensitive nature.[4-6] To overcome this problem, second generation CPs, for example poly(thiophene) (**PT**) and poly(3,4-ethylenedioxythiophene) (**PEDOT**), which do not show as high conductivities as polyacetylene but still enough for using these as semiconducting materials, have been later developed and their applications in organic electronic devices such as organic field effect transistors (**OFETs**),[7, 8] organic photovoltaics (**OPVs**),[9, 10] as well as organic light emitting diodes

(**OLEDs**)[11] became one of the most vibrant research field in the area of organic materials, both in academia and industry.

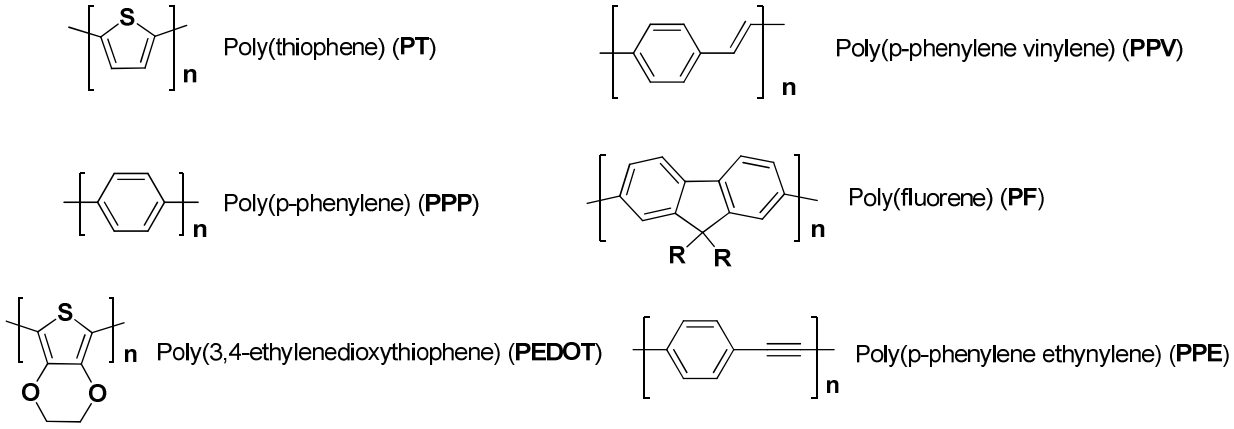

Figure 1.1. Examples of most common semiconducting polymers for organic electronics.

1.2 Fabrication Techniques and Intrinsic Drawbacks of Conventionally Prepared Thin Film Devices.

Lower cost of raw materials, easy fabrication process, as well as possibility to manufacture flexible devices with thin-film semiconducting layer spur the development of organic electronics. Gas phase deposition and solution techniques are usually employed to prepare a thin film CP active layer on top of a solid substrate. Small-molecule compounds or polymers with low vapor pressure yield highly ordered thin layers with high charge carrier mobility or dramatically improved exciton (a coupled pair of hole and electron[12]) diffusion length through physical vapor deposition (**PVD**) or chemical vapor deposition (**CVD**) methods.[13, 14] Although such techniques need lower processing temperature than those traditionally used for deposition of inorganic materials (e.g. 180 ˚C for polyethylene terephthalate vs. 350 ˚C for amorphous silicon), relatively slow deposition rate and higher cost for manufacturing make alternative solution-based techniques more favorable. Using polymer solutions in common organic solvents, CP thin films can be deposited via spin-casting, inkjet printing, or screen printing. Despite advantage of easy and fast manufacturing of the organic electronic devices, solution technique has intrinsic

drawbacks, such as low electroluminescent efficiency or charge mobility, as well as thin films poor physical and chemical stabilities.

Bulky solubilizing groups such as hexyl side chains attached to the conjugated backbone intrinsically increase low solubility of CPs in common organic solvents and make them more suitable for processing. However, use of solubilizing groups interferes with the formation of molecularly ordered structures and results in amorphous thin films with charge carrier mobilities far less than optimal value. Conductivity and charge mobility can be expressed by the following equations:[15]

$$\sigma = n\mu e \qquad \text{(eqn. 1)}$$

$$\mu_{tot} = \mu_{intra} + \mu_{inter} \quad \text{(eqn. 2)}$$

Conductivity σ depends on number of charge carriers *n* and how fast they can move through the material (mobility μ), with *e* being the electron charge. The total mobility μ_{tot} can be expressed as sum of intramolecular mobility μ_{intra} and intermolecular mobility μ_{inter}. In an amorphous CP thin film where charge carriers are mainly transferred through hopping to neighboring CPs, total mobility mainly depends on slow intermolecular mobility (the portion of faster μ_{intra} in total mobility is small).[15] For example, theoretical intramolecular mobility of poly(3-hexylthiophene) (**P3HT**) is $\mu_{intra} = 3.34$ cm^2 V^{-1}s^{-1} and $\mu_{inter} = 7.13 \times 10^{-3}$ cm^2 V^{-1}s^{-1}.[16] Thus, solution processed CP thin film devices exhibit relatively low conductivity due to low charge carrier mobility. In organic photovoltaic (**OPV**) devices, low efficiency due to amorphous thin films and disordered molecular structure is also affected by a number of additional factors. To better understand the problems related to OPV thin-film materials, photon to power conversion mechanism and architecture of OPV devices is outlined below. The mechanism of current generation in OPV devices involves the following steps:[17]

1. Absorption of incident light ranged from 700 to 1000 nm (1.3 ~ 2.0 eV), which corresponds to average sunlight on the surface of the earth at the latitude of 48° (air mass 1.5 (AM1.5)).
2. Exciton generation.
3. Exciton migration to interface between donor and acceptor.
4. Exciton dissociation at the interface to electron and hole driven by the electric field resulting from different electron affinity of donor and acceptor.
5. Diffusion of the free charge carriers toward electrodes.
6. Charge collection at electrodes.

Since lifetime of exciton is short (due to radiative and nonradiative decay), typical exciton migration length in amorphous polymer thin film is around 5 - 10 nm.[17] Furthermore, exciton migration is affected by morphologies of active layer and presence of impurities which result in exciton trapping. Therefore, preparation of highly ordered and defect-free OPV thin-films is essential for efficient exciton migration.[18] Indeed, only a small portion of excitons can reach the interface of donor and acceptor in solution processed thin-film OPVs. Recently, it was found that exciton diffusion length of crystalline structure can be extended up to few micrometers and this discovery may explain why amorphous OPVs have shown lower efficiencies than their maximum theoretical values.[12] To overcome these difficulties, bulk-heterojunction (**BHJ**) type solar cells, which are prepared by spin-coating of blend solution of mutually immiscible donor and acceptor materials, have been introduced in 1995 by Heeger et al.[19] The ideal structure of BHJ OPV promises optimal area of donor-acceptor interface within exciton diffusion length. Furthermore, through variation of experimental conditions such as solvents, annealing time, as well as blending ratio of donor and acceptor, phase separations and molecular organization of resulting thin film can be controlled.[20, 21] However, it has failed to address the issue of precise

control of architecture, with most devices having deviant structures as a result. (Figure 1.2) The deviant structure is responsible for less efficient exciton migration and high probability of hole-electron recombination during free charge carriers diffusion to electrodes. Therefore, even with greatly enhanced number of photogenerated charge carriers, only a small portion of them can be converted to photo-induced power.

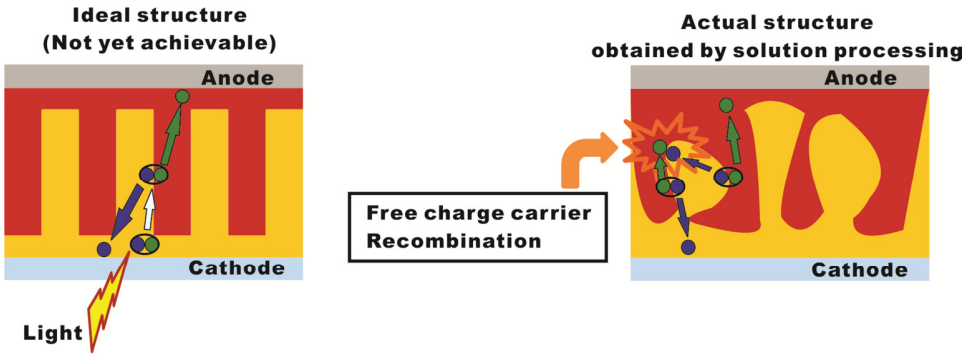

Figure 1.2. Structure of BHJ solar cell and photon to power generation mechanism.

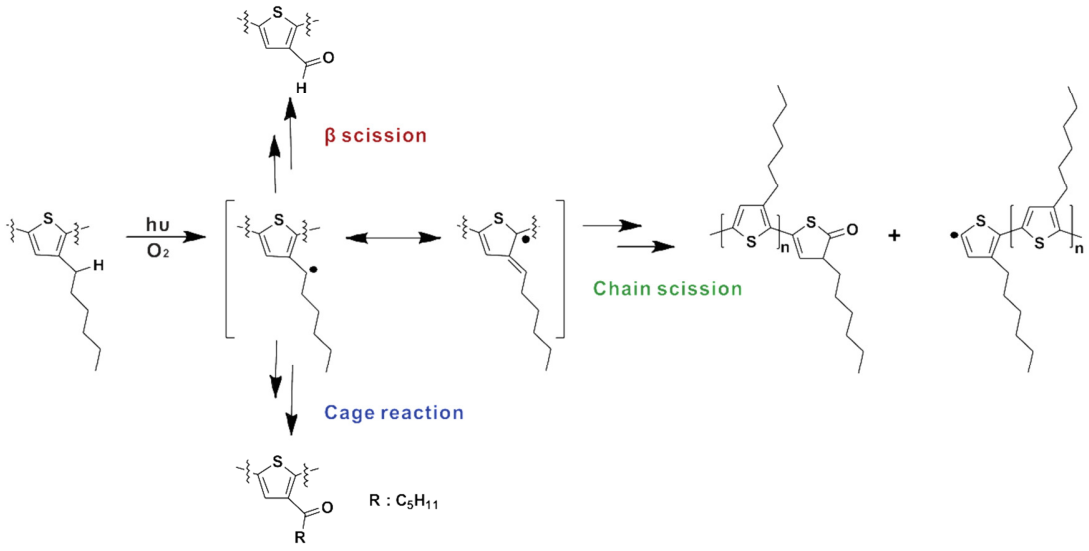

Figure 1.3. Proposed photodegradation mechanism of P3HT (from ref 22, 23).

Another major bottleneck of solution processed organic electronics is the poor physical and chemical stabilities of active polymer layer which greatly reduces device operating time. So far, exact mechanism of thermal or photodegradation of CPs in thin film has not been accurately

elucidated, however, it is likely that abstraction of an α-hydrogen on long alkyl chain can act as the starting point of such degradation[22, 23] (Figure 1.3).

The conjugated backbone fragmentation results in destruction of active layer which can be monitored through hypsochromic spectral shift as well as gradual reduction of optical density of devices. Consequently, P3HT which is the most widely employed OPV material shows failing against light, moisture, as well as oxygen. For example, it was reported that a 80 nm thick spin-casted P3HT film decreased optical density from 0.8 to 0.1 within 13 hour under 130 mW/cm^2 of white light at 8 bar pressure of oxygen, with absorption λ_{max} of P3HT shift from 554 nm to less than 500nm.[24] Furthermore, gradual decreasing of the intensity of 600 nm peak indicated that photodegradation induced further disordered structure.[24] In addition to chemical instability, poor physical stability, not to mention mechanical stability, is another commonly recognized problem. As an example, BHJ OPV exhibited contrasting results in their efficiency depending on annealing time and temperature. P3HT/ Phenyl-C61-butyric acid methyl ester (**PCBM**) BHJ device showed a gradual decrease of power conversion efficiency after 1 hour annealing at 140 ˚C due to phase separation and formation of PCBM and P3HT micrometer sized grains in thin film, therefore making exciton migration to donor-accept interface even less efficient. Furthermore, at higher temperature, rate of aggregation was further accelerated.[25]

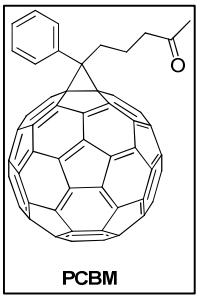

PCBM

To improve this situation, enormous efforts have been paid during the last decade. Some more promising efforts included encapsulation of devices, modification of CPs or PCBM, etc.[26, 27] Although such modifications showed some improvements, they could not be seen as a universal solution. Consequently, development of a novel paradigm based on "bottom-up" approach (in contrast to traditional "top-down" paradigm) can be viewed as a radical way to improve the situation.

1.3 Novel Bottom-up Approach; Grafting of Conjugated Polymer Brushes.

Similar with hairs on body, polymer brushes are surface-tethered polymers prepared by surface-initiated *in situ* polymerization or reaction between anchoring-group attached polymers and functionalized surface. (The details of preparation methods will be considered in the following sections.) The advantages of surface-immobilized polymer brushes are not only in improved physical stability but also in their unique property, namely stretching of tethered polymers.[28] When polymer brush density is high, grafted polymers stretch out away from the surface to minimize interactions with crowded neighboring polymer chains; therefore, thick polymer monolayer can be obtained with high surface coverage. This aggregation phenomenon of surface-immobilized polymers allowed prevalence of these materials in many areas including formations of organic semiconducting thin films.

When CPs are grown via *in situ* polymerization, some improvements can be expected in several aspects. Firstly, highly dense semiconducting thin film can be formed. For conventional solution processing, CPs should be functionalized with bulk solubilizing groups, however, for *in situ* prepared thin film, unsubstitued CPs are polymerized from the surface directly and highly dense surface coverage can be obtained. Moreover, stretching behavior of resulting polymer brushes will allow formation of CP chains without kinks and other conformation defects which reduce conjugation length. Another major benefit would be preparation of defect-free thin films. As we discussed above, to achieve highly efficient organic electronic devices, manufacturing of defect-free thin films is essential. For this purpose, solution processed thin films have to be fabricated inside of special dust-free chambers. Moreover, the chance of formation of pin-hole area in spin-cast thin films, which induce shortcuts and make resulting devices useless, becomes higher upon increasing scale of devices.[29, 30] Since polymer tethering is carried out inside a sealed reaction vessel similar to common organic reactions, this promises high density, defect

and pin-hole free thin films. So far, many previous efforts have produced some promising results (such as polymer brush gate dielectrics in OFET) for defect-free thin films.[31, 32] Due to covalent attachments between polymers and surface, grafting of polymer brushes induces good mechanical strength. Furthermore, lack of solubilizing groups would reduce a chance of photodegradation originating from α-hydrogen. That is, more durable organic semiconducting thin films can be prepared.

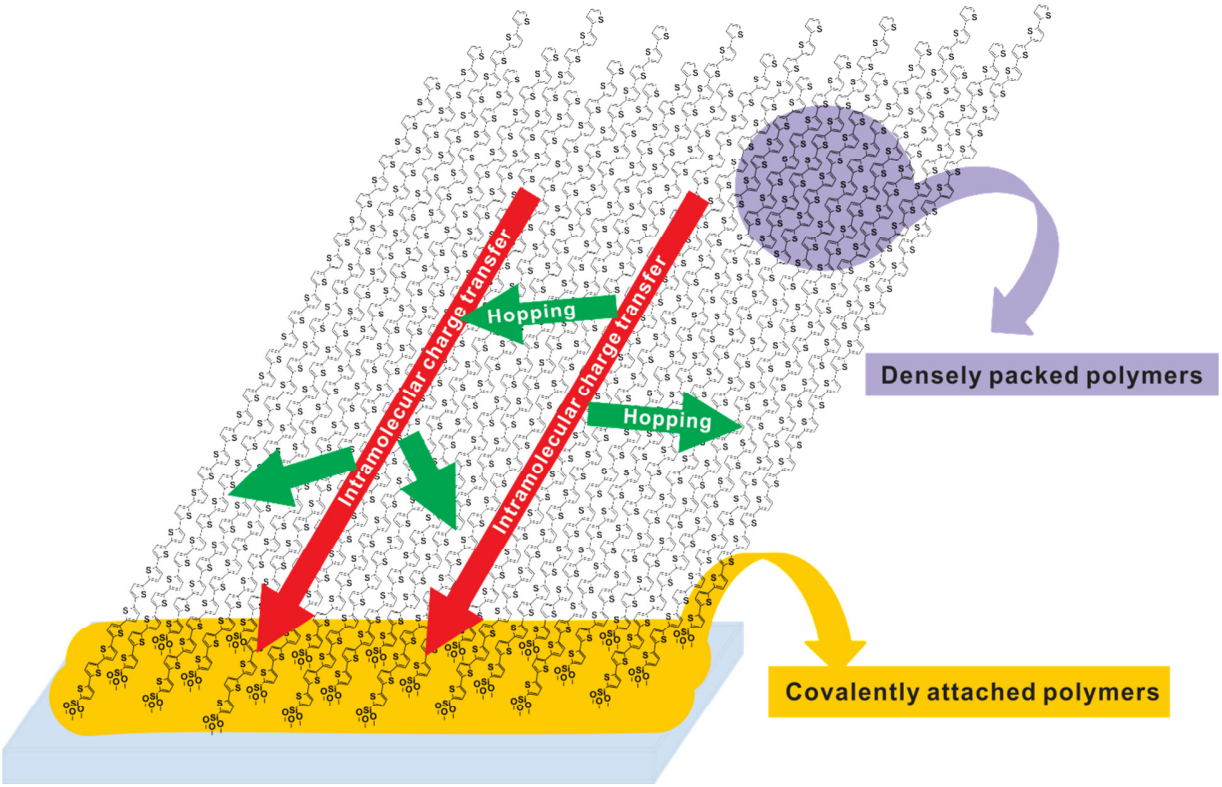

Figure 1.4. Surface-immobilized polythiophene brushes on a substrate.

The most valuable achievement with surface-immobilized CP brushes would be improvement in charge mobility. All surface-anchored polymers are directly bound to electrode and polymer chains are close to each other, thus, more efficient three dimensional charge carrier transport can be expected through charge hopping to close neighboring CP brushes as well as more efficient intramolecular charge transfer (Figure 1.4). Currently, the majority of *in situ*

polymerized thin films described in literature have been manufactured by electrochemical polymerizations and some examples were prepared by novel metal-catalyzed surface-initiated living polymerizations. In the following sections, details of these two methods are briefly reviewed.

1.4 Electrochemical Polymerization.

Electrochemical polymerization is a powerful and fast surface-initiated polymerization method to give surface-immobilized CP brushes. Conventionally, conducting working electrodes such as platinum, gold or indium tin oxide (**ITO**) coated glass are used as solid substrates. Although the detailed mechanism of electropolymerization is not completely understood, Figure 1.5 shows an accepted mechanism of anodic electropolymerization of heteroarenes via oligomers.[33]

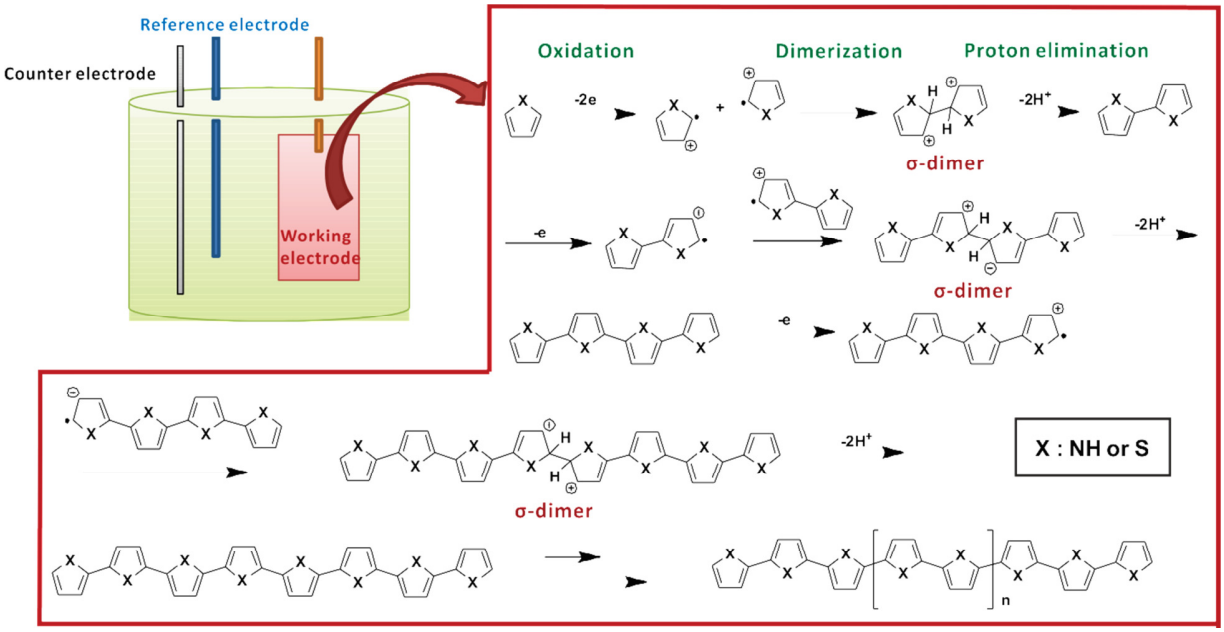

Figure 1.5. Mechanism of electropolymerization via σ-bonded intermediates.

In this mechanism, monomers dimerize at α-position to give doubly charged σ-dimers after oxidation of monomers which produces radical cations. Dimers formed by proton elimination are

oxidized again followed by generation of tetramers through dimerization with subsequent proton elimination. Through repetition of the above reactions, CPs can be grafted on top of a working electrode. Typically properties of resulted thin films are strongly affected by experimental conditions.

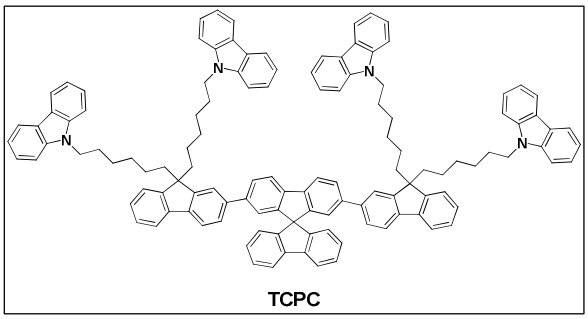

TCPC

As described in many publications,[34-36] "water effect" (i.e. water content in organic solvent) strongly affects the quality of resulting films. When anhydrous acetonitrile was used as a solvent for electropolymerization of pyrrole, short-chain oligomers were mainly generated due to inefficient proton elimination induced by weak acidity of σ-bonded intermediates. However, addition of 1 wt % of water, which acts as a base and aids in proton elimination, results in polypyrrole thin film with improved morphologies as well as longer chain length. Ma et al. noted that electrolyte and cyclic voltammetry (**CV**) scan rate are also key factors determining properties of the thin films produced by electrochemical polymerization.[37] In their report, electrochemically polymerized TCPC polymer was electrodeposited on ITO surface under scan rates of 50, 100, 200, 300, 400 mV/s. Upon increasing scan rates, size and number of grains were reduced. At the rate of 400 mV/s with 80 scan cycles, the resulted thin film showed smooth morphology (RMS 2.8 nm). The choice of electrolyte also affects morphologies of resulting films. TCPC polymer thin film prepared with tetrabutylammonium hexafluorophosphate (**$TBAPF_6$**) exhibited lower extent of aggregation relative to thin film prepared using tetrabutylammonium tetrafluoroborate (**$TBABF_4$**) electrolyte. Consequently, electroluminescence quantum efficiency in OLED devices of electrochemically deposited film with $TBAPF_6$ was 45.5 %, substantially higher than 25.5 % from samples electropolymerized with $TBABF_4$.

Upon variation of experimental conditions, electropolymerization can produce molecularly organized surface-immobilized thin films, with polymer chains oriented linear or parallel to the electrode. In the past, such polymer brushes have been prepared starting from self-assembled monolayers of surface-immobilized conjugated oligomers. As an example of horizontally oriented CP thin film, Roncali et al. prepared an EDOT-thiophene copolymer thin film by electropolymerization of surface-immobilized bithiophenic precursors on gold surface.[38] Unlike most reports which mainly produced dimers or oligomers, the resulting polymer thin film demonstrated reduced HOMO-LUMO energy gap due to formation of a more extended conjugated polymer system. Since Zotti et al. reported the first surface-initiated electropolymerization to give polypyrrole brushes oriented normally to the surface, starting from terthiophene or bisEDOT surface-anchored monolayer,[39] many further research developments have been described. For example, Armstrong et al. manufactured a nanocomposite thin film of PEDOT (a hole transporting material) and 3,4-propylenedioxythiophene (Pro-DOT) capped CdSe nanocrystals to offer percolation pathway for electron transfer in hybrid solar cells.[40] Surface-initiated electropolymerization from 10-((3-methyl-3,4-dihydro-2H-thieno[3,4-b][1,4]dioxepin-3-yl)-methoxy)-10-oxo-decanoic acid (ProDOT-CA) immobilized on ITO electrode resulted in tethered PEDOT brushes. After cross-linking between PEDOT thin film and ProDOT-CA modified CdSe nanocrystal via electropolymerization, surface-immobilized nanocomposite thin film was obtained (Figure 1.6).

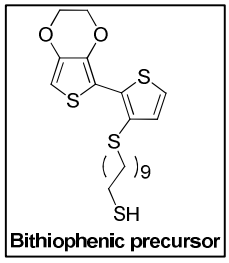

Bithiophenic precursor

More recently, polypyrrole tethered TiO_2 nanotubes were prepared by Zhou to use in chemically bonded p-n heterojunctions.[41] The material was obtained via immobilization of biomimetic anchor of *N*-(3,4-dihydroxyphenethyl)-pyrrole-2-carboxamide on electrochemically anodized TiO_2 foil followed by surface-initiated electropolymerization of pyrrole monomer

(Figure 1.7). Comparing with electrochemically deposited polypyrrole on bare TiO_2, the resulting polypyrrole brushes from surface-initiated polymerization demonstrated reduced film resistance as well as enhanced charge transfer efficiency.

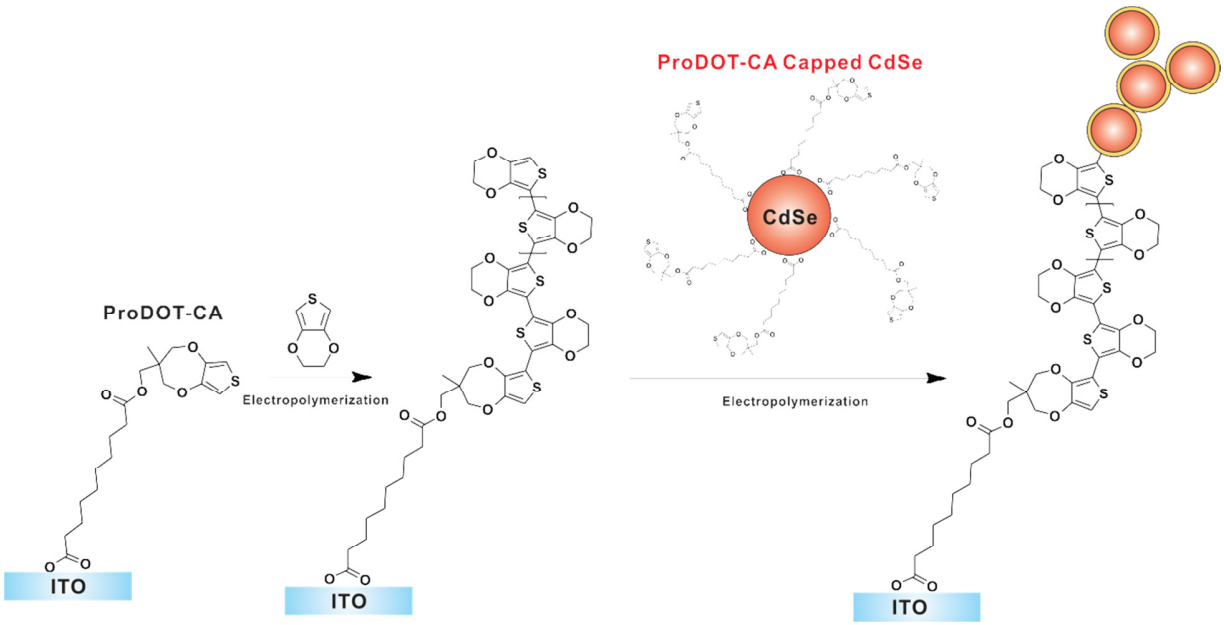

Figure 1.6. Preparation scheme of PEDOT-semiconductor nanoparticle composite thin film tethered to ITO via electropolymerization (from ref. 40).

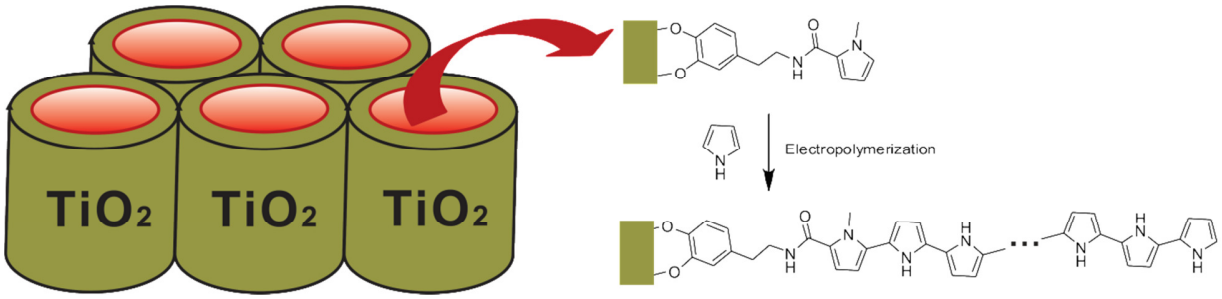

Figure 1.7. Surface-immobilized p-n heterojunctions via surface-initiated electropolymerization (from ref. 41).

Although electropolymerization promises a fast solution to obtain thick surface-immobilized CP thin films, limitation toward mass production, dependence of the outcome on complicated experimental conditions, relatively poor surface morphology of the polymer films,

electrochemical coupling between surface-immobilized precursors which would reduce surface coverage, as well as limited choice of monomers capable of electrochemical polymerization restrict the application of this method and stimulate search for alternative polymerization approaches.

1.5 Chemically Grafted Conjugated Polymer Brushes.

Conventional polymer brushes have been prepared via two pathways, "grafting to" and "grafting from" methods.[28, 42] Polymer brushes through "grafting to" method are typically manufactured by physisorption, i.e. attachment of sticky block copolymers to surface, or chemisorption which relies on covalent bonding between terminal anchoring groups on polymers and complementary groups on surface via highly efficient reactions such as click chemistry. Although "grafting to" method seems to promise convenient way to yield tethered polymers with desired optical and electrical properties, some limitations preclude it from being universal. Steric repulsion between approaching polymers and tethered polymers on surface hinder the formation of densely packed polymer brushes. Furthermore, with higher molecular weight of polymer, the reaction efficiency between polymers and surface becomes lower. Consequently, thickness of resulting film could be severely limited. In case of physisorption, thin films showed relatively poor stabilities and would be prone to peeling off.

Surface-initiated polymerization, so called "grafting from" method, is an alternative pathway to yield tethering of dense and thick polymers on the surface. Such polymer brushes can be obtained through a two-step procedure. First, initiators are immobilized on the surface of a substrate. Unlike surface-initiated electropolymerization, any choice of substrate can be employed, even those that are not conductive. Using an initiator-modified substrate, surface-initiated polymerization from solutions containing monomers and catalyst gives a dense and thick polymer brushes covalently attached to the surface.

Although many successful results using both methods were previously reported for non-conjugated polymers, conjugated polymers were mainly attached to surface using "grafting to" method.[43, 44] Recently, ethynyl group terminated regioregular P3HT (M_n = 5,900 g mol^{-1}, PDI (polydispersity) 1.2) was grafted on azide functionalized silicon dioxide surface via click reaction and resulting thin film was utilized to fabricate OFET (Figure 1.8). [43] In this work, it was demonstrated that the surface coverage of resulting P3HT thin film was 0.5 chain per nm^2 and hole mobility of resulting OFET was 5 x 10^{-5} cm^2 V s^{-1}, higher than the mobility obtained with the low molecular weight P3HT spin-casted OFET. Although "grafting to" method allows to attach polymers with low polydispersity, the necessity to use bulky solubilizing groups, low molecular weight, as well as low polymer brush density still remain a bottleneck for further applications in organic electronics.

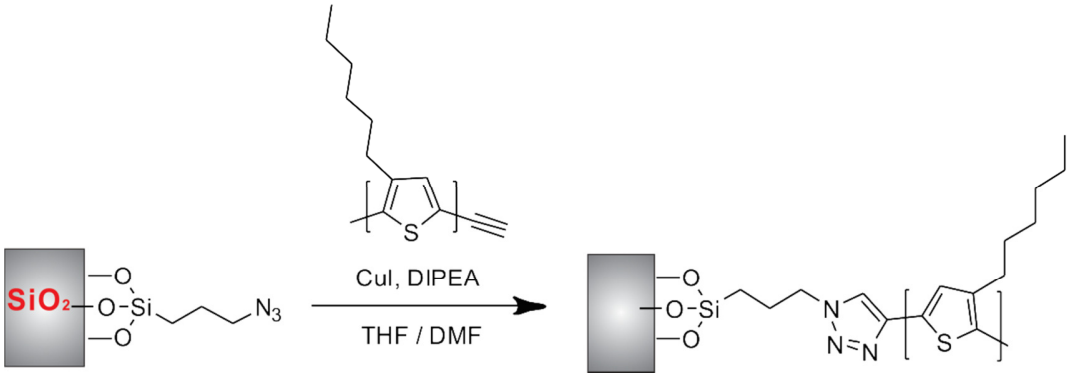

Figure 1.8. Surface-immobilized P3HT via "graft to" method (from ref 43).

In 2007, Kiriy et al. suggested a way to graft CP brushes via metal catalyst transfer surface-initiated polycondensation.[45] To graft surface-immobilized P3HT brushes on Si wafer or glass, an anchoring layer consisting of poly(glycidyl methacrylate) (**PGMA**) / cross linked poly(4-bromostyrene) (**PS-Br**) was deposited by spin-coating of PS-Br on PGMA layer followed by UV irradiation. This layer was then activated with $Ni(PPh_3)_4$ to produce surface-immobilized macroinitiators. Subsequent surface-initiated Kumada polycondensation from the initiator layer

yielded surface-attached red colored P3HT thin film (Figure 1.9). This was certainly a remarkable ground-breaking achievement. However, there was one complicating issue: Thickness of the initiating PGMA / cross-linked PS-Br layer was a major factor determining thickness of P3HT layer. For example, with 1.7 nm thickness of the anchoring layer, only 5 nm of P3HT layer was formed. On the contrary, 110 nm thick PGMA / PS-Br layer gave 150 nm thick P3HT brushes. The authors initially assumed that such behavior would originate from a poor stability of anchoring layer during polymerization. Thus, thicker anchoring layer would give thicker P3HT layer. However, later the same authors determined the actual reason.[46] This was originating from the fact that the resulting films had interpenetrated network structure, that is, P3HT brushes were grafted not only from topmost layer but also from inside of PGMA / PS-Br initiating layer. Therefore, thickness of the resulting thin films was mainly determined by thickness of the macroinitiator layer. This behavior was most likely due to the low reactivity of employed Ni(II) catalytic system, which resulted in inefficient externally-initiated polymerization and high probability of chain transfer to the monomers in solution.

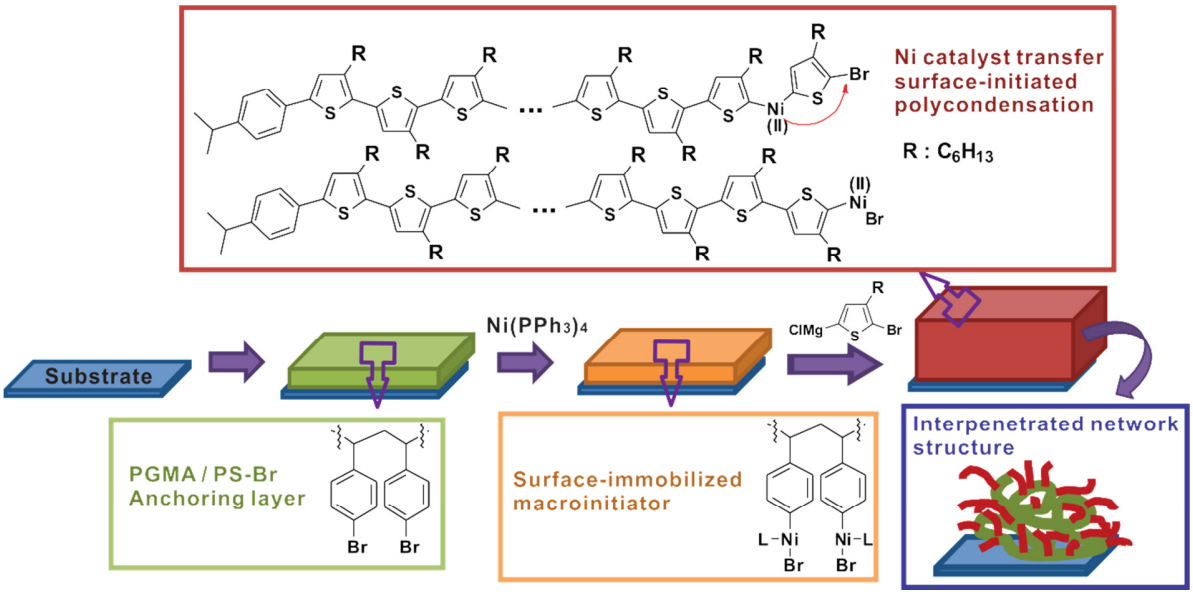

Figure 1.9. Metal catalyst transfer surface-initiated living Kumada polycondesation (from ref 46, 47).

The first real "grafting from" CP films were demonstrated by Locklin et al. in 2009.[47] In this report, the authors mentioned that $Ni(PPh_3)_4$ did not generate surface-immobilized Ni(II) complex and resulted in inefficient polymerization. Thus, they developed a new catalytic system generated via ligand exchange promising an efficient activation of aryl halide. To obtain surface immobilized PT or poly(p-phenylene) (**PPP**) on the surface of gold, hexylthiol-terminated 2-bromothiophene was anchored on top of gold substrate followed by oxidative addition to $Ni(COD)_2$ (which has a better reactivity than $Ni(PPh_3)_4$). 14 nm thick layer of P3HT or 42 nm layer of PPP brushes were grafted from this surface immobilized macroinitiators in the conditions of *in situ* Kumada polycondensation (Figure 1.10A).

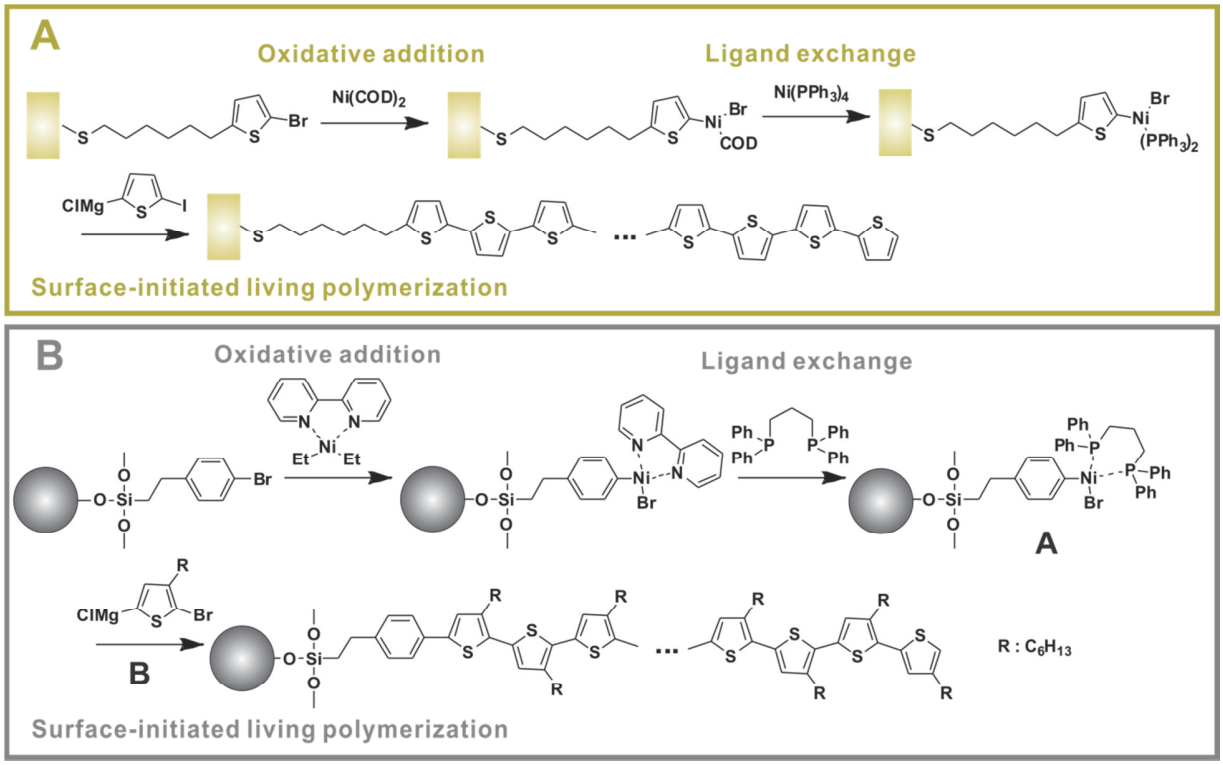

Figure 1.10. Surface-immobilized PT brushes via ligand exchange (from ref 47, 48).

To develop a more efficient catalytic system, Kiriy et al. compared the solution polymerization efficiencies of two Ni(II) catalyst, Ph-$Ni(PPh_3)_2$-Br and $Ni(dppp)Cl_2$. Based on the better polymerization performance with $Ni(dppp)Cl_2$, the authors further developed a ligand

exchange method to produce surface-immobilized initiator layer with more efficient bidentate ligand in $Et_2Ni(bipy)$ Ni(II) complex.[48] As a first step, oxidative addition of 4-bromobenzene to $Et_2Ni(bipy)$ followed by ligand exchange with 1,3-bis(diphenylphosphino)propane (**dppp**) resulted in surface-immobilized Ar-Ni(dppp)-Br (**A** in Figure 1.10) active initiator. When this surface was exposed to solution of the Grignard monomer **B**, surface-initiated Kumada polycondensation yielded P3HT brushes with M_n 43,000 g/mol that were immobilized on surface of Si particles (Figure 1.10B).

Such surface-initiated living polycondensation is not limited only by Kumada polycondensation. Kiriy also achieved a surface initiated Suzuki polycondensation based on recent report from Yokozawa that the chain growth Suzuki polycondensation with three-coordinate complex [$(tBu_3P)Pd(Ph)Br$] occurrs in the living fashion.[49, 50] Like previously reported procedures, oxidative addition of cross linked PS-Br to $Pd(PtBu_3)_2$ followed by living polymerization of 7-bromo-9,9-bis(2-ethyl-hexyl)-9H-fluoren-2-ylboric acid ester monomer gave a network-structured surface-immobilized polyfluorene thin film with thickness of up to 100 nm.

1.6 Research Focus.

The ultimate goal of this research dissertation centers on development of "bottom-up" approaches to thin films of conjugated polymers. This new paradigm will offer an improved free charge carrier transfer efficiency in the films made of densely packed CPs without any bulky solubilizing groups as well as more efficient intramolecular transfer. Additionally, control of the nanoscale structure and morphology of the resulting thin films through combination of nanoparticle lithography and efficient surface-initiated *in situ* polymerization will allow fabricating ideally structured BHJ OPV devices. Enhancement in chemical and physical stability of the thin films and resulting devices would be an additional benefit of the strategy.

In initial attempts, we developed preparation of surface-tethered PEDOT / PT block copolymers (analogue of PEDOT/PSS / P3HT layers in conventional spin-coated OPV) via surface-initiated electropolymerization which was chosen due to its practical convenience. Using this strategy, we prepared a half PV devices consisting of donor layer on ITO electrode which demonstrated better photovoltaic efficiency and higher photostability than spin-casted devices. This research is described in chapter 2.

Chapter 3 describes development of Ni catalyst transfer surface-initiated Kumada polycondensation. To obtain thick and dense thin films, we carried out systematic studies to improve experimental conditions using novel highly efficient Ni(II) external catalytic initiator currently being developed in the group. As a result, we successfully grafted thin PT films with improved surface morphology on top of various substrates such as Si wafer, ITO, and quartz. In addition to development of chemical "grafting from" method, we also prepared nanopatterned surface-immobilized columnar PT thin films as a hole transporting counterpart of the ideal structured BHJ OPV.

Chapter 4 describes an alternative approach to surface-immobilized thin films prepared by stepwise *in situ* polymerization method using Cu catalyzed Huisgen 1,3-cycloaddition reaction ("click" reaction). Along this line, it was found that stepwise prepared conducting polymer thin films not only promise complete control over surface morphology, thickness, and molecular composition of resulting polymer film but also allow building complex copolymer thin films with desired photophysical properties.

1.7 References.

(1) Shirakawa, H.; Louis, E. J.; MacDiarmid, A. G.; Chiang, C. K.; Heeger, A. J., Synthesis of electrically conducting organic polymers: halogen derivatives of polyacetylene, (CH), *J. Chem. Soc. Chem. Commun.* **1977**, 578-580.

(2) Advanced information - The Nobel Prize in Chemistry, 2000: Conductive polymers, *THE ROYAL SWEDISH ACADEMY OF SCIENCE*.

(3) Chiang, C. K.; Druy, M. A.; Gau, S. C.; Heeger, A. J.; Louis, E. J.; MacDiarmid, A. G.; Park, Y. W.; Shirakawa, H., Synthesis of highly conducting films of derivatives of polyacetylene, (CH)x, *J. Am. Chem. Soc.* **1978**, *100*, 1013-1015.

(4) Huq, R.; Farrington, G. C., Stability of Undoped and Oxidized Polyacetylene, *J. Electrochem. Soc.* **1984**, *131*, 819-823.

(5) Rolland, M.; Lefrant, S.; Aldissi, M.; Bernier, P.; Rzepka, E.; Schue, F., Stablility of various doping species in trans-polyacetylene, *J. Electron. Mater.* **1981**, *10*, 619-630.

(6) Yen, S. P. S.; Somoano, R.; Khanna, S. K.; Rembaum, A., Stability of polyacetylene films, *Solid State Commun.* **1980**, *36*, 339-343.

(7) Usta, H.; Risko, C.; Wang, Z.; Huang, H.; Deliomeroglu, M. K.; Zhukhovitskiy, A.; Facchetti, A.; Marks, T. J., Design, Synthesis, and Characterization of Ladder-Type Molecules and Polymers. Air-Stable, Solution-Processable n-Channel and Ambipolar Semiconductors for Thin-Film Transistors via Experiment and Theory, *J. Am. Chem. Soc.* **2009**, *131*, 5586-5608.

(8) Herlogsson, L.; Crispin, X.; Robinson, N. D.; Sandberg, M.; Hagel, O. J.; Gustafsson, G.; Berggren, M., Low-Voltage Polymer Field-Effect Transistors Gated via a Proton Conductor, *Adv. Mater.* **2007**, *19*, 97-101.

(9) Liang, Y.; Yu, L., A New Class of Semiconducting Polymers for Bulk Heterojunction Solar Cells with Exceptionally High Performance, *Acc. Chem. Res.* **2010**, *43*, 1227-1236.

(10) Kim, Y.; Cook, S.; Tuladhar, S. M.; Choulis, S. A.; Nelson, J.; Durrant, J. R.; Bradley, D. D. C.; Giles, M.; McCulloch, I.; Ha, C. S.; Ree, M., A strong regioregularity effect in self-organizing conjugated polymer films and high-efficiency polythiophene: fullerene solar cells, *Nat. Mater.* **2006**, *5*, 197-203.

(11) Gross, M.; Muller, D. C.; Nothofer, H. G.; Scherf, U.; Neher, D.; Brauchle, C.; Meerholz, K., Improving the performance of doped pi-conjugated polymers for use in organic light-emitting diodes, *Nature* **2000**, *405*, 661-665.

(12) Najafov, H.; Lee, B.; Zhou, Q.; Feldman, L. C.; Podzorov, V., Observation of long-range exciton diffusion in highly ordered organic semiconductors, *Nat. Mater.* **2010**, *9*, 938-943.

(13) Vaeth, K. M.; Jensen, K. F., Chemical vapor deposition of thin polymer films used is polymer-based light emitting diodes, *Adv. Mater.* **1997**, *9*, 490-493.

(14) Gommans, H. H. P.; Kemerink, M.; Andersson, G. G.; Pijper, R. M. T., Charge transport and trapping in Cs-doped poly(dialkoxy-p-phenylene vinylene) light-emitting diodes, *Phys. Rev. B* **2004**, *69*, 155216.

(15) Coropceanu, V.; Cornil, J.; da Silva Filho, D. A.; Olivier, Y.; Silbey, R.; Brédas, J.-L., Charge Transport in Organic Semiconductors, *Chem. Rev.* **2007**, *107*, 926-952.

(16) Lan, Y. K.; Yang, C. H.; Yang, H. C., Theoretical investigations of electronic structure and charge transport properties in polythiophene-based organic field-effect transistors, *Polym. Int.* **2010**, *59*, 16-21.

(17) Lane, P.; Kafafi, Z. In *Organic Photovoltaics*; CRC Press, 2005.

(18) Hoppe, H.; Sariciftci, N. S., Morphology of polymer/fullerene bulk heterojunction solar cells, *J. Mater. Chem.* **2006**, *16*, 45-61.

(19) Yu, G.; Gao, J.; Hummelen, J. C.; Wudl, F.; Heeger, A. J., Polymer photovoltaic cells - enhanced efficiencies via a network of internal donor-acceptor heterojunctions, *Science* **1995**, *270*, 1789-1791.

(20) Morana, M.; Koers, P.; Waldauf, C.; Koppe, M.; Muehlbacher, D.; Denk, P.; Scharber, M.; Waller, D.; Brabec, C., Organic field-effect devices as tool to characterize the bipolar transport in polymer-fullerene blends: The case of P3HT-PCBM, *Adv. Funct. Mater.* **2007**, *17*, 3274-3283.

(21) Hoppe, H.; Niggemann, M.; Winder, C.; Kraut, J.; Hiesgen, R.; Hinsch, A.; Meissner, D.; Sariciftci, N. S., Nanoscale morphology of conjugated polymer/fullerene-based bulk-heterojunction solar cells, *Adv. Funct. Mater.* **2004**, *14*, 1005-1011.

(22) Manceau, M.; Rivaton, A.; Gardette, J. L.; Guillerez, S.; Lemaitre, N., The mechanism of photo- and thermooxidation of poly(3-hexylthiophene) (P3HT) reconsidered, *Polym. Degrad. Stab.* **2009**, *94*, 898-907.

(23) Abdou, M. S. A.; Holdcroft, S., Mechanisms of photodegradation of poly(3-alkylthiophenes) in solution, *Macromolecules* **1993**, *26*, 2954-2962.

(24) Hintz, H.; Egelhaaf, H. J.; Lüer, L.; Hauch, J.; Peisert, H.; Chassé, T., Photodegradation of P3HT−A Systematic Study of Environmental Factors, *Chem. Mater.* **2010**, *23*, 145-154.

(25) Sivula, K.; Ball, Z. T.; Watanabe, N.; Fréchet, J. M. J., Amphiphilic Diblock Copolymer Compatibilizers and Their Effect on the Morphology and Performance of Polythiophene:Fullerene Solar Cells, *Adv. Mater.* **2006**, *18*, 206-210.

(26) Zhang, Y.; Yip, H.-L.; Acton, O.; Hau, S. K.; Huang, F.; Jen, A. K. Y., A Simple and Effective Way of Achieving Highly Efficient and Thermally Stable Bulk-Heterojunction Polymer Solar Cells Using Amorphous Fullerene Derivatives as Electron Acceptor, *Chem. Mater.* **2009**, *21*, 2598-2600.

(27) Kim, N.; Potscavage, W. J.; Domercq, B.; Kippelen, B.; Graham, S., A hybrid encapsulation method for organic electronics, *Appl. Phys. Lett.* **2009**, *94*.

(28) Barbey, R. l.; Lavanant, L.; Paripovic, D.; Schüwer, N.; Sugnaux, C.; Tugulu, S.; Klok, H.-A., Polymer Brushes via Surface-Initiated Controlled Radical Polymerization: Synthesis, Characterization, Properties, and Applications, *Chem. Rev.* **2009**, *109*, 5437-5527.

(29) Pinto, J. C.; Whiting, G. L.; Khodabakhsh, S.; Torre, L.; Rodríguez, A.; Dalgliesh, R. M.; Higgins, A. M.; Andreasen, J. W.; Nielsen, M. M.; Geoghegan, M.; Huck, W. T. S.; Sirringhaus, H., Organic Thin Film Transistors with Polymer Brush Gate Dielectrics Synthesized by Atom Transfer Radical Polymerization, *Adv. Funct. Mater.* **2008**, *18*, 36-43.

(30) Rutenberg, I. M.; Scherman, O. A.; Grubbs, R. H.; Jiang, W.; Garfunkel, E.; Bao, Z., Synthesis of Polymer Dielectric Layers for Organic Thin Film Transistors via Surface-Initiated Ring-Opening Metathesis Polymerization, *J. Am. Chem. Soc.* **2004**, *126*, 4062-4063.

(31) Park, K.; Park, S. H.; Kim, E.; Kim, J. D.; An, S. Y.; Lim, H. S.; Lee, H. H.; Kim, D. H.; Ryu, D. Y.; Lee, D. R.; Cho, J. H., Polymer Brush As a Facile Dielectric Surface Treatment for High-Performance, Stable, Soluble Acene-Based Transistors, *Chem. Mater.* **2010**, *22*, 5377-5382.

(32) Pinto, J. C.; Whiting, G. L.; Khodabakhsh, S.; Torre, L.; Rodriguez, A. B.; Dalgliesh, R. M.; Higgins, A. M.; Andreasen, J. W.; Nielsen, M. M.; Geoghegan, M.; Huck, W. T. S.; Sirringhaus, H., Organic thin film transistors with polymer brush gate dielectrics synthesized by atom transfer radical polymerization, *Adv. Funct. Mater.* **2008**, *18*, 36-43.

(33) Heinze, J. r.; Frontana-Uribe, B. A.; Ludwigs, S., Electrochemistry of Conducting Polymers—Persistent Models and New Concepts, *Chem. Rev.* **2010**, *110*, 4724-4771.

(34) Marchal, D.; Boireau, W.; Laval, J. M.; Bourdillon, C.; Moiroux, J., Kinetics of redox conversion at a gold electrode of water-insoluble ubiquinone (UQ((10))) and plastoquinone (PQ((9))) incorporated in supported phospholipid layers, *J. Electroanal. Chem.* **1998**, *451*, 139-144.

(35) Zotti, G.; Schiavon, G.; Zecchin, S.; Sannicolo, F.; Brenna, E., Anion-assisted anodic coupling of 2,2'-bipyrrole-role of tosylate anion in the electrochemical synthesis of polypyrrole, *Chem. Mater.* **1995**, *7*, 1464-1468.

(36) Zotti, G.; Schiavon, G.; Berlin, A.; Pagani, G., The role of water in the electrochemical polymerization of pyrroles, *Electrochim. Acta* **1989**, *34*, 881-884.

(37) Li, M.; Tang, S.; Shen, F. Z.; Liu, M. R.; Xie, W. J.; Xia, H.; Liu, L. L.; Tian, L. L.; Xie, Z. Q.; Lu, P.; Hanif, M.; Lu, D.; Cheng, G.; Ma, Y. G., Electrochemically deposited

organic luminescent films: The effects of deposition parameters on morphologies and luminescent efficiency of films, *J. Phys. Chem. B* **2006**, *110*, 17784-17789.

(38) Ocafrain, M.; Tran, T. K.; Blanchard, P.; Lenfant, S.; Godey, S.; Vuillaume, D.; Roncali, J., Electropolymerized self-assembled monolayers of a 3,4-ethylenedioxythiophene-thiophene hybrid system, *Adv. Funct. Mater.* **2008**, *18*, 2163-2171.

(39) Zotti, G.; Zecchin, S.; Vercelli, B.; Berlin, A.; Grimoldi, S.; Groenendaal, L.; Bertoncello, R.; Natali, M., Surface-initiated polymerization of thiophene and pyrrole monomers on poly(terthiophene) films and oligothiophene monolayers, *Chem. Mater.* **2005**, *17*, 3681-3694.

(40) Shallcross, R. C.; D'Ambruoso, G. D.; Korth, B. D.; Hall, H. K.; Zheng, Z. P.; Pyun, J.; Armstrong, N. R., Poly(3,4-ethylenedioxythiophene) - Semiconductor nanoparticle composite thin films tethered to indium tin oxide substrates via electropolymerization, *J. Am. Chem. Soc.* **2007**, *129*, 11310-11311.

(41) Wang, D.; Ye, Q.; Yu, B.; Zhou, F., Towards chemically bonded p-n heterojunctions through surface initiated electrodeposition of p-type conducting polymer inside TiO2 nanotubes, *J. Mater. Chem.* **2010**, *20*, 6910-6915.

(42) Edmondson, S.; Osborne, V. L.; Huck, W. T. S., Polymer brushes via surface-initiated polymerizations, *Chem. Soc. Rev.* **2004**, *33*, 14-22.

(43) Paoprasert, P.; Spalenka, J. W.; Peterson, D. L.; Ruther, R. E.; Hamers, R. J.; Evans, P. G.; Gopalan, P., Grafting of poly(3-hexylthiophene) brushes on oxides using click chemistry, *J. Mater. Chem.* **2010**, *20*, 2651-2658.

(44) Acharya, J. R.; Zhang, H.; Li, X.; Nesterov, E. E., Chemically Controlled Amplified Ratiometric Fluorescence in Surface-Immobilized End-Capped Oligo(p-phenylene ethynylene)s, *J. Am. Chem. Soc.* **2009**, *131*, 880-881.

(45) Senkovskyy, V.; Khanduyeva, N.; Komber, H.; Oertel, U.; Stamm, M.; Kuckling, D.; Kiriy, A., Conductive polymer brushes of regioregular head-to-tail poly(3-alkylthiophenes) via catalyst-transfer surface-initiated polycondensation, *J. Am. Chem. Soc.* **2007**, *129*, 6626-6632.

(46) Khanduyeva, N.; Senkovskyy, V.; Beryozkina, T.; Bocharova, V.; Simon, F.; Nitschke, M.; Stamm, M.; Grotzschel, R.; Kiriy, A., Grafting of Poly (3-hexylthiophene) from Poly(4-bromostyrene) Films by Kumada Catalyst-Transfer Polycondensation: Revealing of the Composite Films Structure, *Macromolecules* **2008**, *41*, 7383-7389.

(47) Sontag, S. K.; Marshall, N.; Locklin, J., Formation of conjugated polymer brushes by surface-initiated catalyst-transfer polycondensation, *Chem. Commun.* **2009**, 3354-3356.

(48) Senkovskyy, V.; Tkachov, R.; Beryozkina, T.; Komber, H.; Oertel, U.; Horecha, M.; Bocharova, V.; Stamm, M.; Gevorgyan, S. A.; Krebs, F. C.; Kiriy, A., "Hairy" Poly(3-

hexylthiophene) Particles Prepared via Surface-Initiated Kumada Catalyst-Transfer Polycondensation, *J. Am. Chem. Soc.* **2009**, *131*, 16445-16453.

(49) Beryozkina, T.; Boyko, K.; Khanduyeva, N.; Senkovskyy, V.; Horecha, M.; Oertel, U.; Simon, F.; Stamm, M.; Kiriy, A., Grafting of Polyfluorene by Surface-Initiated Suzuki Polycondensation, *Angew. Chem., Int. Ed.* **2009**, *48*, 2695-2698.

(50) Yokoyama, A.; Suzuki, H.; Kubota, Y.; Ohuchi, K.; Higashimura, H.; Yokozawa, T., Chain-growth polymerization for the synthesis of polyfluorene via Suzuki-Miyaura coupling reaction from an externally added initiator unit, *J. Am. Chem. Soc.* **2007**, *129*, 7236-7237.

CHAPTER 2 SELF-ASSEMBLED MONOLAYER INITIATED ELECTROCHEMICAL POLYMERIZATION: A ROUTE TO THIN FILM MATERIALS WITH ENHANCED PHOTOVOLTAIC PERFORMANCE.[1]

2.1 Introduction.

The development of organic photovoltaic (PV) devices based on semiconducting conjugated polymers has attracted significant research attention because it promises to deliver an inexpensive versatile basis for the conversion of solar light to electricity.[1] Currently, there are two major classes of organic PV devices: small molecular PV and conductive polymer PV devices. Small molecular photovoltaic devices are generally manufactured through vacuum vapor deposition. In contrast, polymer solar cells are commonly prepared by simple solution processing of two different materials.[2] Because of high cost and difficulties associated with vacuum vapor deposition processing, organic solar cells based on solution processable conjugated polymers have significant advantages.

Organic heterojunction type solar cells made by sandwiching two different conducting polymers between two metal electrodes have been first introduced by Tang in 1986,[3] and since then were widely investigated. They can be classified into two types: bilayer heterojunction devices and bulk heterojunction devices. A bilayer device has a sandwiched structure with donor and acceptor materials between two different metal electrodes. Similar to conventional inorganic silicon-based PV, exitons (tightly bound hole and electron pairs) can only dissociate at the interface between the two materials.[1] Because of short exciton lifetime, the layers should be thin to allow the exciton reach the interface fastly, and well organized to provide the shortest possible pathways for charge transport. Both factors are important in obtaining better light to power conversion efficiency. However, high degree of disorder, low intermolecular forces in organic

[1] "Reproduced in part with permission from Hwang, E.; de Silva, K.M.N. ; Seevers, C.B.; Li, J.; Garno, J.C.; Nesterov, E.E., *Langmuir.*, 2008, *24(17)*, 9700 - 9706., DOI: 10.1021/la800871r, Copyright 2008 American Chemical Society."

materials, and relatively small interfacial contact area result only in a tiny fraction of the absorbed photons generating photocurrent. In addition, difficulty of the fabrication of two distinct thin layers leads to farther lowering the light to current conversion efficiency of bilayer heterojunction devices. To improve the situations, bulk heterojunction (**BHJ**) devices have been introduced by Heeger in 1995.[4, 5] The basic concept of a bulk heterojunction device is similar to that of bilayer heterojunction devices, but it results in dramatic increase of the area of interfacial contact and decrease of distances required for free charges to travel towards the electrodes. A BHJ device is prepared by blending immiscible donor and acceptor components in a bulk volume. This allows to achieve much better efficiencies as compared to bilayer devices (Figure 2.1).

Figure 2.1. Schematic diagrams of heterojunction type organic solar cells.

Despite recent progress with bulk heterojunction PV systems,[6-9] the design of new alternative platforms to overcome some major drawbacks of the currently available devices remains a high priority. One of the major problems to be resolved is low current generation efficiency, which is partially attributed to the poor charge-transport characteristics of amorphous organic materials as well as loose and poorly organized contacts at interfacial junctions.[10-12] Therefore, optimizing these two factors is a promising way to increase the light-to-current conversion efficiency. Whereas it has been recognized that better molecular organization in the bulk polymer material can result in higher-efficiency devices,[13-15] achieving such organization still poses a challenge. In principle, ordered conducting polymer networks can be prepared by endogenous (i.e., occurring

without the addition of any catalyst or external reagent) polymerization approaches.[16, 17] Electropolymerization is one approach that can yield both electrode-attached and free-standing films and is widely used in the preparation of polythiophene and its derivatives. Polythiophene-derived materials are promising semiconducting polymers for PV applications because they possess a variety of attractive properties such as high stability, good charge mobility, and the possibility to modify their electronic parameters easily by chemical functionalization.[18] In particular, polythiophene without sterically bulky side groups attached to the conjugated backbone would be highly suitable for practical applications because it can adopt a relatively planarized backbone conformation with extended π-electron conjugation. However, unsubstituted polythiophenes cannot be processed because of their low solubility, and those modified with solubilizing groups adopt less planar conformations and tend to form molecularly disordered amorphous systems during conventional spin-cast processing. One way to overcome the low solubility problem during device fabrication would be to use *in situ* preparation of polythiophene from its soluble monomeric precursor by electropolymerization. Despite the relative simplicity of this approach, the preparation of complex multilayered electronic devices by electropolymerization has not been previously demonstrated.

In this project, we developed an approach to prepare highly stable thin-film bilayer materials for building OPV devices with improved performance characteristics. The bilayer films of polythiophene and its derivatives are prepared without the need to have any solubilizing groups, which overcomes the solubility problem that is pertinent to this class of electronic materials. The approach is based on the modification of the surface of a transparent indium tin oxide (**ITO**) electrode with a surface-immobilized precursor or initiator layer of an electroactive compound (e.g., ter(3,4-ethylenedioxythiophene) (terEDOT) derivative). The surface-modified electrode is then used as a working electrode for the electropolymerization of a suitable electroactive

monomer in a controlled cyclic voltammetry (CV) mode. The polymer growth occurs from the monolayer as an initiator site and, because of spatial restrictions in the monolayer, results in the formation of a densely packed polymer film covalently attached to the ITO surface. This film can, in turn, be used to initiate the electropolymerization of the next monomer to produce a covalently interconnected bilayer structure. The sequence can, in principle, be continued to prepare a trilayer film and even further complex systems. Thus, this bottom-up strategy enables the preparation of complex molecularly ordered thin-film multilayer systems, covalently attached to an ITO electrode, with tight covalently bonded interlayer heterojunctions. Importantly, the thickness and other characteristics of each sublayer can be controlled by adjusting the polymerization conditions, such as monomer concentration, number of CV scans, and so forth (Figure 2.2).

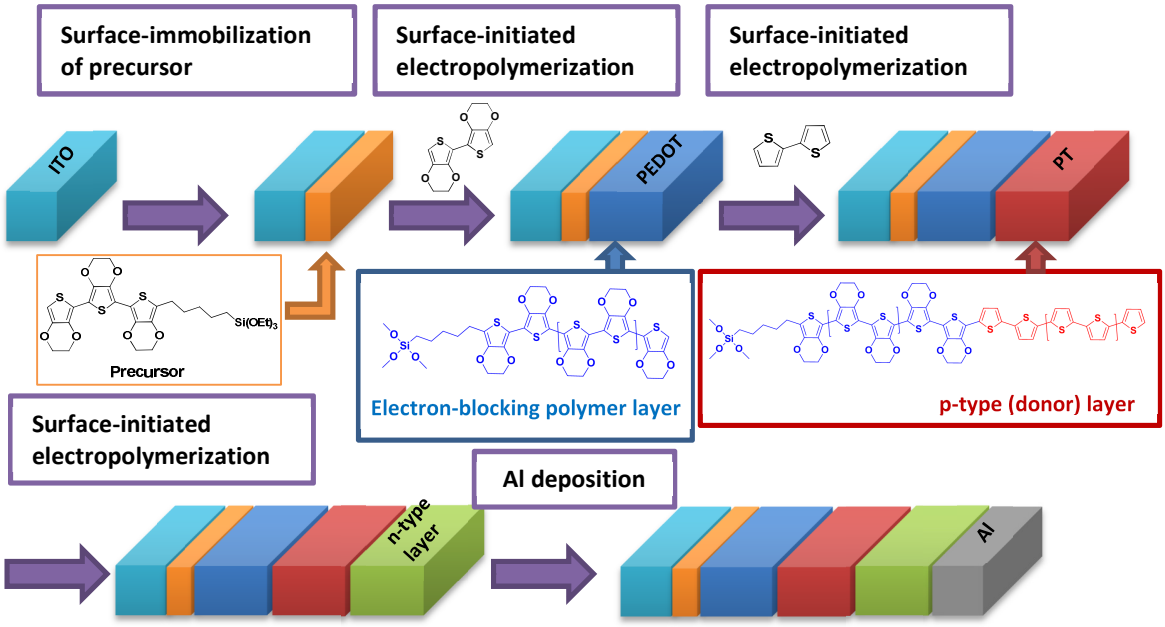

Figure 2.2. Novel strategy based on surface-immobilized precursor layer followed by surface-initiated electropolymerization.

Although the formation of polythiophene and other conducting polymer films by electropolymerization on precursor-tethered electrode surfaces has been previously studied,[19-23]

our study was the first to report on the improved performance and high stability of the complex bilayer thin-film materials prepared in this way to be used in PV applications. In principle, the same approach can be extended to the preparation of other electronic devices requiring improved charge-transport efficiency such as organic polymer light-emitting diodes.

2.2 Experimental Details.

2.2.1 Polymerization Initiators.

Preparation of precursors started with the synthesis of 2,2'-Bis(3,4-ethylenedioxythiophene) (bisEDOT) (**2-A1**) by $CuCl_2$ catalyzed coupling reaction of lithiated 3,4-ethylenedioxythiophene (Scheme 2.1).[24] After lithiation with *n*-BuLi followed by reaction with Me_3SnCl, 5-(Trimethylstannyl)-2,2'-bis(3,4-ethylenedioxythiophene) (**2-A2**) was obtained. 2-(Pent-4-en-1-yl)-3,4-ethylenedioxythiophene (**2-A3**) was prepared from 3,4-ethylenedioxythiophene through lithiation and subsequent nucleophilic substitution reactions. The product was further iodinated to afford 2-Iodo-5-(pent-4-en-1-yl)-3,4-ethylenedioxythiophene (**2-A4**). Stille coupling between **2-A2** and **2-A4** yielded ter(EDOT) derivative **2-A5**. For the formation of covalently attached precursor layer on ITO surface, the terminal alkene group of precursors had to be functionalized through hydrosilylation. Therefore, triethoxysilane-substituted precursor **TEDT** was prepared through hydrosilylation mediated by Karstedt's catalyst.[25] The preparation of comparison OPV without the electron-blolcking PEDOT layer can illustrate how PEDOT improves the performance of the device. For this purpose, the terthiophene analogue **TT** was synthesized following the same route as for **TEDT**. (Scheme 2. 1) Further details are given in the Experimental section.

2.2.2 Preparation of Surface-immobilized Conducting Polymer Thin Film.

Freshly cleaned rectangular ITO-coated glass slides were immersed into precursor solution in toluene for 3 days to tether precursor **TEDT** or **TT** to ITO surface. Subsequent

electropolymerization was accomplished by CV scaning using modified ITO or bare ITO as a working electrode in a 10mM solution of 2,2'-bisthiophene or bisEDOT in the supporting electrolyte.

Scheme 2.1. Synthesis of precursor **TEDT** and **TT.**

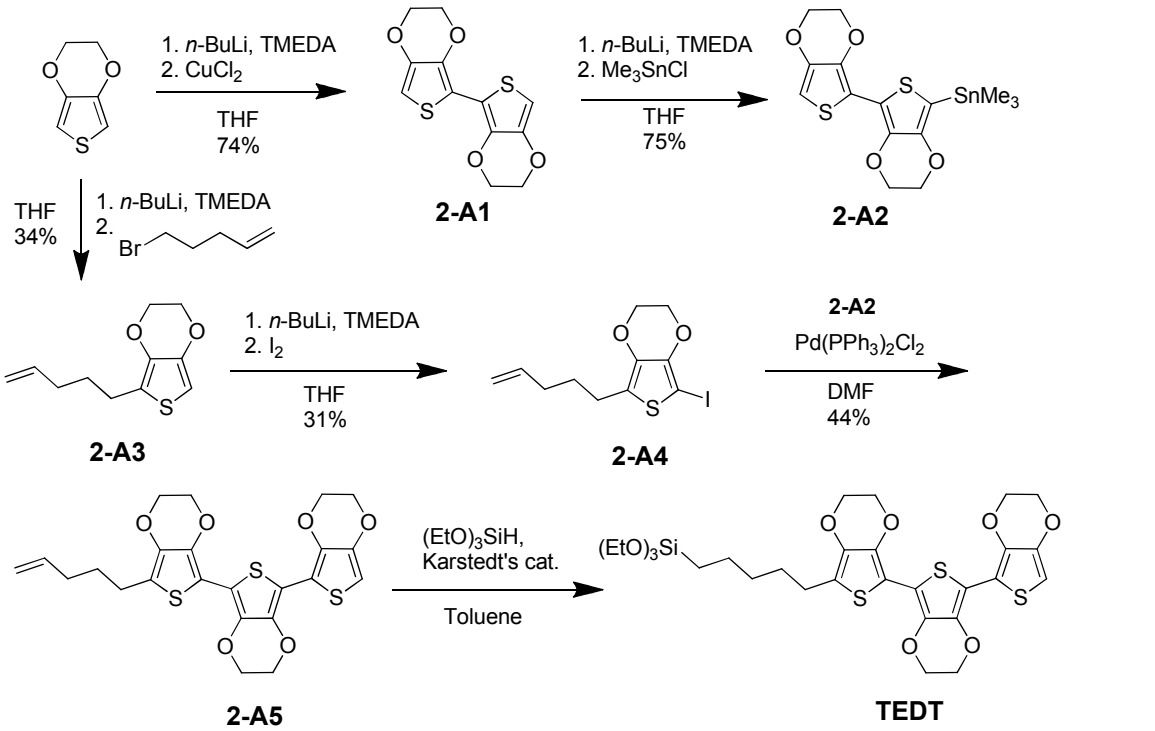

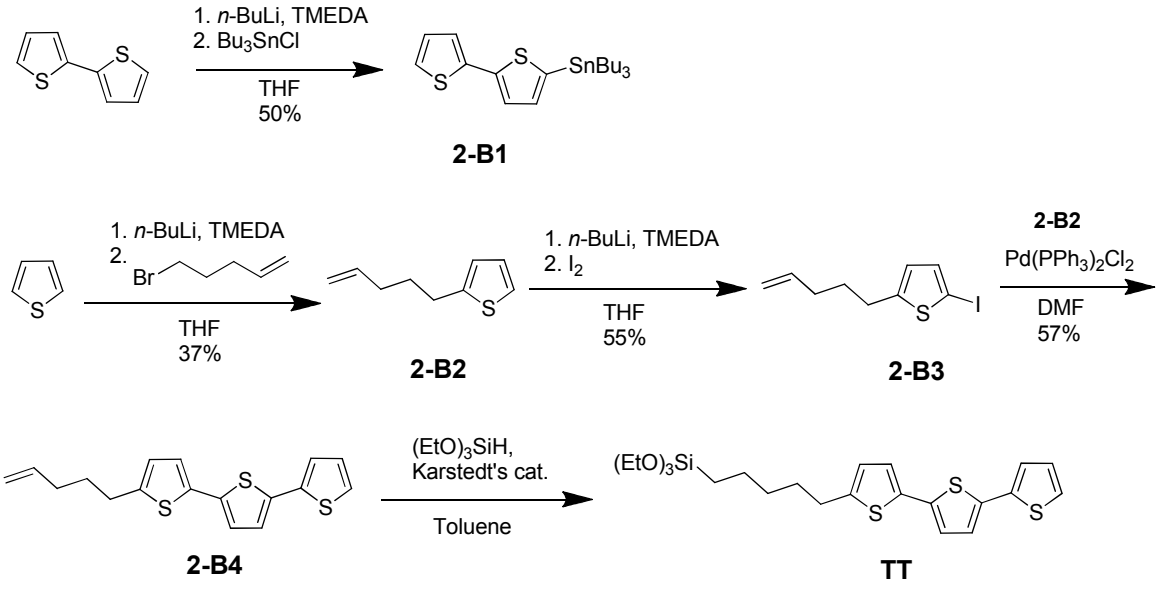

Removing monomer residues on sample slides through washing with copious amount of CH_2Cl_2 followed by ultrasonication gave an electrochemically deposited polymer thin film ITO-coated substrates. Further details are provided in the Experimental section.

2.2.3 Photoelectrochemical Studies.

All photoelectrochemical experiments were performed using monochromatic irradiation produced by a Newport 66353 300W Xe lamp, controlled by a Newport 68945 digital exposure controller through an electromechanical shutter. The monochromatic light of a required wavelength was selected using a Newport 77250 high throughput monochromator. The light intensity was measured by a Newport 70260 radiant power meter equipped with a Newport 70268 probe and was corrected. The photocurrent was measured in a three-electrode arrangement using a custom-made photoelectrochemical cell with a 40-mm-diameter quartz window, modified ITO samples as a working electrode (electrode area ~1.5 cm^2), a Ag/AgCl (3 M KCl) reference electrode, and a Pt wire coil as a counter electrode. An air-saturated 5 mM solution of methyl viologen in 0.1 M aqueous Na_2SO_4 was used as a supporting electrolyte (a deaerated, argon-saturated electrolyte was used in some instances where noted) (Figure 2.3).

The photocurrent measurements were performed at -0.1 V bias using monochromatic irradiation at a wavelength of 505 nm and an optical power of 800 μW cm^{-2}. Photocurrent generation quantum yields (Φ) and incident photon-to-current conversion efficiency (IPCE) values were calculated using the following equations adopted from literature.[26]

$$\phi = \frac{ihc}{eW\lambda(1-10^{-A})} \qquad eqn\ 2.1$$

$$\text{IPCE} = 1240\frac{i}{W\lambda} \qquad eqn\ 2.2$$

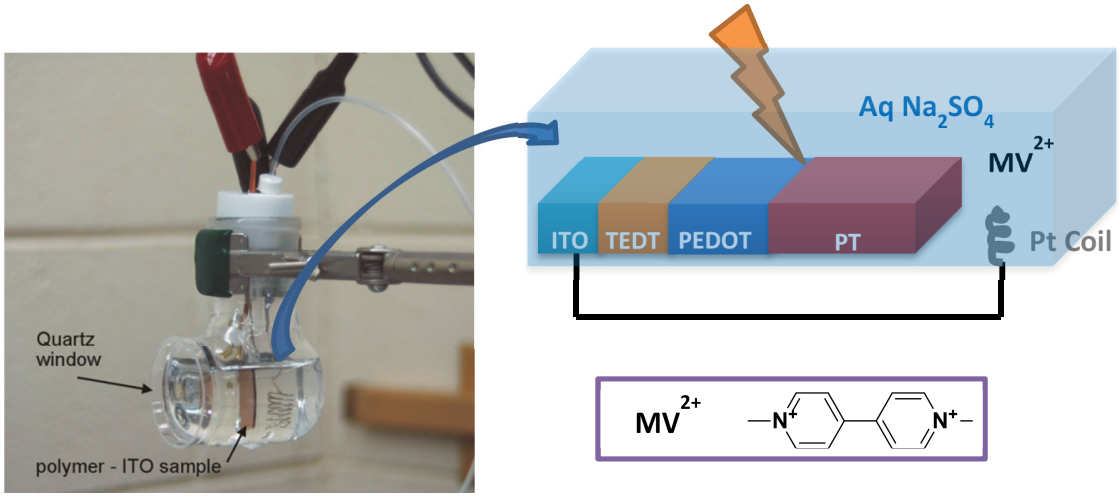

Figure 2.3. Custom-made quartz electrochemical cell used in the photoelectrochemical experiments.

In the formula, i is the photocurrent density, h is the Plank constant, c is the speed of light, e is the elementary charge, λ is the wavelength of incident light with the optical power W, and A is absorbance at this wavelength. Each value reported in Table 1 was obtained through the measurements on three to five independently prepared samples. A photoaction spectrum in Figure 2.4 inset was obtained using the same experimental setup by measuring the photocurrent at the incident light wavelengths being varied in the range from 350 to 810 nm with a step of 10 nm. At each step, the light power was adjusted to 300 μW cm^{-2}.

2.3 Results and Discussion.

2.3.1 Design of Surface-immobilized Semiconducting Polymer Thin Film.

Although the pentamethylene linkage between the electroactive terEDOT unit and the anchoring silyl group in **TEDT** could presumably retard the charge transport to the ITO electrode, this linkage was chosen because it could improve bulk organization in the monolayer. **TEDT** readily forms a uniform monolayer on the surface of ITO as evidenced by UV-vis spectroscopy and CV studies (Figures 2.4 and 2.5). Thus, the disappearance of the fine vibronic structure of the terEDOT electronic absorption band clearly visible in a solution of **2-A5**, along

with a slight bathochromic shift, can be attributed to intermolecular interactions in the monolayer. A CV scan displays a reversible oxidation peak at +0.25 V (vs Ag/Ag^+) that is similar to the oxidation peak of compound **2-A5** in solution.

Unlike *n*-alkyl derivatives that commonly accept uniformly elongated chain conformation in SAMs, precursor **TEDT** possesses bent geometry with an approximately 133° angle between the planar trisEDOT fragment and the *n*-pentane linker (Figure 2.7A). Assuming the bent geometry and considering the monolayer average thickness of 1.4 nm, one can estimate that the *n*-pentane chains are actually very close to the expected normal orientation (estimated tilt angle of only 13° with respect to the surface normal), whereas the electroactive terEDOT groups are almost coplanar with the surface (approximate tilt angle of 73°, Figure 2.7A). Such an unusual orientation of **TEDT** on the surface likely precluded the formation of a tightly packed monolayer. On the basis of the dimensions shown in Figure 2.7B, each molecule of **TEDT** was estimated to occupy approximately 1.5 nm^2 of the surface area, but the experimental value derived from the electrochemically determined surface coverage was 6.7 nm^2.

Despite the obvious inability to form a tightly packed monolayer, the surface-attached film of **TEDT** was relatively uniform and free from experimentally detectable aggregates. Indeed, uniform coverage with few defects was revealed in AFM topography images (Figure 2.8A), where the angularly shaped terraces of the ITO substrate are clearly distinguishable. Simultaneously acquired current-sensing AFM (CS-AFM) images indicated uniform conductivity throughout the surface, which is in good agreement with the topography data.

Despite the obvious inability to form a tightly packed monolayer, the surface-attached film of **TEDT** was relatively uniform and free from experimentally detectable aggregates. Indeed, uniform coverage with few defects was revealed in AFM topography images (Figure 2.8A), where the angularly shaped terraces of the ITO substrate are clearly distinguishable.

Simultaneously acquired current-sensing AFM (CS-AFM) images indicated uniform conductivity throughout the surface, which is in good agreement with the topography data.

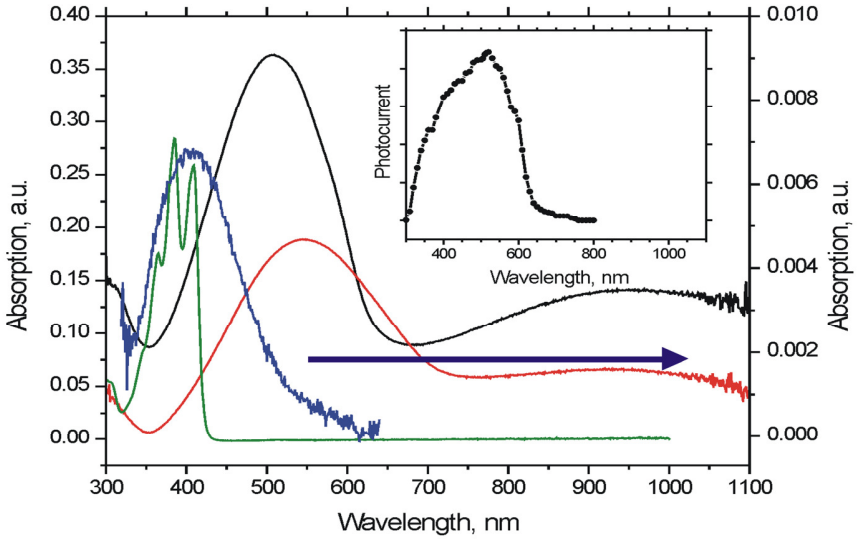

Figure 2.4. UV-Vis absorption spectra of surface-immobilized TEDT on ITO (blue trace), and of **2-A5** in CH_2Cl_2 solution (green trace), ITO/TEDT/PEDOT (red trace), and ITO/TEDT/PEDOT/PT (black trace). The latter three spectra use the left absorption scale. *Inset:* action spectrum of an ITO/TEDT/PEDOT/PT/ MV^{2+}/Pt cell (incident power 300 μW/cm^2, bias potential -0.1 V vs. Ag/AgCl, air-saturated 0.1 M aq. Na_2SO_4 containing 5 mM MV^{2+}).

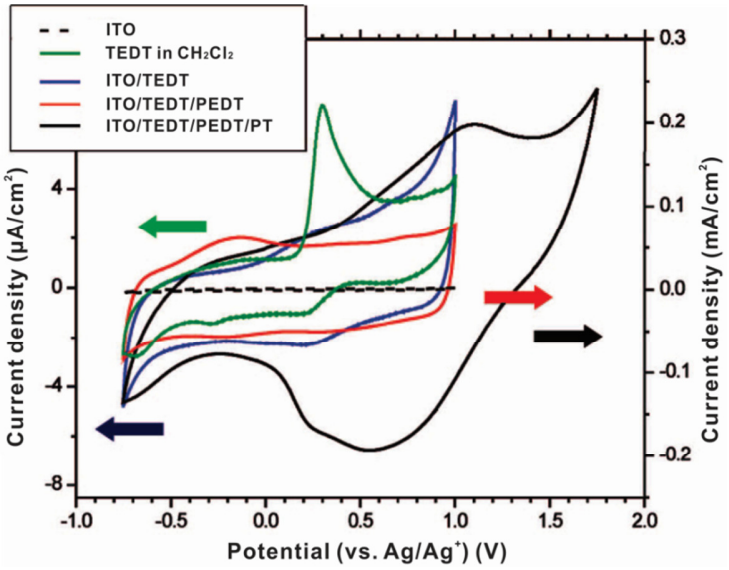

Figure 2.5. Cyclic voltammograms of 1 mM solution of **2-A5** and surface-immobilized precursor TEDT on ITO, as well as of the electropolymerized samples. The arrows of the corresponding color point to the Y-axis applicable for each graph. Experimental conditions: 0.1 M Bu_4NPF_6 in CH_2Cl_2, sweep rate 0.1 V/s.

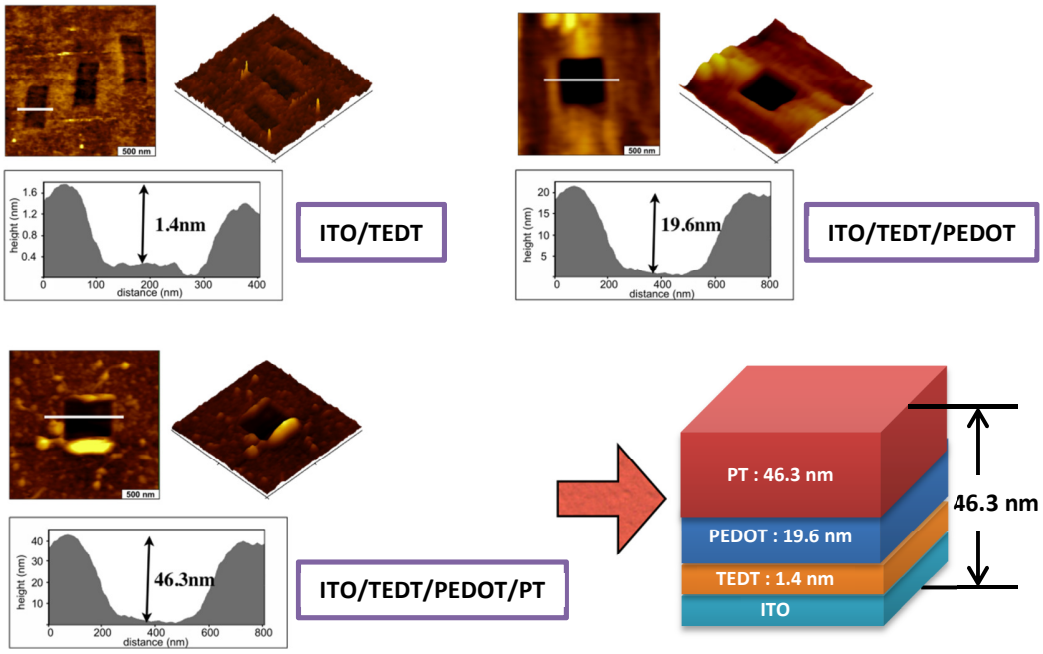

Figure 2.6. Thickness of constituent layers as determined by AFM nanoshaving studies (the area of each image is 2x2 μm^2).

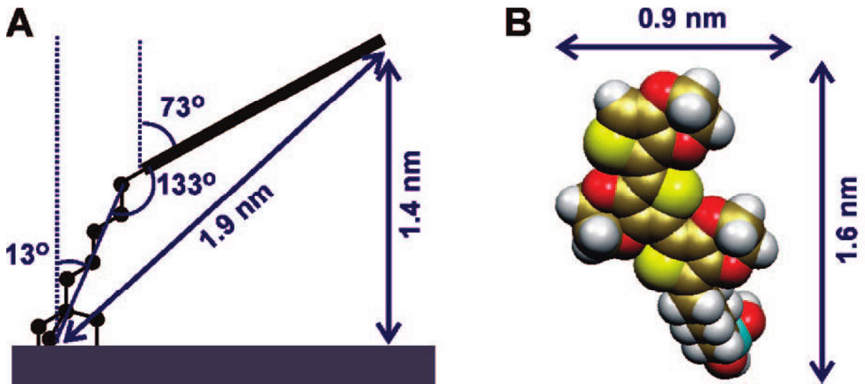

Figure 2.7. (A) Proposed structure of compound TEDT in the surface-immobilized monolayer (based on the experimental monolayer thickness and computed geometry). (B) Top view of TEDT (space-filling model) attached to the surface. The geometry of TEDT was optimized in the gas phase with the RHF/3-21G* method.

A single CV scan in a 10 mM solution of bisEDOT using an ITO slide modified with a SAM of **TEDT** (ITO/TEDT, where / denotes an interface) as the working electrode resulted in the deposition of a deep-blue PEDOT film (ITO/TEDT/PEDOT). The positions of absorption

maximum and CV oxidation peak (Figures 2.4 and 2.5) agree well with the formation of the PEDOT layer. The film exhibited homogeneous coverage and current conduction throughout areas of the film (Figure 2.8B), with the local thickness of the PEDOT layer measuring 18 ± 1 nm (Figure 2.6). In the next step, a covalently attached PT layer was grown on top of the PEDOT layer after two CV scans in a 10 mM solution of bithiophene monomer. The resulting ITO/TEDT/PEDOT/PT system (device **D1**, Table 2.1, page 37) showed a hypsochromically shifted UV-vis absorption band characteristic of PT (Figure 2.4) as well as a new oxidation peak at 1.1 V (Figure 2.5). The absence of the original PEDOT oxidation peak at -0.1 V indicated complete coverage of the underlying PEDOT layer. Indeed, the AFM images (Figure 2.8C) revealed a uniformly covered PT layer with a local thickness of 27 ± 1 nm (Figure 2.6). A side-by-side comparison of the films indicated that the surface roughness increased as layers were added to the device, thus the topography of the underlying substrate was no longer evident in Figure 2.8C.

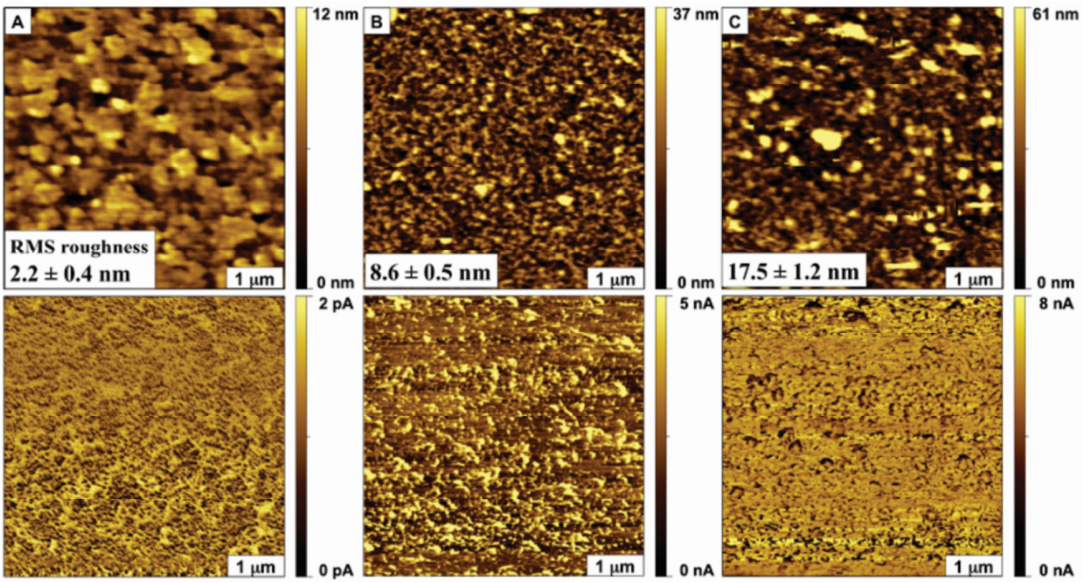

Figure 2.8. Evolution of changes in surface topography *(up column)* and corresponding current-sensing AFM images acquired at a sample bias -4 V *(bottom column)* for device **D1**. A. ITO/TEDT; B. ITO/TEDT/PEDOT; C. ITO/TEDT/PEDOT/PT. The area of each image is 5×5 μm.

2.3.2 Building Prototype PV Devices and Studies of Their Performance.

The electronic properties of bilayer device **D1** were probed using a liquid electrolyte. The liquid electrolyte provides a convenient method to electrically contact the device without the need to build a complete PV device with a deposited metal junction. Indeed, this enabled the rapid screening of a variety of different device architectures to determine the best-performing system. Thus, the photocurrent generation of device **D1** was studied in a photoelectrochemical cell using methyl viologen (MV^{2+}) as an electron carrier in an air-saturated aqueous solution of Na_2SO_4 as a supporting electrolyte and a Pt wire anode (ITO/TEDT/PEDOT/PT/MV^{2+}/Pt). The electrochemical energy diagram explaining photocurrent generation in this case is sketched in Figure 2.9.

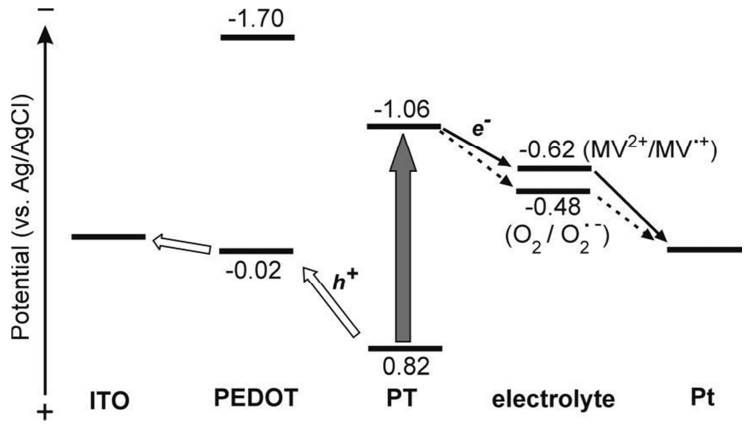

Figure 2.9. Energy diagram for photocurrent generation in an ITO/TEDT/PEDOT/PT/MV^{2+}/Pt cell

In this diagram, the given values for HOMO of PEDOT and PT were obtained from the onset of their oxidation potentials,[29] and the LUMO potentials were derived from the corresponding optical band gaps. We presumed that in D1 the polythiophene (PT) layer would act as a photoactive exciton- generating layer and the PEDOT sublayer would serve to improve the hole transport to the ITO electrode as well as to prevent electron injection from the photoactive PT layer to ITO. A stable cathodic photocurrent appeared immediately upon photoirradiation with

monochromatic light at a wavelength of 505 nm and disappeared instantly upon turning off the light (Figure 2.10A). The quantum yield of photocurrent generation obtained from this experiment was 5.7 ± 0.6%, and IPCE was 2.4 ± 0.4%.

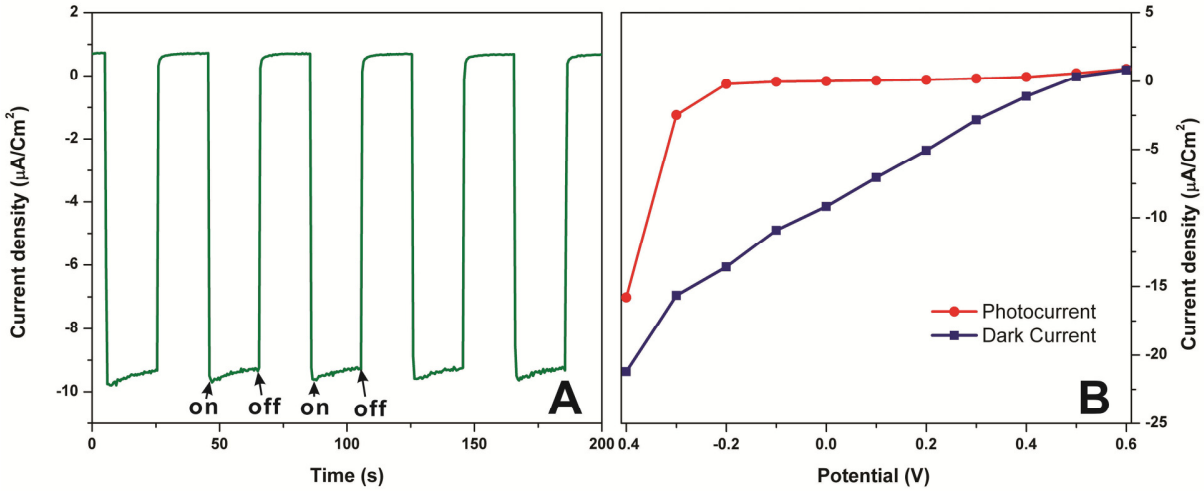

Figure 2.10. (A) Photoelectrochemical response of an ITO/TEDT/PEDOT/PT/MV^{2+}/Pt cell (applied bias of -0.1 V vs Ag/AgCl). (B) Photocurrent vs applied potential for the cell in part A. Experimental conditions: (A) incident power 800 μW cm^{-2} or (B) 300 μW cm^{-2}; λ = 505 nm, air-saturated 0.1 M Na_2SO_4(aq) containing 5 mM MV^{2+}.

It is clear that in this type of liquid electrolyte cell the process of electron transfer from the PT film to an electron carrier is of critical importance to current generation. In air-saturated electrolyte, dissolved oxygen acts as an electron carrier in addition to MV^{2+} (Figure 2.9), therefore increasing the overall efficiency of the device. The reduced electron carriers ($MV^{\bullet+}$ and $O_2^{\bullet-}$) diffuse to release electron to the Pt counter electrode and establish the cathodic current flow. Indeed, with deaerated, argon-saturated electrolyte, both the photocurrent generation quantum yield and IPCE showed substantial decreases to 3.5 ± 0.3% and 1.4 ± 0.1%, respectively (Table 2.1). However, no further increase in current generation efficiency was observed upon increasing the concentration of MV^{2+} beyond 5 mM. This indicates the special role of O_2 as an electron carrier for this system, which is probably due to the suppression of charge recombination from $O_2^{\bullet-}$ to $PT^{\bullet+}$.[30]

The device also demonstrated remarkable photostability, showing no drop in photocurrent upon continuous irradiation for more than 6 h in an air-saturated cell (Figure 2.11). Good agreement between the action spectrum of this device (Figure 2.4, inset) and the absorption spectrum of PT indicated that the excitons were generated in the PT sublayer.

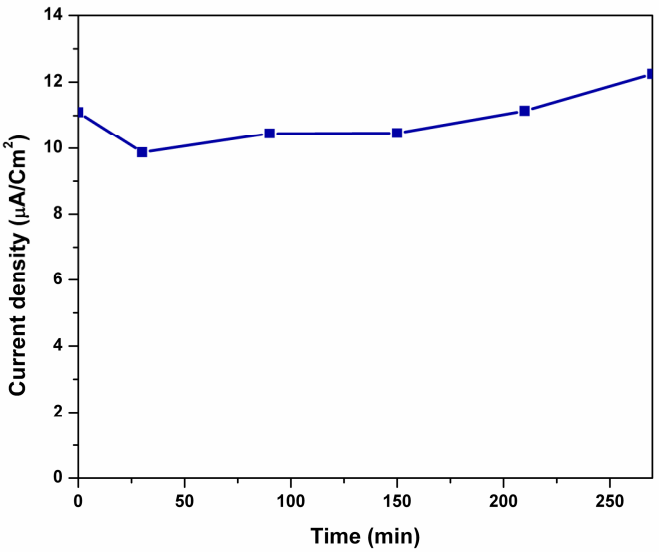

Figure 2.11. Photoelectrochemical response of an ITO/TEDT/PEDOT/PT/MV^{2+}/Pt cell upon continuous monochromatic irradiation at 505 nm. Experimental conditions: incident power 800 μW cm^{-2}, bias of -0.1 V vs Ag/AgCl, 5 mM MV^{2+} in air-saturated 0.1 M aqueous Na_2SO_4.

To demonstrate that the approach described herein leads to improved photovoltaic performance of the resulting thin-film materials, we fabricated a series of comparison devices using different techniques. The structure of devices **D1-D7** and their PV properties are summarized in Table 2.1. Because all of the devices were tested under the same experimental conditions, the relative differences in the photocurrent generation quantum yield (Φ) of the devices are significant and meaningful. Regardless of the fact that the values for the other important parameter, IPCE, depend on the optical absorption of the devices, this parameter can also be used to compare between them because all of the prepared devices had comparable absorption at the wavelength used for irradiation (Table 2.1).

Table 2.1. Structures and PV characteristics of polymer devices **D1-D7.**

Device	structure	Φ, %	IPCE, %	*A*, au	*I*, μA cm^{-2}
D1	ITO/TEDT [a] /PEDOT/PT	5.7 ± 0.6 (3.5 ± 0.3) [c]	2.4 ± 0.4 (1.4 ± 0.1) [c]	0.22	10.32
D2	ITO/PEDOT/PT	3.0 ± 0.8	1.5 ± 0.3	0.30	4.31
D3	ITO/TT [a] /PT	1.5 ± 0.3	0.5 ± 0.2	0.24	2.75
D4	ITO/PT	1.0 ± 0.6	0.4 ± 0.1	0.29	0.73
D5	ITO/TEDT [a] /PEDOT/P3HT	1.7 ± 0.3	0.9 ± 0.2	0.31	3.22
D6	ITO/TEDT [a] /P3HT[b]	0.59 ± 0.12	0.25 ± 0.04	0.25	0.51
D7	ITO/PEDOT/PSS/P3HT[b]	0.78 ± 0.15 (0.61 ± 0.12) [c]	0.35 ± 0.06 (0.35 ± 0.04) [c]	0.26	1.18

Φ - photocurrent generation quantum yield; IPCE - incident photon-to-current conversion efficiency; *A* - optical absorption at λ = 505 nm; *I* - photocurrent density. All measurements were performed in a three-electrode cell with an air-saturated 5 mM solution of MV^{2+} in 0.1 M Na_2SO_4(aq) as a supporting electrolyte with a Pt electrode and a Ag/AgCl reference electrode at an applied bias of -0.1 V using monochromatic irradiation λ_{max} 505 nm and optical power 800 μW cm^{-2}. (a) Surface-immobilized precursor monolayer. (b) The P3HT layer was deposited by spin casting from chlorobenzene solution. (c) Measured in deaerated, argon-saturated electrolyte solution.

Most importantly, device **D1** prepared following the described approach exhibited remarkably better PV performance relative to that of all the comparison devices. It showed an almost 2-fold increase in photocurrent generation efficiency and substantial improvements in other parameters when compared to those of device **D2** made by the same procedure as **D1** but using bare, unmodified ITO glass (ITO/PEDOT/PT). This clearly illustrates the role of the covalently surface-attached precursor TEDT, which likely improves the tightness of the ITO-polymer junction, as well as increases the uniformity of the layers as a result of the higher nucleation density during the electropolymerization originating from the surface-immobilized

precursor layer. Indeed, a simple side-by-side comparison of the surface morphology of **D1** and **D2** by AFM at different stages of device preparation reveals the substantially more uniform surface of the layers and reduced roughness in the case of **D1** (Figure 2.12). The higher surface uniformity may also be a reflection of the increased molecular order in the surface-initiated electropolymerized bulk layers giving rise to additional improvement in charge-transport characteristics. This is evidenced by a 2.5-fold increase in the measured photocurrent (*I*) in **D1** vs **D2** (Table 2.1) that can be attributed to the enhanced mobility of charge carriers in the former, which is related to the improved bulk layer molecular organization.[31, 32]

At the same time, the presence of the intermediate PEDOT sublayer proved to be necessary for achieving high efficiency, possibly through facilitating the hole injection and preventing the electron injection to ITO. Thus, device **D3** lacking a PEDOT sublayer was prepared by surface-initiated electropolymerization of dithiophene with terthiophene derivative TT as a surface-immobilized initiator (ITO/TT) and turned out to be significantly less efficient than **D1** (Table 2.1). This provided spectacular evidence of the unique role of the electropolymerized PEDOT sublayer for increasing the efficiency of polymer PV devices. The most dramatic difference was observed upon comparing **D1** with reference device **D7**. The device was prepared by spin-casting regioregular poly(3-hexylthiophene) (P3HT) from its solution in chlorobenzene on ITO. Spin casting is the most typically used method for fabricating organic polymer photovoltaics, including BHJ devices. Therefore, **D7** can serve as an excellent reference point for comparison with the devices prepared by more advanced approaches. When tested under the same conditions as for device **D1**, **D7** showed a 7 times lower current generation efficiency (photocurrent quantum yield 0.78 (0.15%) compared to that of **D1**. The partial addition of some of the features of device **D1** to the reference device resulted in consistent improvement of the poor PV performance of **D7**. As a general rule, using the layers obtained by in situ electropolymerization

instead of solution spin casting consistently improved performance, even if only one layer was prepared by electropolymerization (e.g., as in device **D5**, Table 2.1). Even the simplest device prepared by the electropolymerization of bithiophene on the surface of a bare ITO electrode (**D4**, Table 2.1) showed, in average, better PV characteristics than did reference device **D7**.

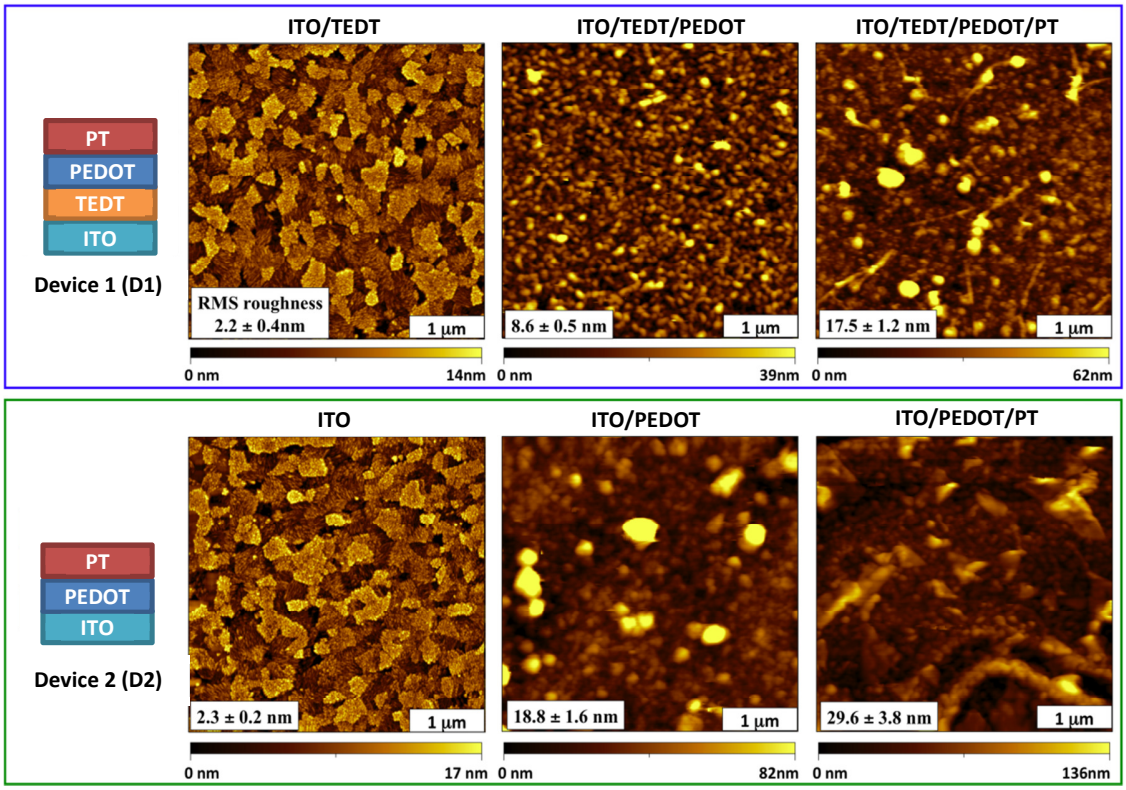

Figure 2.12. Comparison of the surface morphology of constituent layers of the TEDT-electropolymerized device **D1** *(top row)* and bare ITO electropolymerized device **D2** *(bottom row)*. The area of each AFM topograph is 4×4 µm.

One important point to be considered when comparing different devices using liquid electrolyte as the electron carrier is the morphology of the interface between the device surface and electrolyte. The less-uniform surfaces with higher roughness would provide more extended interfacial area, therefore facilitating charge injection. A similar effect is responsible for the high efficiency of dye-sensitized photoelectrochemical cells.[33, 34] If considering only this factor, one would expect the devices with higher surface roughness, such as those prepared by

electropolymerization without surface-immobilized initiator (e.g., devices **D2** and **D4**), to exhibit higher PV efficiency. Although there is no easy way to estimate the contribution of this effect, it does not seem to be able to overcome substantial enhancement in the devices due to surface-initiated electropolymerization. Overall, both electroactive **TEDT** and **TT** modification and *in situ* electropolymerization contribute significantly to the PV performance enhancement, with the better performance observed in the devices incorporating two polymer layers.

Another advantage of the PV thin-film materials prepared by the electropolymerization approach is that it allows to obtain pinhole-free films. The formation of pinholes is often difficult to avoid in conventional solution spin-casting methods, and this results in a high percentage of short-circuited PV devices after vacuum vapor deposition of metal electrodes. To check for current leakage due to the presence of pinholes, we carried out CV experiments using device **D1** as a working electrode and a 5 mM solution of hexyl viologen (HV^{2+}) in 0.1 M Bu_4NPF_6 in acetonitrile as an electrolyte. Using HV^{2+} instead of MV^{2+} was necessary because the latter proved to be insoluble in organic solvents used for electrochemical experiments. The sharp reversible redox peak of HV^{2+} appeared at -0.71 V (vs Ag/ Ag^{+}) with bare ITO employed as a working electrode (Figure 2.13). However, only a very subtle peak was visible in this region when **D1** was used instead of a bare ITO working electrode. This clearly indicated the pinhole-free nature of thin-film device **D1** and the overall robustness of the reported approach.

In addition to enhanced PV performance, devices prepared by surface-initiated electropolymerization possess greater mechanical stability than analogues prepared by conventional spin-casting methods because of the covalent interconnections between the layers. For example, **D1** could be ultrasonicated in CH_2Cl_2 for hours without destruction whereas the treatment of **D2** under the same conditions caused peeling of the polymer film in a few minutes and **D7** could not even be exposed to organic solvents.

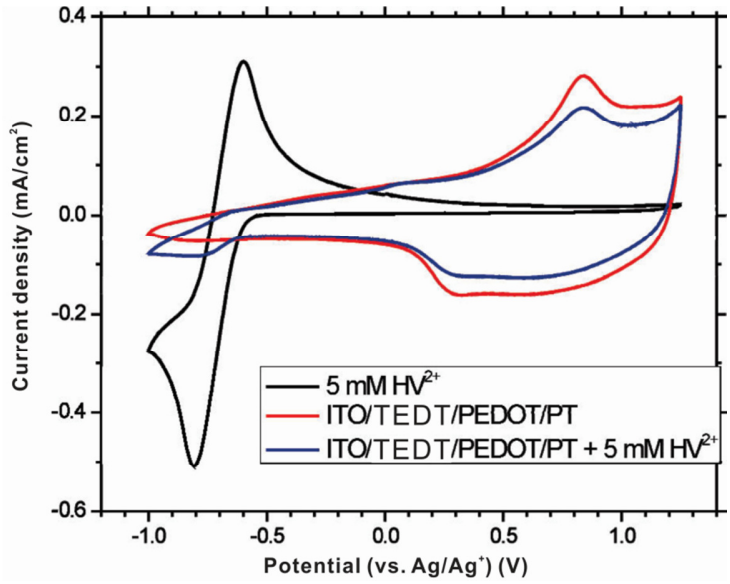

Figure 2.13. Cyclic voltammograms of a 5 mM solution of HV^{2+} and device **D1** in the absence and in the presence of HV^{2+}. Experimental conditions: 0.1 M Bu_4NPF_6 in CH_3CN, sweep rate 0.1 V s^{-1}.

2.4 Conclusions.

We demonstrated that thin-film multilayer organic polymer PV materials can be prepared by *in situ* electropolymerization on electrode surfaces modified with covalently attached electroactive monolayers. The devices prepared by this method showed superior PV performance relative to that of the control devices prepared by conventional spin-casting procedures. In the future, we will try to extend this method toward the preparation of complete solid-state organic PV devices as well as investigating the general scope of this method, the influence of various parameters on the device functioning, and the possibilities of further structural manipulations to improve performance.

2.5 References.

(1) Günes, S.; Neugebauer, H.; Sariciftci, N. S., Conjugated Polymer-Based Organic Solar Cells, *Chem. Rev.* **2007**, *107*, 1324-1338.

(2) Hirsch, A.; Brettreich, M. *Fullerenes: Chemistry and Reactions*; VCH, 2005.

(3) Tang, C. W., 2-layer organic photovoltaic cell, *Appl. Phys. Lett* **1986**, *48*, 183-185.

(4) Hoppe, H.; Sariciftci, N. S., Organic solar cells: An overview, *J. Mater. Res.* **2004**, *19*, 1924-1945.

(5) Yu, G.; Gao, J.; Hummelen, J. C.; Wudl, F.; Heeger, A. J., Polymer photovoltaic cells: enhanced efficiencies via a network of internal donor-acceptor heterojunctions, *Science* **1995**, *270*, 1789-1791.

(6) Kim, J. Y.; Lee, K.; Coates, N. E.; Moses, D.; Nguyen, T.-Q.; Dante, M.; Heeger, A. J., Efficient Tandem Polymer Solar Cells Fabricated by All-Solution Processing, *Science* **2007**, *317*, 222-225.

(7) Taranekar, P.; Qiao, Q.; Jiang, H.; Ghiviriga, I.; Schanze, K. S.; Reynolds, J. R., Hyperbranched Conjugated Polyelectrolyte Bilayers for Solar-Cell Applications, *J. Am. Chem. Soc.* **2007**, *129*, 8958-8959.

(8) Wong, W.-Y.; Wang, X.-Z.; He, Z.; Djurisic, A. B.; Yip, C.-T.; Cheung, K.-Y.; Wang, H.; Mak, C. S. K.; Chan, W.-K., Metallated conjugated polymers as a new avenue towards high-efficiency polymer solar cells, *Nat. Mater.* **2007**, *6*, 521-527.

(9) Peet, J.; Kim, J. Y.; Coates, N. E.; Ma, W. L.; Moses, D.; Heeger, A. J.; Bazan, G. C., Efficiency enhancement in low-bandgap polymer solar cells by processing with alkane dithiols, *Nat. Mater.* **2007**, *6*, 497-500.

(10) Schmidt-Mende, L.; Fechtenkötter, A.; Müllen, K.; Moons, E.; Friend, R. H.; MacKenzie, J. D., Self-Organized Discotic Liquid Crystals for High-Efficiency Organic Photovoltaics, *Science* **2001**, *293*, 1119-1122.

(11) Brabec, C. J.; Winder, C.; Scharber, M. C.; Sariciftci, N. S.; Hummelen, J. C.; Svensson, M.; Andersson, M. R., Influence of disorder on the photoinduced excitations in phenyl substituted polythiophenes, *J. Chem. Phys.* **2001**, *115*, 7235-7244.

(12) Nelson, J., Organic photovoltaic films, *Curr. Opin. Solid State Mater. Sci.* **2002**, *6*, 87-95.

(13) Berson, S.; De Bettignies, R.; Bailly, S.; Guillerez, S., Poly(3-hexylthiophene) Fibers for Photovoltaic Applications, *Adv. Funct. Mater.* **2007**, *17*, 1377-1384.

(14) Kim, Y.; Cook, S.; Tuladhar, S. M.; Choulis, S. A.; Nelson, J.; Durrant, J. R.; Bradley, D. D. C.; Giles, M.; McCulloch, I.; Ha, C.-S.; Ree, M., A strong regioregularity effect in self-organizing conjugated polymer films and high-efficiency polythiophene:fullerene solar cells, *Nat. Mater.* **2006**, *5*, 197-203.

(15) Mingirulli, N.; Biro, D.; Preu, R.; Glunz, S. W.; Riepe, S., Method for determination of recombination activity of cylindric conduction channels for back-contacted solar cells, *Appl. Phys. Lett.* **2007**, *91*, 183512-3.

(16) Meng, H.; Perepichka, D. F.; Wudl, F., Facile Solid-State Synthesis of Highly Conducting Poly(ethylenedioxythiophene), *Angew. Chem., Int. Ed.* **2003**, *42*, 658-661.

(17) Hulvat, J. F.; Stupp, S. I., Liquid-Crystal Templating of Conducting Polymers, *Angew. Chem., Int. Ed.* **2003**, *42*, 778-781.

(18) Otsubo, T.; Aso, Y.; Takimiya, K., Functional oligothiophenes as advanced molecular electronic materials, *J. Mater. Chem.* **2002**, *12*, 2565-2575.

(19) Xia, C.; Advincula, R. C., Surface Grafting of Conjugated Polymers onto Self-assembled Monolayer Modified Conducting Substrates by Electrochemistry, *Chem. Mater.* **2001**, *13*, 1682-1691.

(20) Zotti, G.; Zecchin, S.; Vercelli, B.; Berlin, A.; Grimoldi, S.; Groenendaal, L.; Bertoncello, R.; Natali, M., Surface-initiated polymerization of thiophene and pyrrole monomers on poly(terthiophene) films and oligothiophene monolayers, *Chem. Mater.* **2005**, *17*, 3681-3694.

(21) Kang, J. F.; Perry, J. D.; Tian, P.; Kilbey, S. M., Growth and morphology of polythiophene on thiophene-capped monolayers: 1. Single component monolayers, *Langmuir* **2002**, *18*, 10196-10201.

(22) Vercelli, B.; Zotti, G.; Berlin, A., Star-shaped and linear terthiophene-thiol self-assembled monolayers as scaffolds for gold nanoparticles, *Chem. Mater.* **2007**, *19*, 443-452.

(23) Berlin, A.; Zotti, G.; Schiavon, G.; Zecchin, S., Adsorption of carboxyl-terminated dithiophene and terthiophene molecules on ITO electrodes and their electrochemical coupling to polymer layers. The influence of molecular geometry, *J. Am. Chem. Soc.* **1998**, *120*, 13453-13460.

(24) Gregory A. Sotzing, J. R. R. P. J. S., Poly(3,4-ethylenedioxythiophene) (PEDOT) prepared via electrochemical polymerization of EDOT, 2,2?-Bis(3,4-ethylenedioxythiophene) (BiEDOT), and their TMS derivatives, *Adv. Mater.* **1997**, *9*, 795-798.

(25) Chernyshev, E. A.; Belyakova, Z. V.; Knyazev, S. P.; Turkel'taub, G. N.; Parshina, E. V.; Serova, I. V.; Storozhenko, P. A., Hydrosilylation of ethylene, *Russ. J. Gen. Chem.* **2006**, *76*, 225-228.

(26) Imahori, H.; Kimura, M.; Hosomizu, K.; Sato, T.; Ahn, T. K.; Kim, S. K.; Kim, D.; Nishimura, Y.; Yamazaki, I.; Araki, Y.; Ito, O.; Fukuzumi, S., Vectorial electron relay at ITO electrodes modified with self-assembled monolayers of ferrocene-porphyrin-fullerene triads and porphyrin-fullerene dyads for molecular photovoltaic devices, *Chem.--Eur. J* **2004**, *10*, 5111-5122.

(27) Xu, S.; Liu, G. Y., Nanometer-scale fabrication by simultaneous nanoshaving and molecular self-assembly, *Langmuir* **1997**, *13*, 127-129.

(28) Liu, G. Y.; Xu, S.; Qian, Y. L., Nanofabrication of self-assembled monolayers using scanning probe lithography, *Acc. Chem. Res.* **2000**, *33*, 457-466.

(29) Hou, J. H.; Tan, Z. A.; Yan, Y.; He, Y. J.; Yang, C. H.; Li, Y. F., Synthesis and photovoltaic properties of two-dimensional conjugated polythiophenes with bi(thienylenevinylene) side chains, *J. Am. Chem. Soc.* **2006**, *128*, 4911-4916.

(30) Yamada, H.; Imahori, H.; Nishimura, Y.; Yamazaki, I.; Ahn, T. K.; Kim, S. K.; Kim, D.; Fukuzumi, S., Photovoltaic properties of self-assembled monolayers of porphyrins and porphyrin-fullerene dyads on ITO and gold surfaces, *J. Am. Chem. Soc.* **2003**, *125*, 9129-9139.

(31) Savenije, T. J.; Kroeze, J. E.; Yang, X. N.; Loos, J., The effect of thermal treatment on the morphology and charge carrier dynamics in a polythiophene-fullerene bulk heterojunction, *Adv. Funct. Mater.* **2005**, *15*, 1260-1266.

(32) van Duren, J. K. J.; Yang, X.; Loos, J.; Bulle-Lieuwma, C. W. T.; Sieval, A. B.; Hummelen, J. C.; Janssen, R. A. J., Relating the Morphology of Poly(p-phenylene vinylene)/Methanofullerene Blends to Solar-Cell Performance, *Adv. Funct. Mater.* **2004**, *14*, 425-434.

(33) Hagfeldt, A.; Grätzel, M., Molecular Photovoltaics, *Acc. Chem. Res.* **2000**, *33*, 269-277.

(34) Law, M.; Greene, L. E.; Johnson, J. C.; Saykally, R.; Yang, P., Nanowire dye-sensitized solar cells, *Nat. Mater.* **2005**, *4*, 455-459.

CHAPTER 3 SURFACE-IMMOBILIZED NANOSTRUCTURED CONJUGATED POLYMER THIN FILM PREPARED BY LIVING CHAIN-GROWTH CHEMICAL POLYMERIZATION.

3.1 Introduction.

Conjugated polymer (CP) thin films are core materials in organic electronics, as well as in sensory devices.[1, 2] Convenient solution processing via conventional spin-casting allows preparation of organic semiconducting thin films in a short production time. To enable spin-casting processing, functionalization of CP with bulk solubilizing side groups is required for processibility (such as hexyl groups in P3HT) to overcome poor solubility of unsubstituted CPs. On the other hand, it can diminish the resulting device performance by decreasing carrier mobility caused by disturbed close packing of CPs and disrupted molecular organization.[3-5] Thus, it would be beneficial to develop an alternative thin film fabrication method to improve this situation. Among many possibilities, surface-initiated *in situ* polymerization would be a promising pathway to build dense thin films of organic CPs without solubilizing groups via *in situ* polymerization of small-molecule monomers.[6] Such immobilized CP thin films are expected to have enhanced charge carrier mobilities because of improved intermolecular and intramolecular charge transport. Another major advantage of such thin films would be their exceptional mechanical and chemical stability. Despite remarkable recent developments in "grafting from" method for conventional polymers (such as ring-opening polymerization, anionic polymerization, as well as free radical polymerization),[7, 8] thin films of conjugated polymers were rarely prepared through *in situ* process[9] and, of the known examples, surface-initiated electropolymerization is one of the most powerful and popular pathways.[10, 11] As described in the previous chapter, we have also developed an approach to PEDOT-PT block copolymer brushes immobilized on ITO surface through surface-initiated electropolymerization. The resultant thin

films demonstrated improved performance when used as donor layers in PV.[12] However, poor surface morphologies, limitation for mass production, limited number of potential electrochemically active monomers and possibility of side reactions (electrochemical coupling of surface-immobilized precursors reducing polymer brushes density), as well as complicated and poorly reproducible reaction conditions would be obvious bottlenecks of this method. Thus, the necessity of chemical *in situ* preparation becomes clear and metal-catalyzed chemical polymerization, with a broad variety of different methodologies available, looks a very promising candidate to yield densely packed surface immobilized CP films under simple and reproducible reaction conditions.

Polythiophene (**PT**) and its derivatives are among the most important organic electronic materials due to high charge transport efficiency, as well as thermal stability and photostability. One of the most widely used PT derivatives is P3HT, a semicrystalline polymer when it is in its highly regioregular form.[13] Depending on regioregularity, charge carrier mobility of spin-coated thin films can be affected by molecular orderness in the thin film. For example, 96% regioregular P3HT exhibited mobility of 1.1 x 10^{-3} cm^2 V^{-1} s^{-1} but 86% regioregular P3HT showed only 6.4 x 10^{-4} cm^2 V^{-1} s^{-1}. Furthermore, highly regioregular P3HT demonstrated higher absorption maximum wavelength, λ_{max}, at 556nm, as compared to less regioregular P3HT.[13] Therefore, for application in organic electronics, high regioregularity of P3HT would be one of the major factors to obtain optimal device performance. Among synthetic methodologies towards such polymers, metal-catalyst transfer Kumada polycondensation which is well-established due to the efforts by Yokozawa and McCullough would be the most powerful synthetic pathway promising a highly regioregular P3HT in a chain-growth manner [14, 15] (Scheme 3.1).

As a first step of Kumada polycondensation, coupling reaction between Ni(II) catalyst, typically Ni(dppp)Cl_2 (dppp: 1,3-bis(diphenylphosphino)propane), and 2 equivalents of Grignard

thiophene monomer forms Ni(II) complex **A** in Scheme 3.1. Next, intramolecular Ni catalyst transfer occurrs to form complex **B** (Ni catalyst is inserted into Carbon-halide bond). Complex **D** with one additional repeating unit is obtained by another coupling reaction with a Grignard monomer followed by intramolecular Ni catalyst transfer. By repetition of above processes, highly regioregular P3HT is produced in a chain growth manner.

Scheme 3.1. Chain-growth polycondensation of poly(3-alkylthiophene)s (from ref. 14).

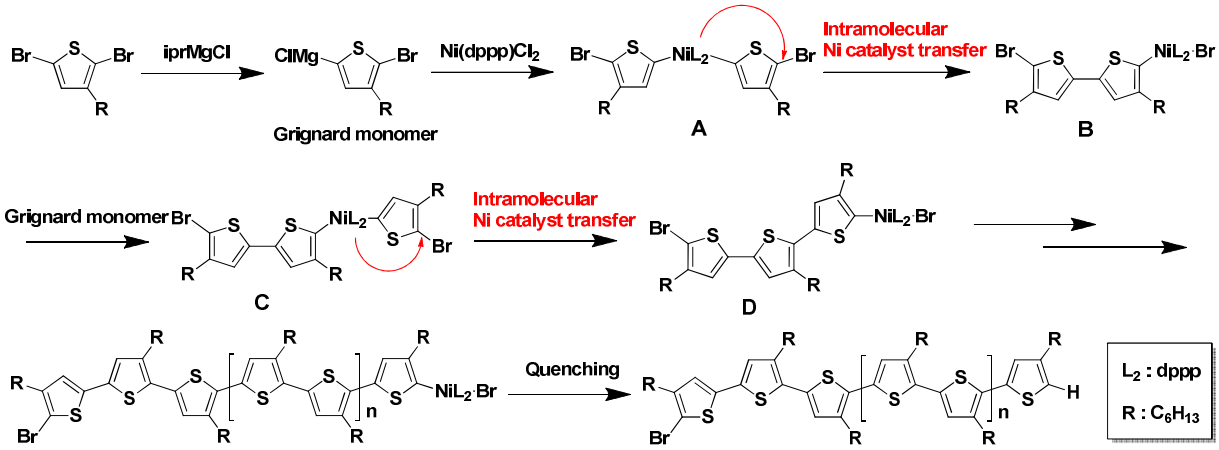

In 2007, Kiriy et al. developed an externally initiated Kumada-type catalyst-transfer polymerization and opened the possibility for surface-initiated *in situ* polymerization via chemical reactions. As a key step in this strategy, surface-immobilized external macroinitiator was formed by oxidative addition of $Ni(PPh_3)_4$ to surface-adhered crosslinked poly(4-bromostyrene) (**PS-Br**) layer on solid substrate.[16] The subsequent Ni-catalyst transfer Kumada polycondensation originating from the macroinitiator resulted in a surface-tethered P3HT obtained in a chain growth manner.

Although this groundbreaking discovery could be seen as a promising tool for CP thin film manufacturing, only very thin P3HT film (5nm thickness starting from 1.7 nm thick PS-Br layer) was obtained, most likely due to two possible reasons.[17] Based on the reported slow rate of

oxidative addition of Ni catalysts,[18] the first factor could be an insufficient reactivity in oxidative addition of $Ni(PPh_3)_4$ to surface-immobilized PS-Br precursor layer. Furthermore, it was also predicted that the poor reactivity resulted in low polymer brush density in the final thin film. Indeed, more reactive $Ni(COD)(PPh_3)_2$ (where COD is cyclooctadiene) prepared *in situ* from surface-immobilized $Ni(COD)_2$-based precursor by ligand exchange gave 14 nm thick surface-bound PT on top of gold-coated glass surface while less reactive $Ni(PPh_3)_4$ did not.[19] Even if the macroinitiator was formed efficiently, the stability of the Ni(II) catalyst would be another key factor in determining the quality of the thin film. Due to low bond energy between Ni catalyst coordinated with monodentate ligands and ethylene group,[20] surface-bound Ni(II) center could transfer to the monomer in solution therefore resulting in early premature chain termination. Thus, the more stable bidentate Ni catalyst which has higher bond energy would produce thicker, higher molecular weight PT in the surface-attached film. Based on this consideration, Kiriy et al. reported surface-initiated polymerization with Ni(II) catalytic center bearing bidentate dppp ligand (prepared by ligand exchange) and successfully grafted high molecular weight P3HT brushes on the surface of Si particles.[21] Thus, it is obvious that structure of Ni catalyst determines the quality of PT thin films made through surface-initiated Kumada polycondensation. Recently, it was discovered in our group (Jinwoo Choi) that oxidative addition of Ni(0) complex $Ni(dppp)_2$ to 2-bromobithiophene produces an extremely efficient external catalytic initiator of living step-growth Kumada polycondensation. In the case of 5-bromo-4-hexyl-2-thienylmagnesium chloride, the polymerization in ambient conditions gave 100% regioregular P3HT with Mn > 50,000 g mol^{-1} and low polydispersity in very short reaction times. Furthermore, using $Ni(dppp)_2$ enabled a simple one step procedure (mixing of aryl halide and $Ni(dppp)_2$) to produce a stable bidentate Ni(II) external initiator. Here, we describe our research

efforts toward a densely packed and thick surface-immobilized PT thin film based on using this novel catalytic system.

To improve organic electronic device performance, it would be essential to build controlled nanostructured thin film architectures presenting a well-defined donor-acceptor interface.[22-24] Although the concept of bulk-heterojunction OPV devices offers a practical solution,[25] a ny deviations from actual BHJ structure prepared through conventional spin-coating interfere with achieving the optimal performance of the PV devices. Moreover, there is a well-recognized dilemma that high crystallinity of CP (which promises high carrier mobility) also leads to donor-acceptor segregated domains of few hundred micrometer size which reduce device performance.[13] Consequently, a conceptual paradigm shift is required to achieve fabrication of nanopatterned CP thin films. This would enable building physically separated nanoscale donor-acceptor interfaces by combination of nanolithography and selective surface-initiated *in situ* polymerization using electropolymerization, or metal-catalyst transfer surface-initiated polycondensation.[26, 27] Simultaneous presence of high crystallinity and controlled nanoscale donor-acceptor phase separation would be the major of the expected advantages of this novel strategy. In this manner, we used a combination of latex nanoparticle-lithography technique[28] with our modified surface-initiated chemical polymerization. This work was performed in close collaboration with Prof. Jayne C. Garno group, and is described in this chapter.

3.2 Experimental Details.

3.2.1 Synthesis of Precursors.

Precursor **3-1** (or **3-2)** was synthesized by the substitution reaction of chlorotriethoxysilane with the Grignard reagent, prepared by treatment of 2,5-diiodothiophene (or 1,4-diiodobenzene) with iPrMgCl. After iodination of **2-B4**, terminal alkene group of compound **3-3A** was

functionalized through hydrosilation with Karstedt's catalyst to afford precursor **3-3**. Further details are given in Chapter 5.

Scheme 3.2. Synthesis of Precursors.

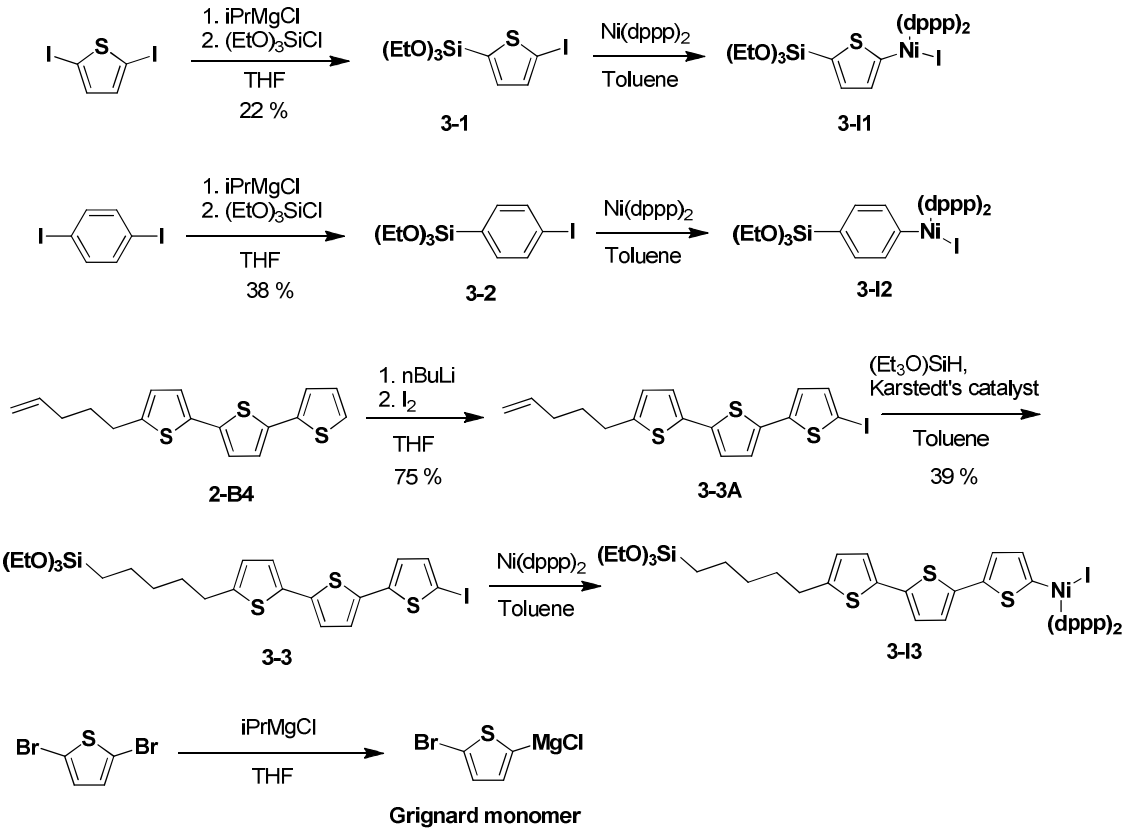

3.2.2 Surface-initiated *in situ* Polymerization.

Freshly cleaned rectangular quartz substrates were immersed into precursor solution in toluene for 3 days to tether precursor **3-1**, **3-2**, or **3-3** to quartz surface. Subsequent *in situ* activation was accomplished by immersing surface-immobilized precursor monolayer into $Ni(dppp)_2$ solution in toluene for 2 days. In an alternative procedure, solution-prepared initiator **3-I1** was synthesized through oxidative addition of $Ni(dppp)_2$ to precursor **3-1**. Subsequent surface-immobilization was performed to obtain surface-bound initiator monolayer. Surface-bound PT thin films were deposited through repeated *in situ* Kumada polycondensation followed

by intermediate regeneration of active Ni(II) catalytic center. Further details are provided in the Chapter 5.

3.2.3 Preparation of Nanoscale Patterned PT Thin Film.

Scheme 3.3. Preparation of surface-immobilized nano-patterned PT.

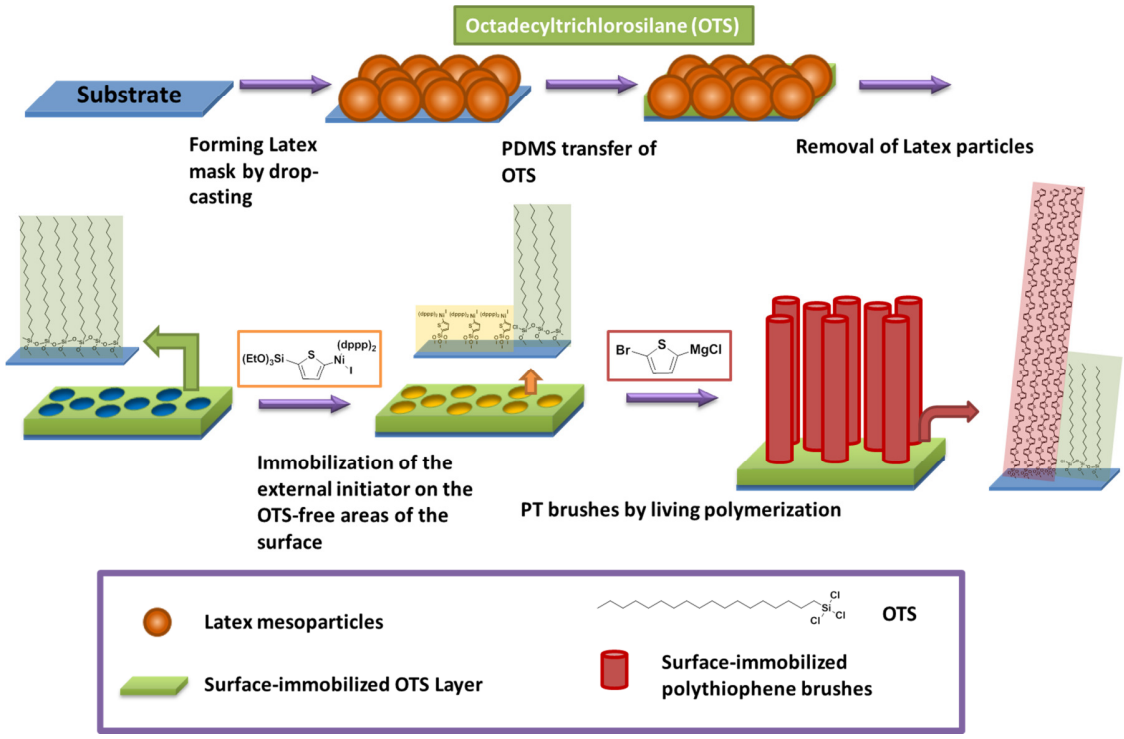

Fabrication of nanopatterned PT thin films begins with forming a latex mask by drop-casting from aqueous suspension on Si(111). Subsequent PDMS transfer of OTS yielded a surface-tethered OTS mask. Nanopatterned columnar PT thin film was fabricated through immobilization of solution-prepared initiator **3-I1** to OTS-uncovered areas on Si(111) followed by surface-initiated Kumada polycondesation with intermediate regeneration of catalytic center.

3.3 Results and Discussion.

3.3.1 Surface-immobilized Precursor.

Based on the mechanism of surface-initiated *in situ* polymerization, the surface coverage of the catalytic external initiator initially determines the polymer brush density. Initiators were

typically prepared through oxidative addition of Ni(0) catalyst to surface-bound aryl halide (i.e. compounds **3-1**, **3-2**, or **3-3**), thus there would be at least 2 factors controlling the quality of surface-immobilized initiators. First, the precursor has to be efficiently immobilized on solid surface. When polymer thin films were prepared through the "grafting to" method, low polymer brush density was often caused by insufficient reaction between polymer and surface (since surface-immobilized polymers interfere with polymer molecules approaching the surface).[7] To increase the polymer film surface density, we directly attached the anchoring triethoxysilyl group to the aromatic core of precursor molecules without any long alkyl chain (Scheme 3-2). To elucidate the effect of the alkyl group, we also synthesized a long alkyl chain attached precursor **3-3**, starting from the previously prepared compound **2-B4**. Absence of a long alkyl chain was expected to be advantageous when the thin films are used in organic electronics. Owing to the insulating nature of saturated hydrocarbon chain, a separating alkyl chain may act as an added series resistor and diminish the charge carrier transport to the electrode as a result. In this sense, precursors **3-1** and **3-2** could transfer charge carriers to the electrode more efficiently.

As an initial step, polythiophene (**PT**) thin films were grafted from surface-bound **3-1**, **3-2**, and **3-3** on quartz slides through activation of the slides with $Ni(dppp)_2$ followed by surface-initiated Kumada polycondensation with the Grignard monomer, (5-bromothiophen-2-yl)magnesium chloride. In this approach, the active external catalytic initiators **3-I1**, **3-I2**, and **3-I3** were prepared *in situ* by the reaction of surface-bound aryl halides **3-1** – **3-3** with $Ni(dppp)_2$. In the UV-Vis absorption spectra, **3-3** exhibited a notably lower optical density than other two samples. This was likely the result of low precursor density originating from the hindered approach of the precursor to the substrate (Figure 3.1).

Based on the slightly more intense absorption of the PT thin film grafted from **3-1**, we assumed that less dense PTs polymerized from surface-immobilized **3-2** might result from less

efficient oxidative addition in the latter case. To start polymerization, initiators have to undergo oxidative addition with a Grignard monomer. Since oxidative addition of Ni catalyst becomes more efficient in the presence of an electron donating group,[18] a more electron rich molecule, thiophene, might start surface-initiated *in situ* polymerization easier and more uniformly while the precursor **3-2** would start polymerization at randomly scattered sites. Thus, sample **3-2** would suffer hindered approach of Grignard monomer to the surface by early grown PT or oligothiophenes. To minimize experimental uncertainty, we repeated the same experiment several times and, in all cases, slightly higher optical density was obtained with initiators derived from **3-1**.

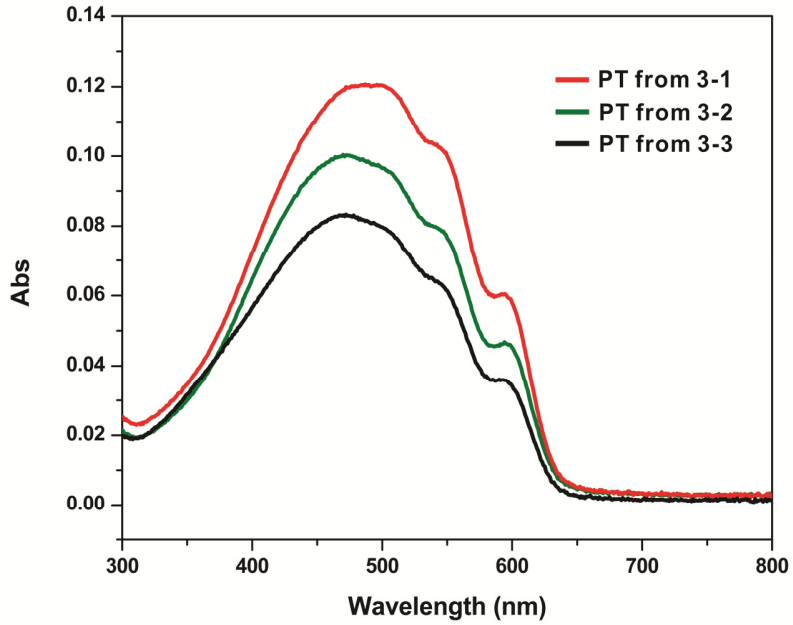

Figure 3.1. UV-Vis absorption spectra of surface-immobilized PT prepared by *in situ* surface activation and polymerization for 15 h.

Another factor determining surface-coverage with an active initiator would be the efficiency of activation reaction. Poor efficiency of a heterogeneous reaction as well as steric hindrance between relatively bulky dppp ligands on the surface-bound initiator and the approaching catalyst molecule would diminish the conversion ratio of surface-immobilized aryl halides **3-1** –

3-3 to initiators **3-I1** – **3-I3**. To prove this hypothesis, a surface-immobilized initiator **3-I1** was generated by immobilization of the precursor **3-1** on a quartz surface followed by activation with $Ni(dppp)_2$. I3d bands in X-ray photoelectron spectroscopy (**XPS**) experiments were then observed (Figure 3.2). From XPS measurements, two different Iodine species were found to be present on the surface. Based on the fact that higher binding energy is observed when an atom is surrounded by electron-withdrawing groups, Iodine bound to a more electronegative carbon has a more electron-deficient nature and showed higher binding energy than anionic iodine attached to Ni(II). Therefore, two pairs of $I3d_{5/2}$ and $I3d_{3/2}$ iodine peaks of the surface-immobilized initiator would be strong evidence suggesting incomplete activation.

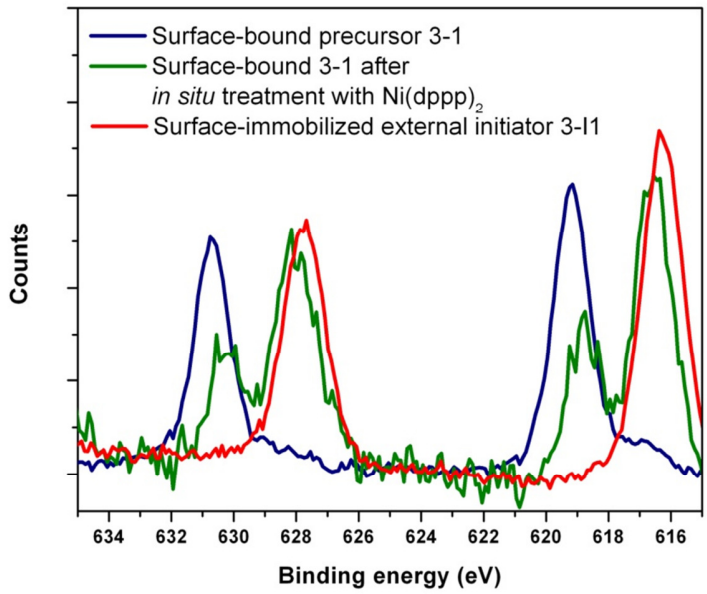

Figure 3.2. I3d X-ray photoelectron spectra of the activated initiators immobilized on the quartz surface.

To improve the catalytic initiator density, we developed a modified procedure. In the first step, external initiator was synthesized in solution by reacting **3-1** with $Ni(dppp)_2$. Complete conversion to **3-I1** was observed with 2 equivalents of $Ni(dppp)_2$ as determined by ^{31}P NMR. To avoid experimental errors due to high reactivity of triethoxysilyl groups, 2-iodothiophene

without the anchoring group was used to figure out optimal reaction conditions by ^{31}P NMR spectroscopy. If 2-iodothiophene is completely converted to the Ni(II) catalytic initiator with 2 equivalents of $Ni(dppp)_2$, the integration ratio of P signals from dppp on initiator and dppp on $Ni(dppp)_2$ should be 1:4. ^{31}P NMR of the reaction mixture exhibited the ratio of 0.7 : 4 after heating at 40 °C for 2 days. Considering an experimental error due to small amount of 2-iodothiophene in the reaction mixture, the agreement between expected and experimentally observed data was reasonable. By immersing a quartz substrate into a solution of **3-I1**, surface-immobilized layer of catalytic initiator was obtained. I3d XPS spectra revealed that only two peaks were observed at 616 and 628 eV corresponding to $I3d_{5/2}$ and $I3d_{3/2}$ transitions and indicated that no unreacted precursor **3-1** was present in the initiating monolayer. Because I3d XPS measurements could only provide qualitative information on the composition of the surface-immobilized initiator, it was necessary to obtain more quantitative information of immobilized initiators for each sample. To estimate surface coverage of the *in situ* generated external catalytic initiator and solution-prepared **3-I1** immobilized on surface, 2,2'-bithiophene thin films on ITO (which has lower oxidation potential relative to thiophene) were prepared through Kumada coupling reaction between the initiator monolayer and thiophen-2-ylmagnesium chloride (Figure 3.3). Subsequent cyclic voltammetry (CV) studies indicated that the surface density of solution prepared initiators was 50 $Å^2$ per one molecule whereas it was 60 $Å^2$ per one molecule for *in situ* initiators.[29] Based on I3d XPS data, ~30 % of unreacted 2-iodothiophene also existed in *in situ* prepared initiator layer. Therefore, CV of bithiophene formed from this initiator would reflect presence of both unreacted 2-iodothiophene and bithiophene. In such a case, the actual difference in surface-coverage of the two samples could be even bigger than the obtained estimate of 10 $Å^2$. Therefore, a higher surface density of the initiator can be accomplished by our modified method, involving surface-immobilization of solution-prepared catalytic initiator **3-I1**.

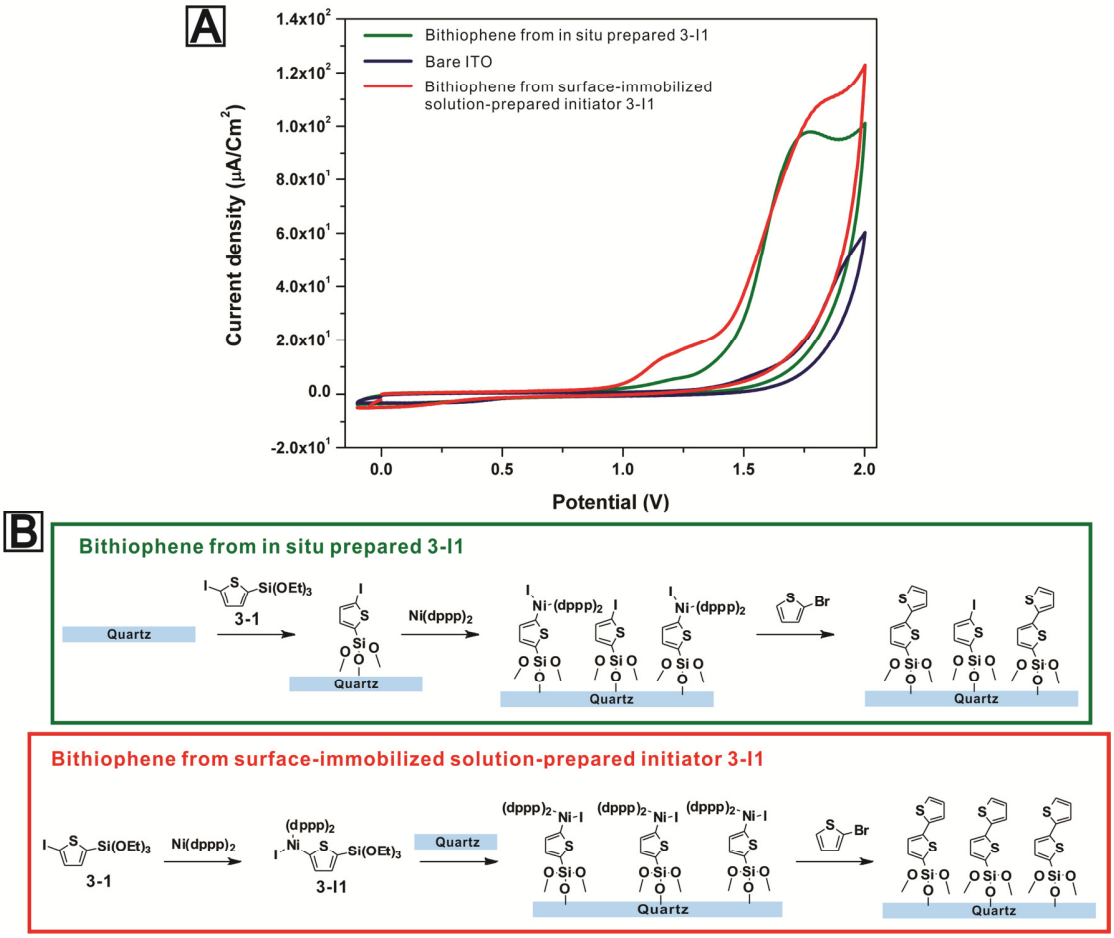

Figure 3.3. (A) Cyclic voltammetry of ITO surface-immobilized bithiophene from *in situ* prepared initiator (green trace) and surface-bound solution prepared **3-I1** (red trace). (B) Preparation of surface-immobilized bithiophene monolayer.

3.3.2 Surface-initiated *in situ* Polymerization via Regeneration of Ni Catalytic Center.

When we started our experiments, it was expected that Ni(II) active catalytic complex with bidentate ligand (dppp) would not suffer intermolecular catalyst transfer. However, during polymerization from surface-immobilized catalytic initiators, we also observed formation of insoluble PT in the Grignard monomer solution which was likely caused by Ni(II) catalyst transfer to monomer.[19] Whereas such intermolecular Ni(II) catalyst transfer prematurely terminates surface polymerization, it also generates a bromide terminus on the surface-bound polymer chain resulting from simple Kumada coupling reaction with (5-bromothiophen-2-

yl)magnesium chloride. In other words, a new surface-immobilized aryl halide precursor is generated as a result of Ni(II) catalyst transfer to the solution.

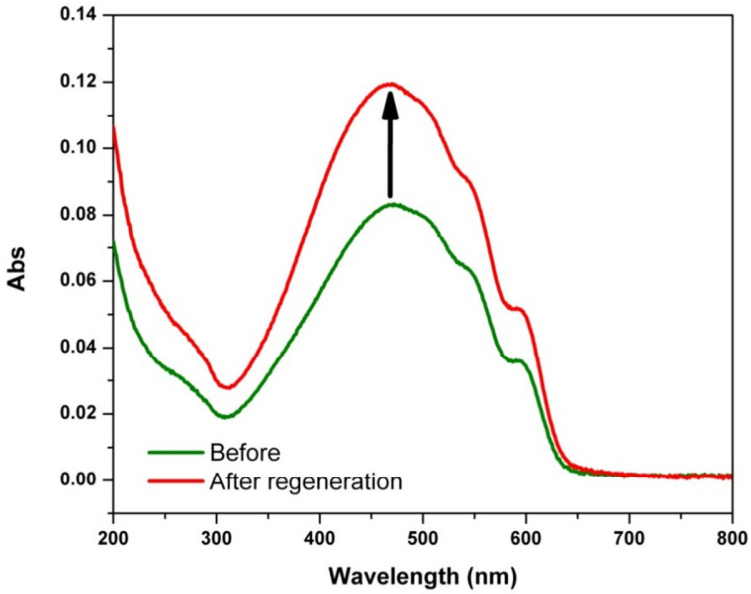

Figure 3.4. UV-Vis absorption spectra of surface-immobilized PT before active catalytist regeneration (green trace) and after regeneration followed by surface initiated polymerization.

With this information, the "regeneration of Ni catalytic center" method was designed to reinitiate a prematurely terminated polymerization. For this purpose, oxidative addition of $Ni(dppp)_2$ to prematurely generated 2-bromothiophene terminus was carried out by immersing the PT films into a $Ni(dppp)_2$ solution. In an initial test, we exposed a PT thin film previously prepared through polymerization initiated by the precursor **3-3**, to a 5mM $Ni(dppp)_2$ solution in toluene. Subsequent exposure of this slide to (5-bromothiophen-2-yl)magnesium chloride solution resulted in the enhancement in optical density from 0.08 to 0.12 (Figure 3.4). This result indicated that even a completely quenched PT thin film can be used to reinitiate polymerization again, if a reasonable number of bromothiophene termini was generated by previous premature termination. As a result, voids in PT thin film induced by the premature termination could be

filled with newly polymerized PT and optical density of the thin film (which correlates with density of PT) was increased.

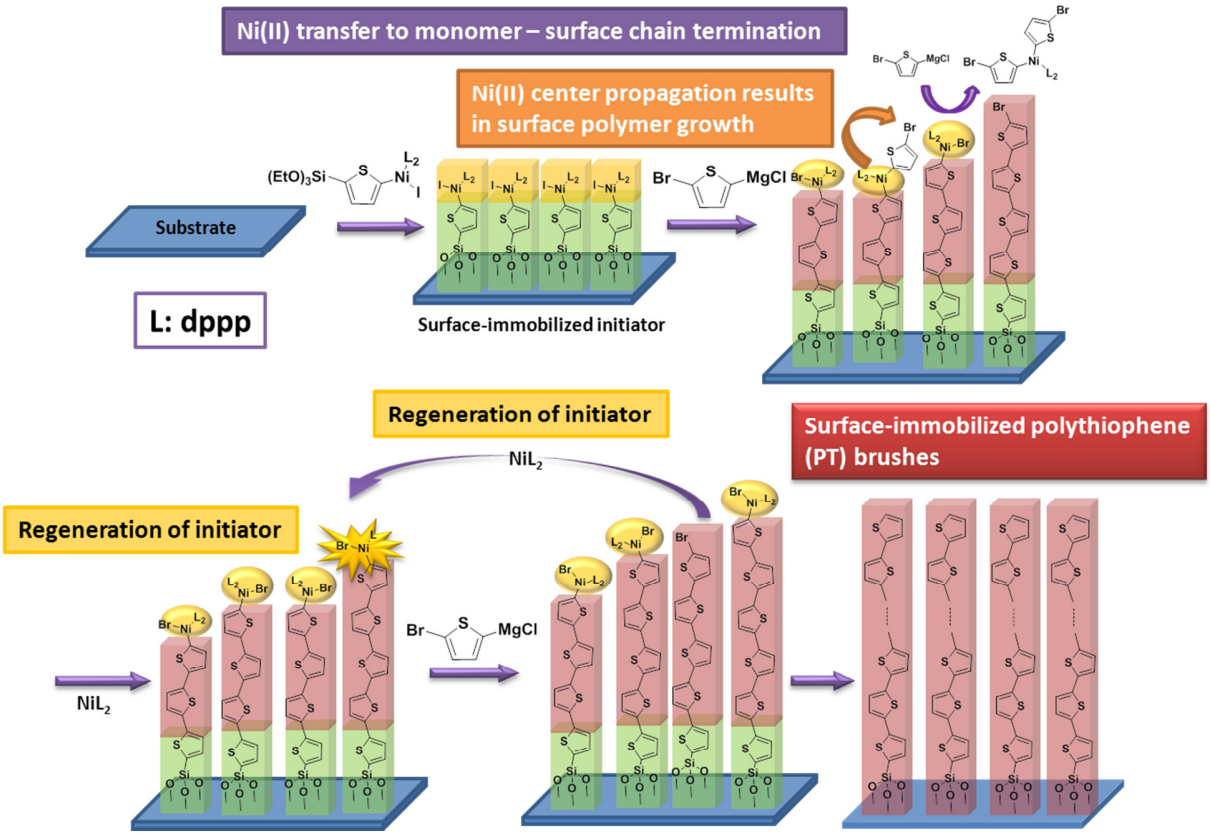

Figure 3.5. Surface-initiated *in situ* polymerization from monolayer of solution-prepared initiator with intermediate regeneration of Ni(II) catalytic center.

Based on our efforts toward the formation of densely packed thick PT brushes, we found that the best result could be achieved by the combination of surface-immobilization of solution – prepared catalytic initiator and the intermediate regeneration of the Ni(II) catalytic center (Figure 3.5). To further optimize this protocol, we prepared three surface-immobilized PT thin films initiated by monolayer of solution prepared catalytic initiator **3-I1** using 1, 2, and 3-day polymerization time followed by intermediate regeneration of the active catalytic center. After many trials with different regeneration and polymerization times, it was found that surface-initiated polymerization for 16 h followed by regeneration of the catalytic surface for 8h gave the

best result. The gradual enhancement of optical density in UV-Vis spectra over increased reaction time indicated that repeated polymerization and regeneration do enhance the thickness and density of the surface-immobilized PT films (Figure 3.6).

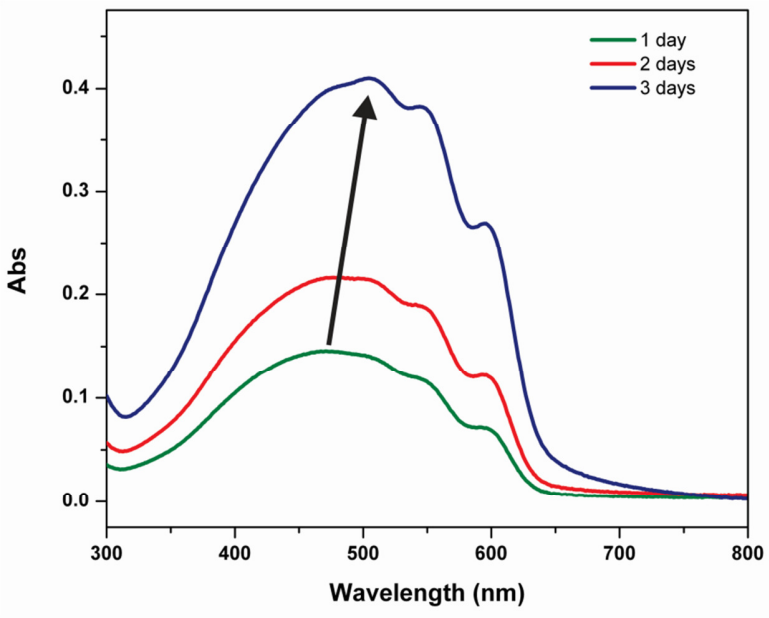

Figure 3.6. UV-Vis absorption spectra of surface-immobilized polythiophene films prepared with intermediate regeneration of the initiator after polymerization for 1 day (green trace), 2 days (red trace), and 3 days (blue trace).

Comparison of UV-Vis absorption spectra of samples with and without Ni catalytic center regeneration was a critical experiment to evaluate the effectiveness of our strategy. In the same manner, we compared absorption spectra of 3 samples prepared via different experimental conditions: polymerization with regeneration (condition 1) or without regeneration (condition 2) from a monolayer of solution-prepared initiator, and conventional process: polymerization without regeneration from *in situ* activated initiator monolayer (condition 3) (Figure 3.7).

After 3 day polymerization under mentioned conditions, λ_{max} of a PT thin film obtained under condition 3 was observed at 470 nm contrasting with λ_{max} 505 nm observed in PT thin films obtained under conditions 1 and 2. Bathochromic shift from the sample obtained with

regeneration (condition 1 and 2) can be rationalized by two reasons. The first possible explanation is that intermolecular Ni(II) catalyst transfer mainly produces surface-immobilized low molecular weight PT due to early termination. Another possible reason can be correlated to empty space. When polymer brush density is high, grafted polymers stretch out away from the surface and orient normally to minimize interactions with crowded neighboring polymer chains.[7]

In other words, if polymer chains were not close enough upon less dense packing, PT molecules would have enough space to form defects (i.e. kinks) in their backbone more easily. As a result, π-electron delocalization length would be decreased resulting in hypsochromic shift. When surface-initiated *in situ* polymerization was initiated by the monolayer of solution-prepared catalytic initiator **3-I1** and carried out with intermediate regeneration of Ni active catalyst, it was found that the quality of PT thin film was substantially improved as compared to the conventional method. Almost two-fold increase in the optical density of PT thin film in the former case is a good evidence in favor of this.

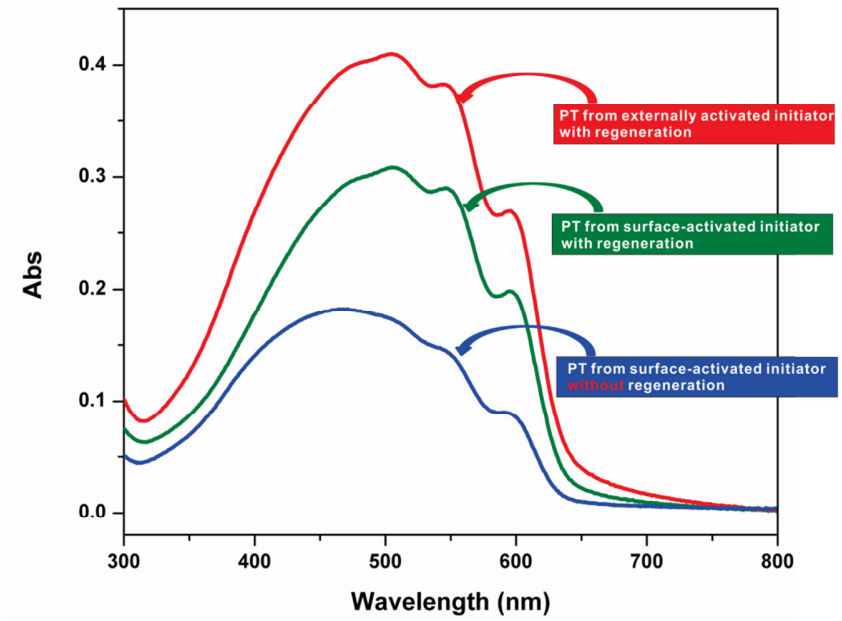

Figure 3.7. Absorption spectra of surface-immobilized polythiophene (PT) thin films after 3 days polymerization (Blue trace – without intermediate regeneration, Green trace – PT prepared from *in situ* surface-activated initiator, and Red trace – PT prepared from surface-immobilized monolayer of solution-prepared initiator **3-I1**).

To determine if the polymer chains were uniformly aligned in the thin films, optical anisotropy measurements have been performed. For the anisotropy measurements, UV-Vis absorption spectra of PT thin films grafted through the combination of immobilized solution-prepared initiator **3-I1** and intermediate regeneration were measured with vertically and horizontally polarized incident light. The twisting angle δ between the incident light and normal to the sample surface was changed between 0° and 40° and absorption spectra were recorded at every 10°.

$$D_{X,Y} = \frac{A_X}{A_Y} = 1 + \frac{2 - 3sin^2\varphi}{sin^2\varphi} sin^2\delta \qquad eqn. 3-1$$

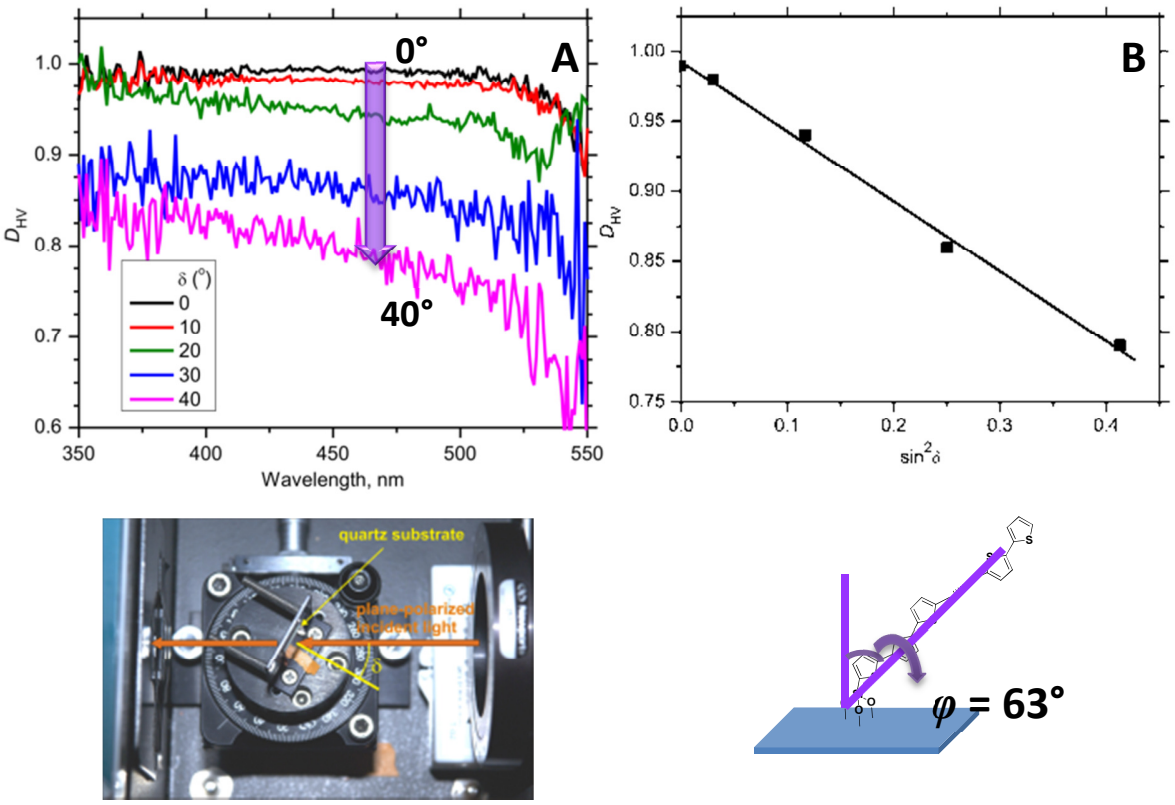

Figure 3.8. (A) Wavelength dependence of dichroic ratio of surface-immobilized PT on quartz substrate at different twisting angles δ. (B) Linear relationship between the dichroic ratio at 460 nm and $sin^2\delta$.

The equation 3-1 gives the dichroic ratio of observed absorption spectra with polarized light as a function of δ, the twisting angle.[30] Linear relationship of $sin^2\delta$ and dichroic ratio at 460 nm indicated that PT brushes in thin film were oriented uniformly. The slope of the linear plot of dichroic ratio vs. the twisting angle δ allowed to obtain tilting angle, φ = 62° (Figure 3.8). An independently conducted Atomic Force Microscopy (**AFM**) study revealed uniform coverage of surface-bound PT thin film with low roughness (RMS value was 1.4 nm) (Figure 3.9). To measure local film thickness accurately, the AFM nanoshaving technique was employed and resulted in ~14 nm PT thin films thickness value. Based on the combination of anisotropy-derived tilting angle φ and AFM-derived film thickness, the length of a single PT brush was estimated to be ~31 nm. With an assumption that the length of a thiophene monomer is around 3.5 Å, surface-immobilized PT brushes would consist of approaximately 90 repeating units. Thus, the estimated molecular weight of a PT brush was approximated at 7,500 g/mol, which was analogous to P3HT with M_n = 15,000 g/mol.

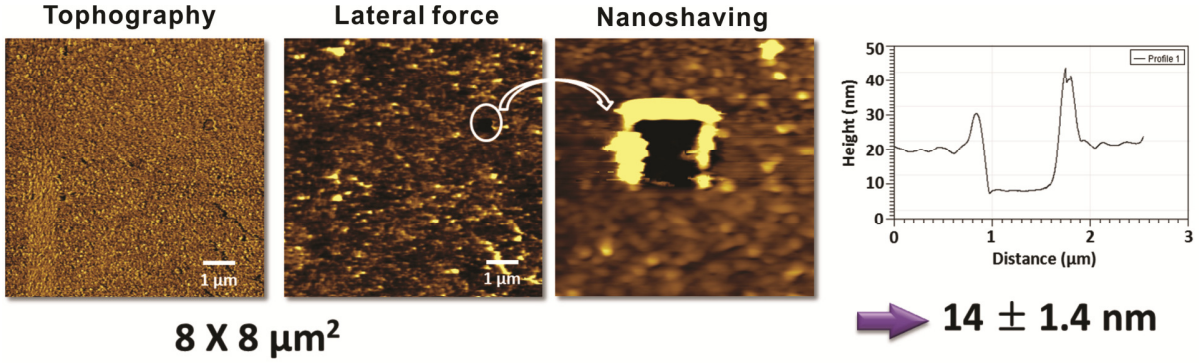

Figure 3.9. Surface mophology and nanoshaving-derived thickness of surface-immobilized PT thin film.

3.3.3 Surface-immobilized Nanopatterned PT Thin Films.

Preparation of surface-immobilized nanopatterned CP thin films (which are required for fabrication of organic electronic devices, especially solar cells) is practically impossible with

currently available "top-down" paradigm relying upon solution processing of pre-synthesized CPs. Development of such a method would reveal the major advantage of the "bottom-up" surface-initiated polymerization described in this dissertation.

To obtain a surface-immobilized nanostructured hole transporting material, we combined particle lithography with *in situ* polymerization initiated by surface-immobilized monolayer of solution-prepared catalytic initiator **3-I1** and intermediate regeneration of Ni catalytic center (Scheme 3.3 in page 51). In a proof-of-concept study, silicon (111) wafer, a widely used material in the field of electronics, was selected as a substrate. Drop-casting with 300 nm diameter latex particles followed by PDMS transfer of octadecyltrichlorosilane (OTS) gave a nanostructured OTS mask. After washing away the latex particles, the OTS-free circular areas were then modified with immobilized monolayer of solution-prepared catalytic initiator **3-I1**, and subsequent surface-initiated polymerization with intermediate regeneration of Ni catalytic center produced columnar nanostructured thin film of PT, covalently attached to the surface of Si (111).

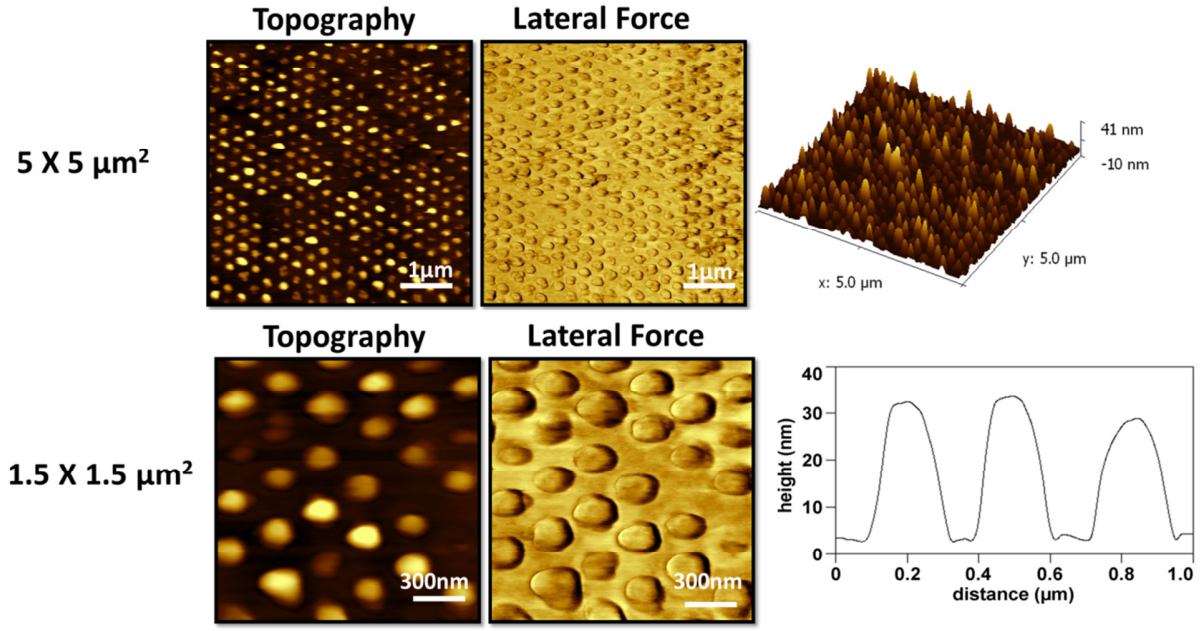

Figure 3.10. AFM image of surface-immobilized nano-patterned PT thin film on top of Si(111).

AFM study demonstrated columnar nanostructures of ~30 nm height uniformly spaced in nearly prefect hexagonal arrangement (Figure 3.10).

3.4 Conclusions.

Toward efficient Ni-catalyst transfer surface-initiated *in situ* polymerization, immobilization of solution-prepared catalytic initiator of living chain-growth Kumada polycondensation and intermediate regeneration of Ni(II) catalytic center methods were developed and optimized resulting in surface-immobilized PT thin films with high surface uniformity and exceptional mechanical stability. The resulting PT thin films demonstrated higher optical density which reflected improved surface coverage of PT brushes than conventionally grafted PT thin films. By combination of the newly developed grafting method and nanoparticle lithography, nanoscale patterned columnar PT films were successfully prepared on the silicon (111) surface. Currently, we are working towards preparation of complete organic photovoltaic devices with controlled nanoscale structure of organic active layer on ITO electrode, and the results will be reported soon.

3.5 References.

(1) Thomas, S. W.; Joly, G. D.; Swager, T. M., Chemical Sensors Based on Amplifying Fluorescent Conjugated Polymers, *Chem. Rev.* **2007**, *107*, 1339-1386.

(2) Arias, A. C.; MacKenzie, J. D.; McCulloch, I.; Rivnay, J.; Salleo, A., Materials and Applications for Large Area Electronics: Solution-Based Approaches, *Chem. Rev.* **2010**, *110*, 3-24.

(3) Kim, Y.; Cook, S.; Tuladhar, S. M.; Choulis, S. A.; Nelson, J.; Durrant, J. R.; Bradley, D. D. C.; Giles, M.; McCulloch, I.; Ha, C.-S.; Ree, M., A strong regioregularity effect in self-organizing conjugated polymer films and high-efficiency polythiophene:fullerene solar cells, *Nat. Mater.* **2006**, *5*, 197-203.

(4) Dimitrakopoulos, C. D.; Malenfant, P. R. L., Organic thin film transistors for large area electronics, *Adv. Mater.* **2002**, *14*, 99-117.

(5) Cates, N. C.; Gysel, R.; Dahl, J. E. P.; Sellinger, A.; McGehee, M. D., Effects of Intercalation on the Hole Mobility of Amorphous Semiconducting Polymer Blends, *Chem. Mater.* **2010**, *22*, 3543-3548.

(6) Zotti, G.; Zecchin, S.; Vercelli, B.; Berlin, A.; Grimoldi, S.; Groenendaal, L.; Bertoncello, R.; Natali, M., Surface-initiated polymerization of thiophene and pyrrole monomers on poly(terthiophene) films and oligothiophene monolayers, *Chem. Mater.* **2005**, *17*, 3681-3694.

(7) Barbey, R. l.; Lavanant, L.; Paripovic, D.; Schüwer, N.; Sugnaux, C.; Tugulu, S.; Klok, H.-A., Polymer Brushes via Surface-Initiated Controlled Radical Polymerization: Synthesis, Characterization, Properties, and Applications, *Chem. Rev.* **2009**, *109*, 5437-5527.

(8) Edmondson, S.; Osborne, V. L.; Huck, W. T. S., Polymer brushes via surface-initiated polymerizations, *Chem. Soc. Rev.* **2004**, *33*, 14-22.

(9) Zhang, Y.; Wang, C. W.; Rothberg, L.; Ng, M. K., Surface-initiated growth of conjugated polymers for functionalization of electronically active nanoporous networks: synthesis, structure and optical properties, *J. Mater. Chem.* **2006**, *16*, 3721-3725.

(10) Shallcross, R. C.; D'Ambruoso, G. D.; Korth, B. D.; Hall, H. K.; Zheng, Z. P.; Pyun, J.; Armstrong, N. R., Poly(3,4-ethylenedioxythiophene) - Semiconductor nanoparticle composite thin films tethered to indium tin oxide substrates via electropolymerization, *J. Am. Chem. Soc.* **2007**, *129*, 11310-11311.

(11) Wang, D.; Ye, Q.; Yu, B.; Zhou, F., Towards chemically bonded p-n heterojunctions through surface initiated electrodeposition of p-type conducting polymer inside TiO2 nanotubes, *J. Mater. Chem.* **2010**, *20*, 6910-6915.

(12) Hwang, E.; de Silva, K. M. N.; Seevers, C. B.; Li, J.-R.; Garno, J. C.; Nesterov, E. E., Self-Assembled Monolayer Initiated Electropolymerization: A Route to Thin-Film Materials with Enhanced Photovoltaic Performance, *Langmuir* **2008**, *24*, 9700-9706.

(13) Woo, C. H.; Thompson, B. C.; Kim, B. J.; Toney, M. F.; Fréchet, J. M. J., The Influence of Poly(3-hexylthiophene) Regioregularity on Fullerene-Composite Solar Cell Performance, *J. Am. Chem. Soc.* **2008**, *130*, 16324-16329.

(14) Yokozawa, T.; Yokoyama, A., Chain-Growth Condensation Polymerization for the Synthesis of Well-Defined Condensation Polymers and π-Conjugated Polymers, *Chem. Rev.* **2009**, *109*, 5595-5619.

(15) Sheina, E. E.; Liu, J.; Iovu, M. C.; Laird, D. W.; McCullough, R. D., Chain Growth Mechanism for Regioregular Nickel-Initiated Cross-Coupling Polymerizations, *Macromolecules* **2004**, *37*, 3526-3528.

(16) Senkovskyy, V.; Khanduyeva, N.; Komber, H.; Oertel, U.; Stamm, M.; Kuckling, D.; Kiriy, A., Conductive polymer brushes of regioregular head-to-tail poly(3-alkylthiophenes) via catalyst-transfer surface-initiated polycondensation, *J. Am. Chem. Soc.* **2007**, *129*, 6626-6632.

(17) Khanduyeva, N.; Senkovskyy, V.; Beryozkina, T.; Bocharova, V.; Simon, F.; Nitschke, M.; Stamm, M.; Grotzschel, R.; Kiriy, A., Grafting of Poly (3-hexylthiophene) from Poly(4-bromostyrene) Films by Kumada Catalyst-Transfer Polycondensation: Revealing of the Composite Films Structure, *Macromolecules* **2008**, *41*, 7383-7389.

(18) Yoshikai, N.; Matsuda, H.; Nakamura, E., Ligand Exchange as the First Irreversible Step in the Nickel-Catalyzed Cross-Coupling Reaction of Grignard Reagents, *J. Am. Chem. Soc.* **2008**, *130*, 15258-15259.

(19) Sontag, S. K.; Marshall, N.; Locklin, J., Formation of conjugated polymer brushes by surface-initiated catalyst-transfer polycondensation, *Chem. Commun.* **2009**, 3354-3356.

(20) Massera, C.; Frenking, G., Energy Partitioning Analysis of the Bonding in $L_2TM–C_2H_2$ and $L_2TM–C_2H_4$ (TM = Ni, Pd, Pt; L_2 = $(PH_3)_2$, $(PMe_3)_2$, $H_2PCH_2PH_2$, $H_2P(CH_2)_2PH_2$), *Organometallics* **2003**, *22*, 2758-2765.

(21) Senkovskyy, V.; Tkachov, R.; Beryozkina, T.; Komber, H.; Oertel, U.; Horecha, M.; Bocharova, V.; Stamm, M.; Gevorgyan, S. A.; Krebs, F. C.; Kiriy, A., "Hairy" Poly(3-hexylthiophene) Particles Prepared via Surface-Initiated Kumada Catalyst-Transfer Polycondensation, *J. Am. Chem. Soc.* **2009**, *131*, 16445-16453.

(22) Shiu, S.-C.; Chao, J.-J.; Hung, S.-C.; Yeh, C.-L.; Lin, C.-F., Morphology Dependence of Silicon Nanowire/Poly(3,4-ethylenedioxythiophene):Poly(styrenesulfonate) Heterojunction Solar Cells, *Chem. Mater.* **2010**, *22*, 3108-3113.

(23) Hu, Z.; Tian, M.; Nysten, B.; Jonas, A. M., Regular arrays of highly ordered ferroelectric polymer nanostructures for non-volatile low-voltage memories, *Nat. Mater.* **2009**, *8*, 62-67.

(24) Hoppe, H.; Niggemann, M.; Winder, C.; Kraut, J.; Hiesgen, R.; Hinsch, A.; Meissner, D.; Sariciftci, N. S., Nanoscale morphology of conjugated polymer/fullerene-based bulk-heterojunction solar cells, *Adv. Funct. Mater.* **2004**, *14*, 1005-1011.

(25) Günes, S.; Neugebauer, H.; Sariciftci, N. S., Conjugated Polymer-Based Organic Solar Cells, *Chem. Rev.* **2007**, *107*, 1324-1338.

(26) Herzer, N.; Wienk, M. M.; Schmit, P.; Spoelstra, A. B.; Hendriks, C. E.; Oosterhout, S. D.; Hoeppener, S.; Schubert, U. S., Fabrication of PEDOT-OTS-patterned ITO substrates, *J. Mater. Chem.* **2010**, *20*, 6618-6621.

(27) Khanduyeva, N.; Senkovskyy, V.; Beryozkina, T.; Horecha, M.; Stamm, M.; Uhrich, C.; Riede, M.; Leo, K.; Kiriy, A., Surface Engineering Using Kumada Catalyst-Transfer Polycondensation (KCTP): Preparation and Structuring of Poly(3-hexylthiophene)-Based Graft Copolymer Brushes, *J. Am. Chem. Soc.* **2008**, *131*, 153-161.

(28) Li, J.-R.; Garno, J. C., Elucidating the Role of Surface Hydrolysis in Preparing Organosilane Nanostructures via Particle Lithography, *Nano Lett.* **2008**, *8*, 1916-1922.

(29) Acharya, J. R.; Zhang, H.; Li, X.; Nesterov, E. E., Chemically Controlled Amplified Ratiometric Fluorescence in Surface-Immobilized End-Capped Oligo(p-phenylene ethynylene)s, *J. Am. Chem. Soc.* **2009**, *131*, 880-881.

(30) Martínez Martínez, V.; López Arbeloa, F.; Bañuelos Prieto, J.; López Arbeloa, I., Orientation of Adsorbed Dyes in the Interlayer Space of Clays. 1. Anisotropy of Rhodamine 6G in Laponite Films by Vis-Absorption with Polarized Light, *Chem. Mater.* **2005**, *17*, 4134-4141.

CHAPTER 4 ORGANIC SEMICONDUCTING POLYMER FILMS BY STEPWISE *IN SITU* POLYMERIZATION VIA SEQUENTIAL CLICK REACTION.

4.1 Introduction.

Polymer brushes, i.e. thin films of surface-immobilized polymers on solid substrates, have been attracting much attention recently for use in stimuli responsive materials and surfaces,[1-3] and organic electronics[4-7] due to their mechanical durability and possibility to fit them with various functional groups. Based on the method of immobilization and/or polymerization, their preparation approaches are broadly classified as "grafting to" and "grafting from" methods. "Grafting to" pathway is accomplished by the attachment of an anchoring-group functionalized polymers previously prepared in solution, to a solid surface-modified substrate. The advantages of the "grafting to" method, such as low polydispersity (**PDI**) and immobilization of the polymer brushes with precisely designed properties, stem from using the appropriately functionalized pre-synthesized polymers with low PDI. However, due to low reactivity in a heterogeneous reaction between the surface and the macromolecules, the "grafting to" method often results in poor, not sufficient surface coverage. Furthermore, due to the trend of even lower reactivity for the polymers with increasing chain length, thickness of the resulting thin films is limited.[8, 9] In this sense, this method would be most appropriate for oligomers or polymers with low molecular weight (M_n).[10] On the other hand, "grafting from" method, such as surface-initiated *in situ* polymerization from covalently attached initiator layer, allows production of thin films with higher surface coverage as well as increased thickness up to a few micrometers. However, the "grafting from" method often suffers from the "needle growth" problem because the reaction between the free monomer and the active chain end is more efficient with bigger polymer molecules than with shorter polymer chains.[11] As a result, high PDI as well as relatively non-uniform, rugged surface morphology of the thin films due to reduced polymer density on topside

of the films could be a typical outcome. In our search for an alternative strategy, we directed our attention to *in situ* stepwise polymerization. In this novel strategy, a polymer brush can be grown by series of discrete steps to attach monomers to an active chain end, in a one-by-one fashion. At a first glance, building a polymer by the repeated reaction between the monomer and the polymer brush seems to be laborious and time-consuming. Nevertheless, it provides full control over polymer structure and composition and can result in thick and dense polymer thin films with low PDI promising uniform surface morphology, especially when the reaction conditions are optimized and each step takes only a short time. As an example, a recent report by Reinecke et al. described deposition of a 115 nm thick polyaramide (Kevlar) film (estimated M_n was around 119,000 g/mol after 1,000 steps) on a silicon wafer via *in situ* stepwise polymerization.[12] Additionally, the overall labor intensiveness and preparation time could be significantly reduced through easy-to-implement automation of stepwise polymerization and repeating immersing-reaction-washing steps. Most importantly, the possibility to achieve complete control over molecular structure and composition of the polymer brushes (and prepare, for example, surface-attached polymers with internal electric field gradient for electronic applications), not achievable by any other means, would dramatically increase the value of this method. Although previous research efforts toward grafting conducting polymer brushes have resulted in noticeable achievements,[13-17] further developments in preparation routes are required to obtain truly dense and thick conducting polymer films for more efficient charge carrier transport in organic electronics. Along this line, we developed a novel grafting method based on a stepwise *in situ* polymerization. For the sufficient growth of surface-immobilized polymer, high reaction efficiency between monomer and surface-tethered polymer is essential for uniform deposition of the surface-attached polymer film. Due to this reason, we chose Cu(I)-catalyzed Huisgen 1,3-cycloaddition (Cu-catalyzed acetylene-azide click reaction (**CuAAC**)) as a robust and efficient

chemistry to build a polymer chain by stepwise addition of the monomers to the surface-immobilized polymer (Figure 4-1). Thermal uncatalyzed 1,3-dipolar cycloaddition reaction between acetylene and organic azide was first discovered by Huisgen in 1960s.[18] However, harsh reaction conditions, such as a high reaction temperature, were required because of the considerably high activation barrier induced by the low polarity character of dipole, and the reaction mainly yielded a mixture of 1,4- and 1,5-isomers (Scheme 4.1).[19, 20]

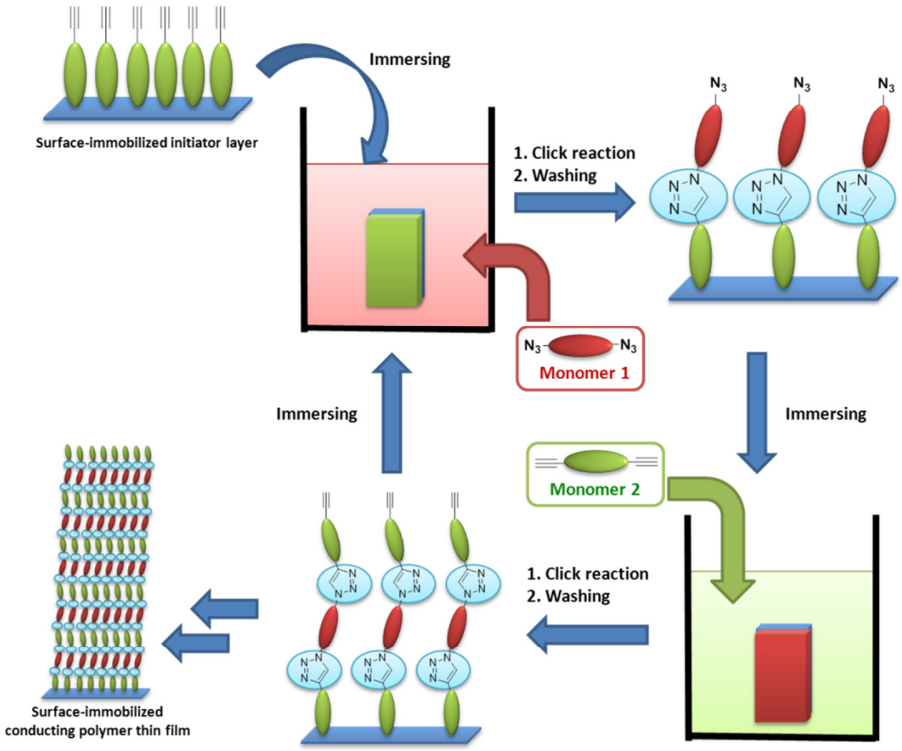

Figure 4.1. General preparation route via stepwise *in situ* polymerization based on click-chemistry.

Scheme 4.1. Thermal uncatalyzed Huisgen 1,3-cycloaddition.

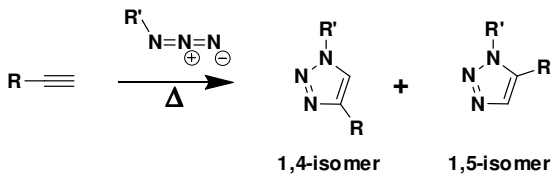

Since the first examples of CuAAC reaction (the so called "click reaction") were reported by Sharpless in 2001,[21] 1,3-cycloaddition between alkyne and azide has become a popular and

powerful choice due to several advantages. First, Cu(I) catalyst greatly improves the rate of 1,3-cycloaddition even at low temperature. Based on the data in Cambridge Crystal Database, more than one copper atom can coordinate to acetylene, thus π-electrons also participate in coordination and the secondary carbon on the acetylene group could aquire enhanced partial positive charge. As a result, the activation barrier of the reaction decreases and the reaction rate increases. Additionally, the formation of a six-membered transition state for the reaction of positively charged secondary carbon on acetylene and terminal nitrogen on azide enhances regioselectivity, yielding a 1,4-isomer as a major product.[19] Simple reaction conditions with easily available starting materials prepared by general synthetic routes would be another advantage of CuAAC. When the reaction gives a product with high product yield within a short reaction time and simple reaction conditions, it can be called a "click reaction" and CuAAC completely satisfies recently outlined qualifications for a click reaction.[22] The following scheme 4.2 shows an accepted mechanism of the click reaction.[19]

Scheme 4.2. Mechanism of Cu(I) catalyzed 1,3-Cycloaddition (from ref. 19).

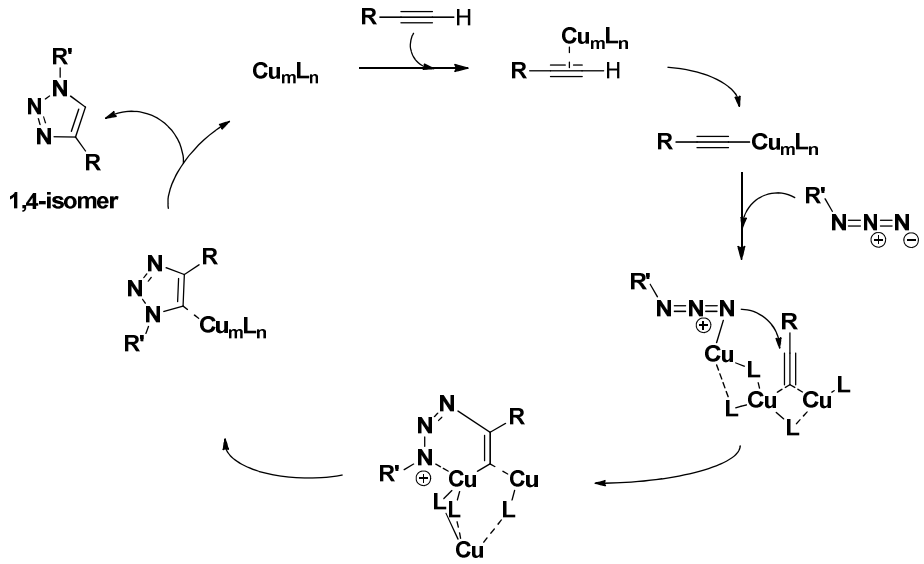

Owing to its robust efficiency and regioselectivity, the click reaction has been widely used in many areas of polymer science[23] and, since it produces a 1,2,3,-triazole linker, is a suitable way

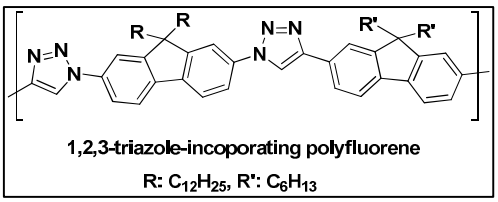

1,2,3-triazole-incoporating polyfluorene
R: $C_{12}H_{25}$, R': C_6H_{13}

to build a semiconducting polymer backbone. The first semiconducting polymer, 1,2,3-triazole-incoporating polyfluorene, prepared via CuAAC was reported in 2005 by van Maarseveen, Reek, and coworkers.[24] Although such polymers would suffer from lacking substantial π-electron delocalization, their potential in electronic devices was demonstrated by their use as active materials in dye-sensitized solar cells.[25, 26] More recently, Ratner and Mirkin demonstrated another possibility to use triazole-incorporating polymers as molecular wires by the construction of a molecular electronic transport junction through *in situ* click polymerization.[27] Besides its use in preparing semiconducting materials, CuAAC has also been widely employed to attach to solid surfaces ("grafting to") or to modify the topmost part of polymer brushes with various functional groups.[10, 28-30] Based on successful results in preparation of bulk semiconducting polymers and surface modification chemistry, it is certain that monomers, functionalized with either acetylene or azide group, can efficiently react with surface-immobilized polymer brushes with the complementary functional group. Furthermore, CuAAC cannot occur between the same functional groups (azide-azide or acetylene-acetylene), thus only one monomeric layer is deposited on top of a conducting polymer film after a single click reaction step. As a result of selective simultaneous stepwise growth, low PDI, which cannot be obtained by bulk polymerization, would be achieved. In this chapter, we describe our efforts to optimize reaction conditions and our initial findings.

4.2 Experimental Details.

4.2.1 Preparation of Monomers and Precursors.

Preparation of monomer **4-m1** was started with iodination of 2,2'-bithiophene to yield 5,5'-diiodo-2,2'-bithiophene (**4-1**). Sonogashira coupling between **4-1** and trimethylsilylacetylene followed by TMS deprotection yielded diacetylene monomer **4-m1**. Diazido monomer, **4-m2**

was prepared through the Sandmeyer reaction with commercially available 9H-fluorene-2,7-diamine. Another diacetylene monomer **4-m3** for preparation of surface-immobilized homopolymer was also synthesized via Sonogashira coupling reaction followed by TMS group deprotection in **4-3**.

Scheme 4.3. Synthesis of monomers and precursors.

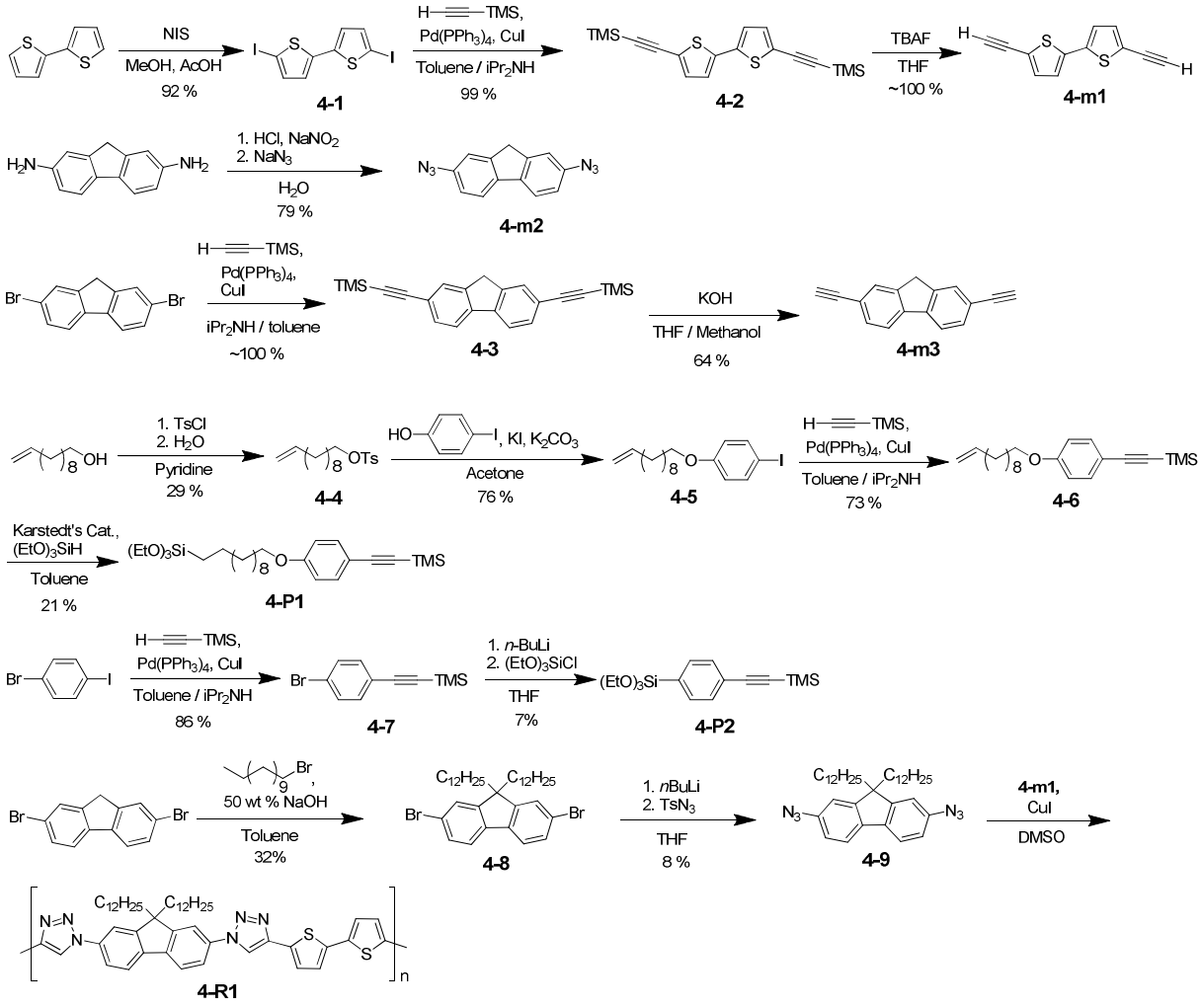

Compound **4-6** was synthesized following the literature procedure.[31] Terminal alkene group of **4-6** was functionalized through hydrosilyation with $(EtO)_3SiH$ Karstedt's catalyst to give triethoxysilane-substituted precursor **4-P1**. After lithiation of ((4-bromophenyl)ethynyl)trimethylsilane (**4-7**), prepared by Sonogashira coupling reaction of 1-

bromo-4-iodobenzene and trimethylsilylacetylene with *n*-BuLi followed by substitution reaction with $(EtO)_3SiCl$, precursor **4-P2** was synthesized as a yellow oil. Soluble reference polymer **4-R1** was synthesized by click polymerization of diazido monomer **4-9** and diacetylene monomer **4-m1**. Synthetic details are described in Chapter 5.

4.2.2 Preparation of Surface-immobilized Polymer Thin Films via Stepwise *in situ* CuAAC Polymerization.

Scheme 4.4. Preparation of surface-bound organic semiconducting polymer thin film through stepwise click polymerization.

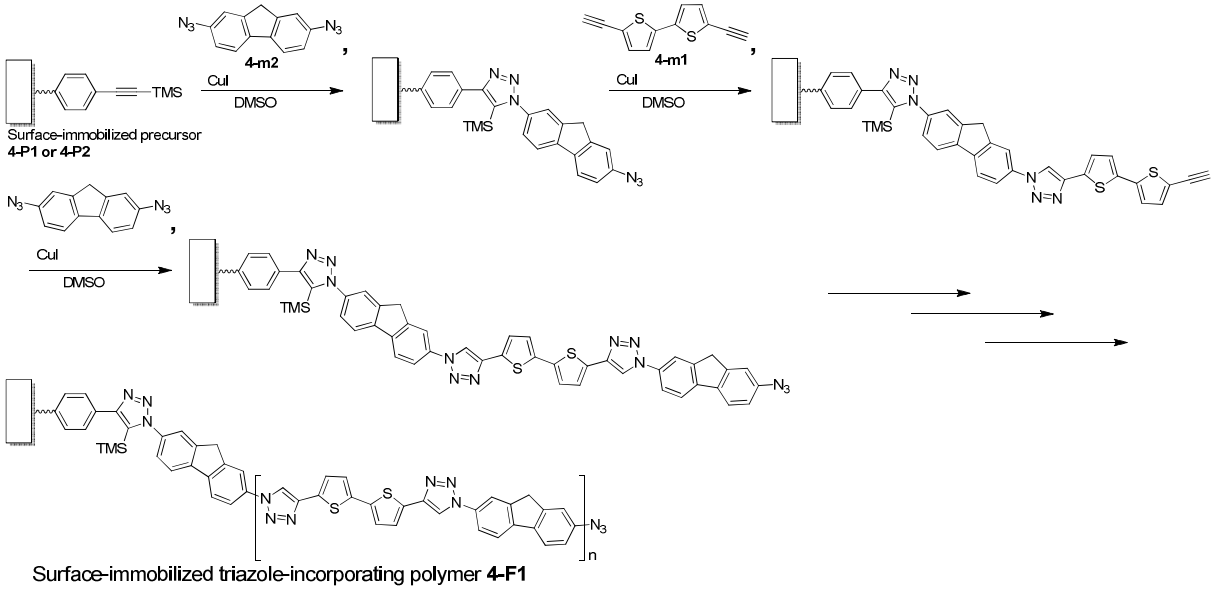

Freshly cleaned rectangular quartz or ITO-coated glass slides were immersed into triethoxysilyl-functionalized precursors **4-P1** or **4-P2** solutions in toluene for 3 days to tether azide functionalized precursor to the substrate surface. Subsequent stepwise *in situ* polymerization was accomplished by sequential immersing of the monolayer-coated substrate into 10 mM solutions of **4-m1** (or **4-m3**) and **4-m2**. Between each click step, sample slides were washed with copious amount of toluene followed by ultrasonication. This procedure gave surface-immobilized triazole incorporating copolymer **4-F1** thin film on substrates. Further details are provided in Chapter 5.

4.3 Results and Discussion.

4.3.1 1,2,3-triazole Incorporating Fluorene-bithiophene Copolymer Brush Thin Films and Their Properties.

In an initial proof-of-concept study, surface-immobilized 1,2,3-triazole incorporating bithiophene-fluorene copolymer thin films (sample **1** in table 4.1) were grafted through 33 steps of sequential one hour CuAAC polymerization with the monomers **4-m1** and **4-m2** starting from the surface-immobilized precursor **4-P1** on quartz substrates (Scheme 4.6). Since the click reaction under inert atmosphere promises a clean reaction[19] and DMSO is a highly hygroscopic solvent, all experiments outlined in this chapter were accomplished inside a glovebox to obtain the best results. Polymer growth in the thin film was monitored by increasing absorption in UV-Vis spectra after every CuAAC step followed by two sets of ten minute ultrasonications in $CHCl_3$ to remove non-attached monomers in the thin film.

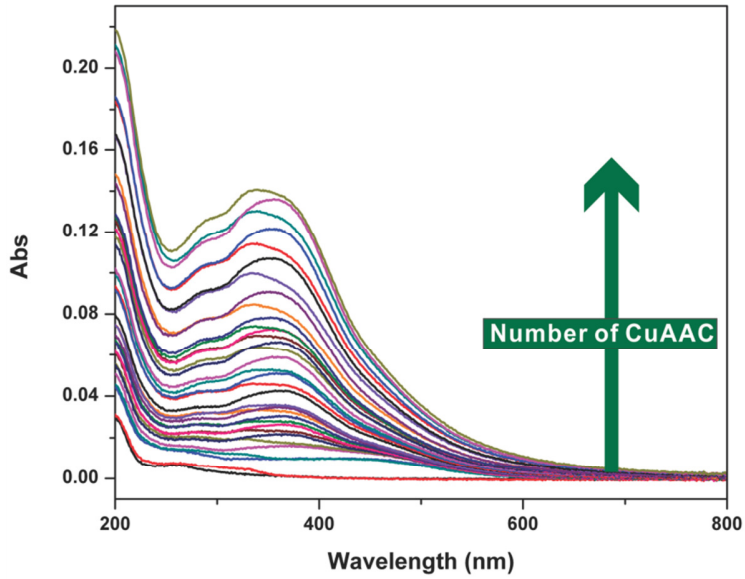

Figure 4.2. UV/Vis monitoring of the growing film immobilized on a quartz surface after 33 Cu(I) catalyzed 1,3-cycloaddition steps.

As shown in Figure 4.2, gradual increase in optical density was observed during repeated sequential click reactions. During stepwise polymerization, it was also observed that the rate of

further enhancement in optical density diminished after 7 or 8 repeated CuAAC stpes. For an efficient click reaction to take place, it is important to maintain Cu(I) at a high level. However, Cu(I) tends to oxidize to Cu(II), thus Cu(II) catalyst with large amount of reducing agent (e.g. ascorbic acid) is typically used for click reactions. Since we use CuI without a reducing agent to simplify reaction conditions, oxidation of CuI resulted in decreasing efficiency of click reactions between the monomers and the growing polymer brushes. Consequently, growth of optical density was slowed down with the increasing number of click steps. To overcome this problem, we were adding additional amount of cheap CuI into the reaction mixture after every 8 click reaction steps. As a result of monitoring and supplying fresh Cu(I), the entire 33-step process was performed with the same monomer solutions without any wasted monomers.

Table 4.1. Experimental conditions used in preparation of surface-immobilized 1,2,3-triazole incorporating polymer thin films on quartz substrates.

Sample	Precursor	Monomer combination	Amount of CuI	Reaction time & temp.	Ultrasonication
1	**4-P1**	**4-m1 + 4-m2**	10 mol%	1 hour (40 °C)	After every CuAAC
2[a]	**4-P1**	**4-m1 + 4-m2**	10 mol%	1 hour (40 °C)	After every CuAAC
3	**4-P1**	**4-m1 + 4-m2**	30 mol%	30 min (60 °C)	After every 5 CuAAC
4	**4-P2**	**4-m1 + 4-m2**	30 mol%	30 min (60 °C)	After every 5 CuAAC
5	**4-P1**	**4-m1 + 4-m2**	30 mol%	30 min (60 °C)	After every 5 CuAAC
6	**4-P2**	**4-m1 + 4-m2**	30 mol%	30 min (60 °C)	After every 5 CuAAC
7	**4-P2**	**4-m3 + 4-m2**	30 mol%	30 min (60 °C)	After every 5 CuAAC

(a): ITO was used as a substrate.

Unlike typical semiconducting polymers, triazole-incorporating polymer lacks substantial π-electron delocalization. This factor was consistent with experimentally observed unusual behavior upon monitoring of the growing film UV/Vis absorption spectra. Although optical density of sample **1** showed systematic increase through the steps, an expected bathochromic spectral shift was not observed. Furthermore, the wavelength of absorption maximum (λ_{max}) of the thin films in the process of stepwise deposition was reversibly altered between two distinct

values after every CuAAC step. When the surface-immobilized polymer film reacted with the fluorene monomer **4-m2**, λ_{max} of the resulting film was found at 330 nm. After subsequent reaction with the bithiophene monomer **4-m1**, λ_{max} would shift to 360 nm. After the next step (reaction with **4-m2**), it would shift back to 330 nm, etc. Based on the absorption spectra of the monomers shown in Figure 4.3 and assuming localized nature of the π-electron system in the polymers, such reversible alteration of the absorption maximum wavelength can be correlated with the relative "concentration" of the monomers in the thin film. Once the polymer chains reacted with diazido functionalized fluorene (**4-m2**), the concentration of fluorene units in the thin film would slightly increase to exceed that of bithiophene units. As a result, λ_{max} of the thin film would shift from 360 nm (almost identical to the λ_{max} of the bithiophene monomer **4-m1**), to 330 nm (close to λ_{max} of **4-m2**).

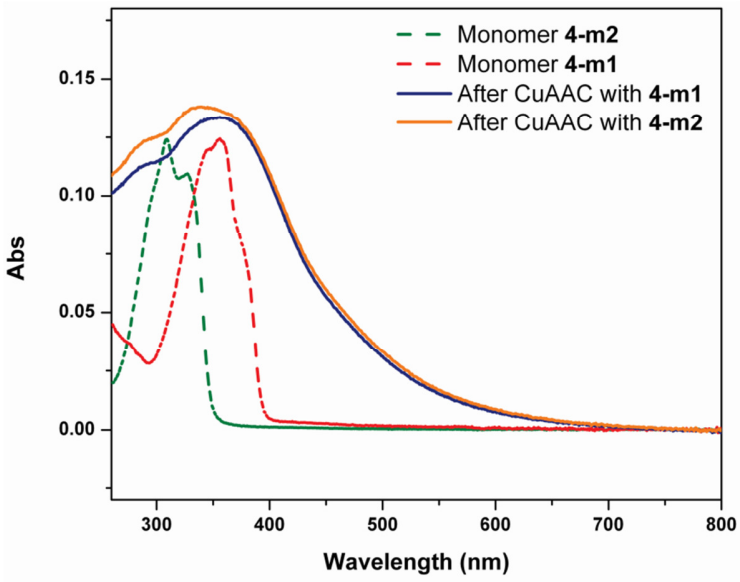

Figure 4.3. Reversible bathochromic and hypsochromic shifts absorption maximum during stepwise *in situ* polymerization via CuAAC. (Orange solid line : hypsochromically shifted λ_{max} after CuAAC with monomer **4-m2**, blue solid line : bathochromically shifted λ_{max} after CuAAC with monomer **4-m1**, green dashed line : absorption spectrum of **4-m2**, red dashed line : absorption spectrum of **4-m1**)

Electrochemical properties of surface-immobilized triazole incorporating fluorene-bithiophene copolymer thin film were studied to estimate energy levels of the highest occupied

molecular orbital (**HOMO**) and to evaluate the lowest unoccupied molecular orbital (**LUMO**), and therefore, the polymer's HOMO-LUMO gap.

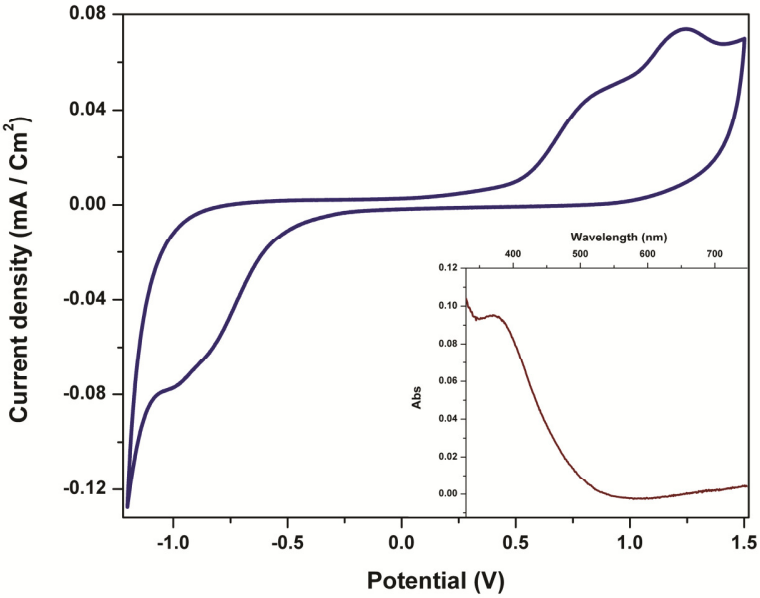

Figure 4.4. Cyclic voltammogram (vs. Ag/Ag^+) of surface immobilized fluorene-bithiophene copolymer thin film **4-F1** on ITO. (Experimental conditions: 0.1M Bu_4NPF_6 in CH_3CN, sweep rate 0.1 V/s) Inset: UV-Vis absorption spectrum of this thin film.

For CV measurements, a new copolymer thin film (sample **2**) was grafted on indium tin oxide (**ITO**) coated glass surface via 33 click steps. Reversible cyclic voltammogram in figure 4.4 exhibited a distinct oxidation potential (E_{ox}) at 1.2 V (vs Ag/Ag^+) with a shoulder peak at 0.9 V and onset oxidation potential (φ_{ox}) at 0.58 V. Following the literature procedure,[32] energy level of HOMO (E_{HOMO}) was estimated at -5.28 eV. The band (HOMO-LUMO) gap energy (E_g) was determined from the onset wavelength of UV-Vis absorption spectrum of triazole copolymer brushes on ITO. Based on the estimated E_g of 2.52 eV, LUMO energy level (E_{LUMO}) was approximated at -2.76 eV. When the estimated values were compared with the reported data determined from CV of 1,2,3-triazole incorporating fluorene homopolymer,[25] E_{HOMO} showed an almost identical value, -5.23 eV. Lower E_{LUMO} of fluorene-bithiophene copolymer originates

from the presence of bithiophene units in the copolymer which showed a bathochromic spectral shift relative to the homopolymer and lower E_g accordingly.

4.3.2 Efforts toward Optimization of Reaction Conditions.

If the reaction time of each CuAAC can be reduced, overall stepwise thin film preparation can be accomplished in a much shorter time. However, shortened reaction time also can cause random deposition of monomers because of the incomplete click reaction between monomers and the topmost part of the polymer brushes which can yield needle-like surface morphology of the resulting thin films. In order to determine if there is any possibility to reduce our initial click reaction time, we deposited a surface-immobilized triazole incorporating polymer thin film via 30 steps of 30 minute per step click reactions (sample **3** in Table 4.1). This time, CuAAC was carried out with increased amount of CuI (30 mol%) and at a higher reaction temperature (60 °C) to compensate for reduced reaction efficiency caused by the shortened reaction time.

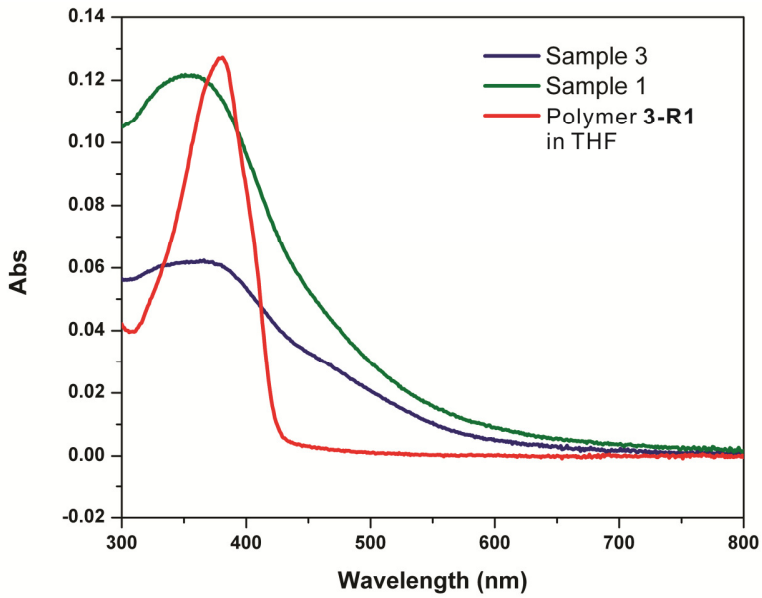

Figure 4.5. Absorption spectra of surface-bound copolymer thin film **4-F1** prepared via 1 hour per step click reaction (green trace) and via 30 min per step reaction (blue trace). Red trace is a spectrum of soluble reference polymer **4-R1** in THF.

UV-Vis absorption spectrum of sample 3 exhibited a somewhat red-shifted absorption maximum at 380 nm, though optical density at the band maximum was almost twice lower than that sample **1** (Figure 4.5).

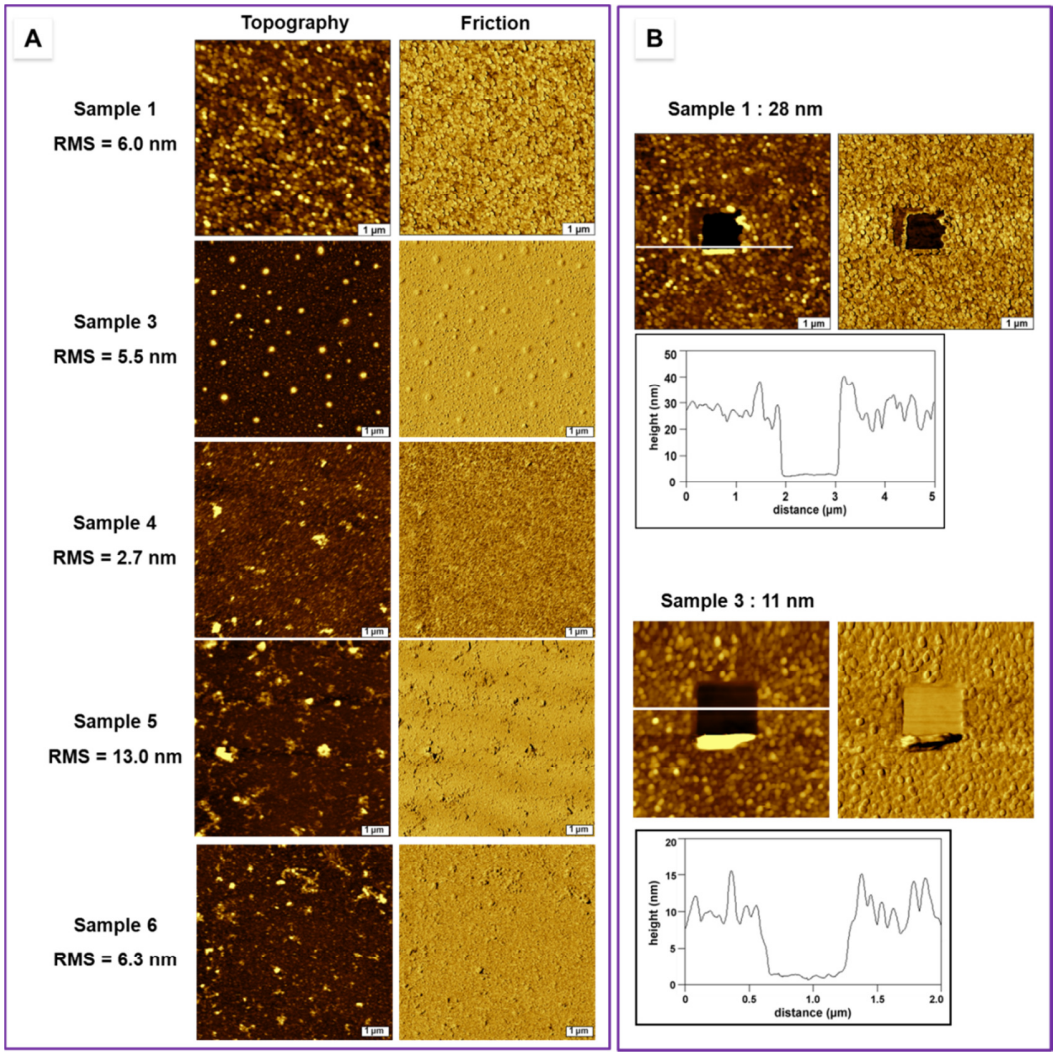

Figure 4.6. (A) AFM surface morphologies of surface-immobilized copolymer (or homopolymer) thin films and (B) Nanoshaving thickness determinations of samples **1** and **3**.

To elucidate the reasons for the lower optical density, surface morphologies of surface-attached thin films were investigated. AFM study revealed formation of random-positioned needle-like grains in sample **3**. In contrast, sample **1** exhibited a uniform surface morphology without outstanding features (Figure 4.6). Based on UV-Vis spectra of the samples and the AFM

study, we hypothesized that a possible reason for lower optical density would be incomplete CuAAC in each deposition step. Therefore, outstanding morphological features in sample **3** might have resulted from a formation of needle-like polymer brushes. Nanoshaving measurements on thin films suggested another explanation for the lower optical density of the sample **3** film. While the thickness of the initially produced sample **1** was around 28 nm, sample **3** deposited under reduced click reaction time per step under moderately harsh conditions showed only 11 nm thickness. If we assume that surface-immobilized polymer brushes were grown uniformly by stepwise *in situ* polymerization, the thickness of the resulting thin film would have to be proportional to the number of CuAAC steps. Hence, lower thickness of the sample **3** produced with shorter reaction time would be a consequence of random deposition of the monomeric layers due to unoptimized click reaction conditions.

In order to further evaluate the properties of surface-bound fluorene-bithiophene copolymer, 1,2,3-triazole-incorporating copolymer bearing dodecyl solubilizing groups (**4-R1** in Scheme 4-3, page 72) was synthesized (M_n = 15,400 g/mol, PDI = 1.8) and its spectroscopic properties were compared with those of thin films (Figure 4.5). While absorption maxima of the reference polymer **4-R1** and sample **3** showed identical λ_{max} at 380 nm, sample **1** exhibited ~20 nm hypsochromically shifted λ_{max}. Considering results from the AFM study on sample **3**, the 20 nm hypsochromically shifted absorption maximum of sample **1** could be rationalized by considering intermolecular electronic interactions (aggregation) of surface-immobilized polymer brushes. Random growth of polymer brushes in sample **3** induced by incomplete click reaction might produce a molecularly disordered structure where polymer chains would not interact efficiently. Furthermore, since concentration of reference solution in THF was very low (~15 µg / ml), the absorption peak at 380 nm most likely represents molecular absorption (M-band) of the 1,2,3,-triazole incorporating fluorene-bithiophene copolymer itself. On the other hand, sample **1**

polymerized in the complete click reaction conditions showed higher optical density due to increased thickness and surface uniformity. Hence, fluorene-bithiophene copolymer brushes in sample **1** seem to be arranged in a more ordered molecular fashion promising efficient interactions with neighboring polymer molecules. After the analysis of literature data on effects of aggregation on UV-Vis absorption spectra of π-electron conjugated dyes, we suggest that hypsochromically shifted λ_{max} of sample **1** originated from H-aggregation.[21, 22, 33] The effect of H-aggregation on optical absorption will be especially pronounced considering limited π-electron delocalization along the polymer backbone, which in fact can be better described as a chain of almost non-interacting chromophores connected in series. Therefore, 1,2,3-triazole incorporating fluorene-bithiophene copolymer brushes in sample **1** would be interact in a face-to-face fashion.

The ultimate advantage of stepwise *in situ* polymerization is that it allows formation of highly ordered conducting polymer thin films with improved surface morphology. In this new strategy, topography of a thin film would be determined by efficiency of the chemistry used for deposition of the monomeric layers, as well as by two additional factors. It is well-known that the quality of surface-immobilized precursor monolayer, which ultimately determines morphology of the resulting thin film, depends on length of the alkyl chain in the anchoring group on initiator molecule (i.e., octadecyl group).[34, 35] Thus, in our initial studyies, we used surface-immobilized initiator **4-P1**, which has a similar chain length as octadecyl group, to prepare sample **1**, even despite the long alkyl chain possible interference with efficient charge transport in electronic devices.[34] In our studies described in Chapter 3, we found that directly surface-immobilized initiator without any separating alkyl chain produced good polymer films with uniform surface morphologies and low RMS values. Therefore, precursor **4-P2** was prepared to deposit a directly surface-bound triazole incorporating copolymer thin film. For convenience and fast result, surface-anchored copolymer brushes (sample **4**) were deposited in

30 CuAAC steps of 30 min per step. Although sample **4** exhibited aggregation features on its surface due to the less complete click reactions, AFM studies revealed that a **4-P2** derived film showed an almost half RMS value, 2.7 nm compared to sample **3** (Figure 4.6). Based on the similarity of surface roughness values (RMS 5.9 and 5.5 nm, respectedly) of samples **1** and **3** (both grafted from **4-P1**), we could conclude that immobilization of the initiator without long alkyl chain gives a better quality surface-immobilized initiator monolayer.

In the attempts descried above, we thoroughly cleaned the substrates with growing polymer film by ultrasonication in $CHCl_3$ to remove adhered monomer residues on the surface or inside of thin films after every CuAAC step. In order to investigate the effect of such laborious cleaning, surface-immobilized copolymer thin films were deposited in identical reaction conditions as discussed above using surface-immobilized initiators **4-P1** (sample **5**) and **4-P2** (sample **6**) except less laborious cleaning process. After each click deposition, slides were just rinsed with a copious amount of toluene. Ultrasonication was performed only after 5 complete CuAAC steps. AFM surface morphologies of the resulted thin films demonstrated lower surface uniformity with larger sized grains as well as two-fold higher RMS values for both samples (Figure 4.6). Like carefully prepared sample **4**, sample **6** also showed a distinctly improved surface-morphology with lower RMS value (6.3 nm) in contrast 12.9 nm for sample **5**. Thus, the best and most uniform surface morphology could be obtained when surface-bound triazole incorporating copolymer was deposited starting with **4-P2** initiator allowing 1 h per each CuAAC step with thorough (ultrasonication in $CHCl_3$) cleaning after each step.

4.3.3 Optimizing UV/Vis Absorption Spectrum through Modification of The Polymer Molecular Composition.

One of the valuable benefits of stepwise *in situ* polymerization would be possibility to tailor spectroscopic properties of the polymer thin films by alteration of the polymer molecular

composition. Lack of substantial π-electron delocalization in these polymers makes it easier to predict spectroscopic properties of the thin films by simply considering the absorption spectra of each monomer.

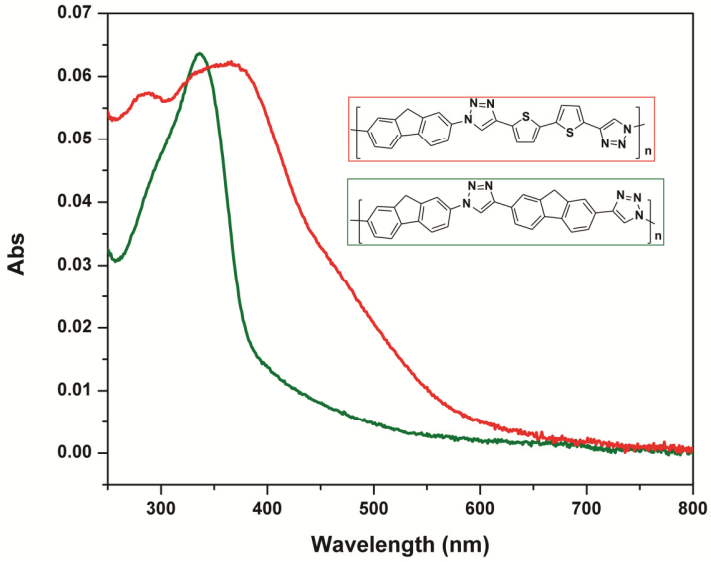

Figure 4.7. UV-Vis absorption spectra of surface-immobilized fluorene-bithiophene copolymer (red trace) and fluorene homopolymer (green trace) thin films.

As shown on Figure 4.3, absorption spectra of fluorene-bithiophene copolymer thin films could be described as a simple superposition of the spectra of the two monomers. Since absorption spectrum of 1,2,3-triazole incorporating fluorene homopolymer was previously reported,[24-26] a fluorene homopolymer thin film (sample **7** in table 4.1) was deposited on a quartz slide as a proof of concept. For quicker result, sample **7** was prepared through 30 elementary CuAAC steps, 30 min per step, starting from surface-immobilized precursor **4-P2** monolayer, and using monomers **4-m2** and **4-m3**. Relatively narrow absorption band with a sharp absorption maximum of sample **7** was found at 336 nm which contrasted with the broad spectra obtained for fluorene-bithiophene copolymer thin films showing λ_{max} at 360 or 380 nm (Figure 4.7). This result demonstrated that spectroscopic and other properties of the polymer films prepared by stepwise polymerization can be easily manipulated by simple variation of the polymer molecular

composition. In further experiments, we will attempt to prepare even more complex polymer brushes, e.g. polymers with internal field gradient.

4.4 Conclusions.

To conclude, novel stepwise *in situ* polymerization method via sequential Cu-catalyzed acetylene-azide click (CuAAC) chemistry was developed to generate highly ordered surface-immobilized organic semiconducting polymer thin films. In initial study, 1,2,3-triazole incorporating fluorene-bithiophene copolymer brushes were surface-deposited and their deposition conditions were optimized. Their spectroscopic, electrochemical, and morphological properties were studied. By comparison of UV-Vis absorption spectra of fluorene homopolymer and fluorene-bithiophene copolymer thin films, the possibility to finely tune spectroscopic properties of surface-immobilized polymer thin films was evaluated. Currently, we are working to further optimize photophysical properties of the thin films using various combinations of monomers.

4.5 References.

(1) Granville, A. M.; Boyes, S. G.; Akgun, B.; Foster, M. D.; Brittain, W. J., Synthesis and characterization of stimuli-responsive semifluorinated polymer brushes prepared by atom transfer radical polymerization, *Macromolecules* **2004**, *37*, 2790-2796.

(2) Zhang, Y. F.; Luo, S. Z.; Liu, S. Y., Fabrication of hybrid nanoparticles with thermoresponsive coronas via a self-assembling approach, *Macromolecules* **2005**, *38*, 9813-9820.

(3) Zhou, J. H.; Wang, G.; Hu, J. Q.; Lu, X. B.; Li, J. H., Temperature, ionic strength and pH induced electrochemical switching of smart polymer interfaces, *Chem. Commun.* **2006**, 4820-4822.

(4) Hwang, E.; de Silva, K. M. N.; Seevers, C. B.; Li, J. R.; Garno, J. C.; Nesterov, E. E., Self-assembled monolayer initiated electropolymerization: A route to thin-film materials with enhanced photovoltaic performance, *Langmuir* **2008**, *24*, 9700-9706.

(5) Berlin, A.; Vercelli, B.; Zotti, G., Polythiophene- and polypyrrole-based mono- and multilayers, *Polym. Rev.***2008**, *48*, 493-530.

(6) Li, L. Q.; Hu, W. P.; Chi, L. F.; Fuchs, H., Polymer Brush and Inorganic Oxide Hybrid Nanodielectrics for High Performance Organic Transistors, *J. Phys. Chem. B* **2010**, *114*, 5315-5319.

(7) Zotti, G.; Vercelli, B.; Berlin, A., Monolayers and multilayers of conjugated polymers as nanosized electronic components, *Acc. Chem. Res.* **2008**, *41*, 1098-1109.

(8) Edmondson, S.; Osborne, V. L.; Huck, W. T. S., Polymer brushes via surface-initiated polymerizations, *Chem. Soc. Rev.* **2004**, *33*, 14-22.

(9) Barbey, R. l.; Lavanant, L.; Paripovic, D.; Schüwer, N.; Sugnaux, C.; Tugulu, S.; Klok, H.-A., Polymer Brushes via Surface-Initiated Controlled Radical Polymerization: Synthesis, Characterization, Properties, and Applications, *Chem. Rev.* **2009**, *109*, 5437-5527.

(10) Paoprasert, P.; Spalenka, J. W.; Peterson, D. L.; Ruther, R. E.; Hamers, R. J.; Evans, P. G.; Gopalan, P., Grafting of poly(3-hexylthiophene) brushes on oxides using click chemistry, *J. Mater. Chem.* **2010**, *20*, 2651-2658.

(11) Milchev, A.; Wittmer, J. P.; Landau, D. P., Formation and equilibrium properties of living polymer brushes, *J. Chem. Phys.* **2000**, *112*, 1606-1615.

(12) Lomadze, N.; Perez, M.; Prucker, O.; Ruhe, J.; Reinecke, H., Step-and-Repeat Assembly of Molecularly Controlled Ultrathin Polyaramide Layers, *Macromolecules* **2010**, *43*, 9056-9062.

(13) Zotti, G.; Zecchin, S.; Vercelli, B.; Berlin, A.; Grimoldi, S.; Groenendaal, L.; Bertoncello, R.; Natali, M., Surface-initiated polymerization of thiophene and pyrrole monomers on poly(terthiophene) films and oligothiophene monolayers, *Chem. Mater.* **2005**, *17*, 3681-3694.

(14) Beryozkina, T.; Boyko, K.; Khanduyeva, N.; Senkovskyy, V.; Horecha, M.; Oertel, U.; Simon, F.; Stamm, M.; Kiriy, A., Grafting of Polyfluorene by Surface-Initiated Suzuki Polycondensation, *Angew. Chem., Int. Ed.* **2009**, *48*, 2695-2698.

(15) Sontag, S. K.; Marshall, N.; Locklin, J., Formation of conjugated polymer brushes by surface-initiated catalyst-transfer polycondensation, *Chem. Commun.* **2009**, 3354-3356.

(16) Senkovskyy, V.; Tkachov, R.; Beryozkina, T.; Komber, H.; Oertel, U.; Horecha, M.; Bocharova, V.; Stamm, M.; Gevorgyan, S. A.; Krebs, F. C.; Kiriy, A., "Hairy" Poly(3-hexylthiophene) Particles Prepared via Surface-Initiated Kumada Catalyst-Transfer Polycondensation, *J. Am. Chem. Soc.* **2009**, *131*, 16445-16453.

(17) Tkachov, R.; Senkovskyy, V.; Horecha, M.; Oertel, U.; Stamm, M.; Kiriy, A., Surface-initiated Kumada catalyst-transfer polycondensation of poly(9,9-dioctylfluorene) from organosilica particles: chain-confinement promoted beta-phase formation, *Chem. Commun.* **2010**, *46*, 1425-1427.

(18) Huisgen, R.; Szeimies, G.; Mobius, L., 1,3-dipolare cycloadditionen. 32. Kinetik der additionen organischer azide an CC-mehrfachbindungen, *Chem. Ber. Recl.* **1967**, *100*, 2494-2507.

(19) Meldal, M.; Tornoe, C. W., Cu-catalyzed azide-alkyne cycloaddition, *Chem. Rev.* **2008**, *108*, 2952-3015.

(20) Amblard, F.; Cho, J. H.; Schinazi, R. F., Cu(I)-Catalyzed Huisgen Azide-Alkyne 1,3-Dipolar Cycloaddition Reaction in Nucleoside, Nucleotide, and Oligonucleotide Chemistry, *Chem. Rev.* **2009**, *109*, 4207-4220.

(21) Kolb, H. C.; Finn, M. G.; Sharpless, K. B., Click Chemistry: Diverse Chemical Function from a Few Good Reactions, *Angew. Chem. Int. Ed.* **2001**, *40*, 2004-2021.

(22) Barner-Kowollik, C.; Du Prez, F. E.; Espeel, P.; Hawker, C. J.; Junkers, T.; Schlaad, H.; Van Camp, W., "Clicking" Polymers or Just Efficient Linking: What Is the Difference?, *Angew. Chem. Int. Ed.* **2011**, *50*, 60-62.

(23) Binder, W. H.; Sachsenhofer, R., 'Click' Chemistry in Polymer and Material Science: An Update, *Macromol. Rapid Commun.* **2008**, *29*, 952-981.

(24) van Steenis, D.; David, O. R. P.; van Strijdonck, G. P. F.; van Maarseveen, J. H.; Reek, J. N. H., Click-chemistry as an efficient synthetic tool for the preparation of novel conjugated polymers, *Chem. Commun.* **2005**, 4333-4335.

(25) Karim, M. A.; Cho, Y. R.; Park, J. S.; Kim, S. C.; Kim, H. J.; Lee, J. W.; Gal, Y. S.; Jin, S. H., Novel fluorene-based functional 'click polymers' for quasi-solid-state dye-sensitized solar cells, *Chem. Commun.* **2008**, 1929-1931.

(26) Karim, A.; Cho, Y. R.; Park, J. S.; Ryu, T. I.; Lee, M. J.; Song, M.; Jin, S. H.; Lee, J. W.; Gal, Y. S., Comparison of Three Different Click Reaction Methods for the Synthesis of Fluorene-Based Polymers and Performance in Quasi-Solid-State DSSCs, *Macromol. Chem. Phys.* **2008**, *209*, 1968-1975.

(27) Chen, X. D.; Braunschweig, A. B.; Wiester, M. J.; Yeganeh, S.; Ratner, M. A.; Mirkin, C. A., Spectroscopic Tracking of Molecular Transport Junctions Generated by Using Click Chemistry, *Angew. Chem., Int. Ed.* **2009**, *48*, 5178-5181.

(28) Ostaci, R. V.; Damiron, D.; Capponi, S.; Vignaud, G.; Leger, L.; Grohens, Y.; Drockenmuller, E., Polymer brushes grafted to "Passivated" silicon substrates using click chemistry, *Langmuir* **2008**, *24*, 2732-2739.

(29) Devaraj, N. K.; Decreau, R. A.; Ebina, W.; Collman, J. P.; Chidsey, C. E. D., Rate of interfacial electron transfer through the 1,2,3-triazole linkage, *J. Phys. Chem. B* **2006**, *110*, 15955-15962.

(30) Lee, J. K.; Chi, Y. S.; Choi, I. S., Reactivity of acetylenyl-terminated self-assembled monolayers on gold: Triazole formation, *Langmuir* **2004**, *20*, 3844-3847.

(31) Acharya, J. R.; Zhang, H.; Li, X.; Nesterov, E. E., Chemically Controlled Amplified Ratiometric Fluorescence in Surface-Immobilized End-Capped Oligo(p-phenylene ethynylene)s, *J. Am. Chem. Soc.* **2009**, *131*, 880-881.

(32) Hou, J. H.; Tan, Z. A.; Yan, Y.; He, Y. J.; Yang, C. H.; Li, Y. F., Synthesis and photovoltaic properties of two-dimensional conjugated polythiophenes with bi(thienylenevinylene) side chains, *J. Am. Chem. Soc.* **2006**, *128*, 4911-4916.

(33) Pinto, J. C.; Whiting, G. L.; Khodabakhsh, S.; Torre, L.; Rodriguez, A. B.; Dalgliesh, R. M.; Higgins, A. M.; Andreasen, J. W.; Nielsen, M. M.; Geoghegan, M.; Huck, W. T. S.; Sirringhaus, H., Organic thin film transistors with polymer brush gate dielectrics synthesized by atom transfer radical polymerization, *Adv. Funct. Mater.* **2008**, *18*, 36-43.

(34) Corain, B.; Bressan, M.; Rigo, P., The behaviour of nickel(0) diphosphine complexes towards unsaturated organic compounds, *J. Organomet. Chem.* **1971**, *28*, 133-136.

(35) Park, K.; Park, S. H.; Kim, E.; Kim, J. D.; An, S. Y.; Lim, H. S.; Lee, H. H.; Kim, D. H.; Ryu, D. Y.; Lee, D. R.; Cho, J. H., Polymer Brush As a Facile Dielectric Surface Treatment for High-Performance, Stable, Soluble Acene-Based Transistors, *Chem. Mater.* **2010**, *22*, 5377-5382.

CHAPTER 5 EXPERIMENTAL SECTION.

5.1 General Information.

All reactions were performed under an atmosphere of dry nitrogen. Melting points were determined in open capillaries and are uncorrected. Column chromatography was performed on silica gel (Sorbent Technologies, 60 Å, 40-63 μm) slurry packed into glass columns. Kugelrohr distillation was performed using a Büchi GKR-50 evaporator equipped with a glass oven. Tetrahydrofuran (THF), dichloromethane, ether, toluene, and acetonitrile were dried by passing through activated alumina, and N,N-dimethylformamide (DMF) – by passing through activated molecular sieves using a PS-400 Solvent Purification System from Innovative Technology, Inc. The water content of the solvents was periodically controlled by Karl Fischer titration (using a DL32 coulometric titrator from Mettler Toledo). All other solvents (HPLC or anhydrous grade) used as received. All reagents were obtained from Aldrich, Acros Organics, and Alfa Aesar and used without further purification. Indium tin oxide (ITO) coated glass slides with 8-12 Ohm/sq. surface resistivity were purchased from Aldrich and Delta Technology. 75 x 25 mm^2 sized rectangular quartz slides were purchased from Chemglass. Silicon (111) wafers were purchased from Virginia Semiconductor Inc. Monodisperse latex mesospheres (300 nm diameter) were supplied by Thermo Scientific. ^1H NMR spectra were recorded at 400 or 250 MHz, and are reported in ppm downfield from tetramethylsilane. UV-visible spectra were recorded on Varian Cary 50 UV-Vis spectrophotometer. All electrochemical and photoelectrochemical experiments were performed using Autolab PGSTAT 302 potentiostat from Eco Chemie. High resolution mass spectra were obtained at the LSU Department of Chemistry Mass Spectrometry Facility using an ESI method, and a peak matching protocol to determine the mass and error range of the molecular ion. All XPS spectra were obtained at Materials Characterization Center at the LSU

Department of Mechanical Engineering using Kratos AXIS 165 X-ray Photoelectron Spectroscope and Scanning Auger Microscope.

5.2 Synthesis.

5.2.1 Preparation of Electropolymerization Initiators in Chapter 2.

Scheme 5.1. Synthesis of precursor **TEDT.**

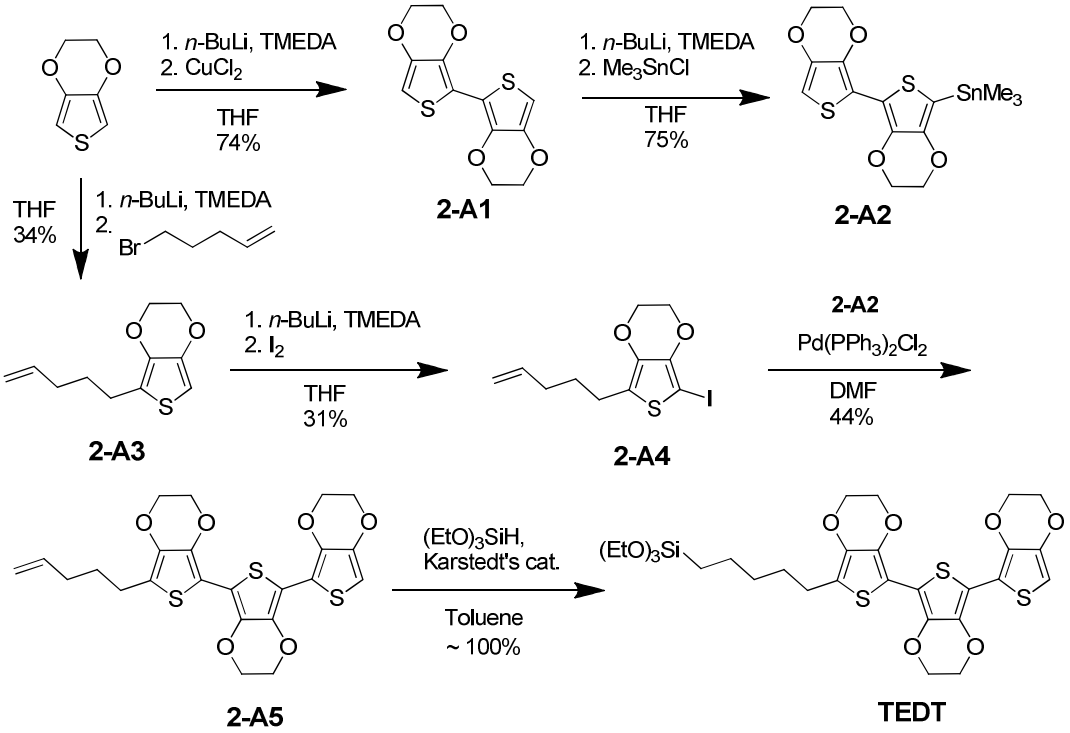

2,2′-Bis(3,4-ethylenedioxythiophene) (bisEDOT) (2-A1) was prepared following a modified literature procedure[1]. A solution of *n*-BuLi (34.0 ml of 1.6 M solution in hexanes, 54.4 mmol) was added dropwise to a stirred at -78 °C solution of 7.5 g (52.8 mmol) of 3,4-ethylenedioxythiophene in 200 ml of THF. After addition was complete, the temperature was slowly raised to and the reaction mixture was stirred for 2 h. Anhydrous $CuCl_2$ (7.4 g, 55.5 mmol) was added in one portion and the stirring was continued for an additional 12 h at 0 °C. The black precipitate was filtered and the solution was poured into crushed ice, extracted with CH_2Cl_2,

washed with brine, water and dried over Na_2SO_4. The solution was filtered and passed through a Celite column. After concentration in vacuo, the product was purified by column chromatography on silica gel (eluent CH_2Cl_2 - hexane 1:1) to yield 5.5 g (74%) of **2-A1** as a white solid, mp 223 °C (lit.[1] mp 203-204 °C). The spectral properties were in agreement with literature data.

5-(Trimethylstannyl)-2,2′-bis(3,4-ethylenedioxythiophene) (2-A2). A solution of *n*-BuLi (9.1 ml of 1.6 M solution in hexanes, 14.6 mmol) was added dropwise to a stirred at -78 °C solution of 4.0 g (14.2 mmol) of **2-A1** in 300 ml of THF. The reaction mixture was stirred for 1.5 h at the same temperature, followed by dropwise addition of a solution of 2.9 g (14.6 mmol) of Me_3SnCl in 20 ml of THF. The resulting solution was stirred at -78 °C for 1 h. After allowing to warm to room temperature, the reaction mixture was concentrated in vacuo, and the residue was extracted with a CH_2Cl_2 – hexane mixture. The combined organic fractions were dried over Na_2SO_4, and concentrated in vacuo. The crude product was thoroughly washed with methanol followed by hexane to yield 4.8 g (75%) of **2-A2** as a colorless solid, mp 153 - 156 °C. ^{1}H NMR ($CDCl_3$) δ 6.25 (s, 1H), 4.40 – 4.10 (m, 8H), 0.35 (s, 9H). HRMS *m/e* 446.9752 $(M+H)^+$ (calcd for $C_{15}H_{19}O_4S_2Sn$ 446.9741).

2-(Pent-4-en-1-yl)-3,4-ethylenedioxythiophene (2-A3). A solution *n*-BuLi (17.6 ml of 1.6 M solution in hexanes, 28.2 mmol) was added dropwise to a stirred at -78 °C solution of 4.0 g (28.2 mmol) of 3,4 ethylenedioxythiophene and 3.29 g (4.24 ml, 28.2 mmol) of TMEDA in 50 ml of THF. The resulting mixture was stirred for 2.5 h at the same temperature and then allowed to warm to room temperature and stirred at this temperature for 15 min. Then the temperature was decreased to -78 °C, and 5-bromo-1-pentene (5.09 g, 4.05 ml, 34.2 mmol) was added dropwise. The resulting solution was allowed to warm to room temperature overnight. It was poured into a conc. NH_4Cl solution and extracted with ether. The organic layer was washed with

water and brine, and dried over Na_2SO_4. After concentration in vacuo, the product mixture was separated by distillation on a Kugelrohr apparatus in vacuo (10 mm Hg) to yield 2.02 g (34%) of **2-A3** as a yellow oil. ^{1}H NMR ($CDCl_3$) δ 6.11 (s, 1H), 5.93 – 5.73 (m, 1H), 5.10 – 4.91 (m, 2H), 4.22 – 4.15 (m, 4H), 2. 65 (t, J = 7.4 Hz, 2H), 2.20 – 2.00 (m, 2H), 1.78 – 1.61 (m, 2H).

2-Iodo-5-(pent-4-en-1-yl)-3,4-ethylenedioxythiophene (2-A4). A solution *n*-BuLi (6.6 ml of 1.6 M solution in hexanes, 10.6 mmol) was added dropwise to a stirred at -78 °C solution of 2.02 g (9.6 mmol) of **2-A3** and 1.24 g (1.6 ml, 10.6 mmol) of TMEDA in 100 ml of THF. The resulting mixture was stirred for 2.5 h at the same temperature and then allowed to warm to room temperature and stirred at this temperature for 15 min. Then the temperature was decreased to -78 °C, and a solution of 3.18 g (12.5 mmol) of iodine in 5 ml of THF was added dropwise. The resulting solution was allowed to warm to room temperature overnight, poured into a conc. $Na_2S_2O_3$ solution, extracted with ether, washed successively with water and brine, and dried over Na_2SO_4. After concentrating in vacuo, the crude product was purified by chromatography on silica gel (column 6x30 cm, eluent CH_2Cl_2 – hexane 2:1), and a fraction with R_f 0.66 afforded 1.0 g (31%) of **2-A4** as a yellow oil. ^{1}H NMR ($CDCl_3$) δ 5.61 – 5.97 (m, 1H), 5.12 – 4.86 (m, 2H), 4.40 – 4.05 (m, 4H), 2.63 (t, J = 7.7 Hz, 2H), 2.18 – 1.99 (m, 2H), 1.77 – 1.54 (m, 2H).

5-(Pent-4-en-1-yl)-2,2′:5′,2″:5″,2‴-ter(3,4-ethylenedioxythiophene) (2-A5). A solution of 0.63 g (1.87 mmol) of **2-A4**, 1.0 g (2.25 mmol) of **2-A2**, and 66 mg (0.094 mmol) of $Pd(PPh_3)_2Cl_2$ in 2.5 ml of anhydrous DMF was stirred at 80°C in a sealed flask for 16 hours. After cooling to room temperature, the reaction mixture was poured into water, extracted with CH_2Cl_2, washed successively with water and brine, and dried over Na_2SO_4. After concentration in vacuo, the crude product was purified by chromatography on silica gel (column 4×34 cm, eluent CH_2Cl_2 – hexane 2:1), and a fraction with R_f 0.35 afforded 0.40 g (44%) of **2-A5** as a yellow solid, mp 167-170 °C. ^{1}H NMR (acetone-D_6) δ 6.36 (s, 1H), 5.92 – 5.72 (m, 1H), 5.08 –

4.88 (m, 2H), 4.42 – 4.17 (m, 12H), 2.64 (t, *J* = 7.6 Hz, 2H), 2.20 – 2.07 (m, 2H), 1.77 – 1.59 (m, 2H). HRMS *m/e* 491.0634 $(M+H)^+$ (calcd for $C_{23}H_{23}O_6S_3$ 491.0651).

5-(5-Triethoxysilylpent-1-yl)-2,2′:5′,2″:5″,2‴-ter(3,4-ethylenedioxy thiophene) (TEDT). A solution of 56 mg (0.11 mmol) of **2-A5** and 1 drop of Platinum(0)-1,3-divinyl-1,1,3,3-tetramethyl-disiloxane complex (Karstedt's catalyst, 0.1 M solution in poly(dimethylsiloxane)) in 3.5 ml of toluene was stirred for 10 min at room temperature, followed by addition of 74 mg (83 μl, 0.45 mmol) of triethoxysilane. The reaction mixture was stirred for 2 days at room temperature, and then filtered through a column with C_{18} reverse-phase silica gel (Sorbent Tech., 60 Å, 40~75 μm). Concentration in vacuo yielded **TEDT** as a greenish yellow solid in a quantitative yield. It was dissolved in toluene to 1 mM concentration to use for self-assembly; the solution can be stored in a freezer for few months. ^{1}H NMR (acetone-D_6) δ 6.37 (s, 1H), 4.45 – 4.11 (m, 12H), 3.80 (q, *J* = 7.0 Hz, 6H), 2.64 (t, *J* = 7.0 Hz, 2H), 1.73 – 1.53 (m, 2H), 1.52 – 1.34 (m, 4H), 1.18 (t, *J* = 7.0 Hz, 9H), 0.73 - 0.42 (m, 2H).

5-(Tributylstannyl)-2,2′-bithiophene (2-B1) was prepared as described in the literature[2]. The crude product was distilled in a Kugelrohr apparatus (oven temperature 240 °C, 0.05 mm Hg) to afford pure **2-B1** as a colorless liquid (yield 50%).

2-(Pent-4-en-1-yl)thiophene (2-B2). A solution *n*-BuLi (20.6 ml of 1.6 M solution in hexanes, 33.5 mmol) was added dropwise to a stirred at -78 °C solution of 2.35 g (28.0 mmol) of thiophene and 3.88 g (5.0 ml, 33.5 mmol) of TMEDA in 125 ml of THF. The resulting mixture was stirred for 1.5 h at the same temperature and then allowed to warm to room temperature and stirred at this temperature for 15 min. Then the temperature was decreased to -78 °C, and 5-bromo-1-pentene (5.0 g, 33.5 mmol) was added dropwise. The reaction mixture was allowed to warm to room temperature overnignt. Then it was poured into ice water, extracted with ether, washed with water and brine, and dried over Na_2SO_4. Conventration in vacuo gave a crude

product, which was purified by vacuum distillation (120 °C, 1 mm Hg) to yield 1.6 g (37%) of **2-B2** as colorless oil. The spectral properties were in agreement with the literature data[3].

Scheme 5.2. Synthesis of precursor **TT.**

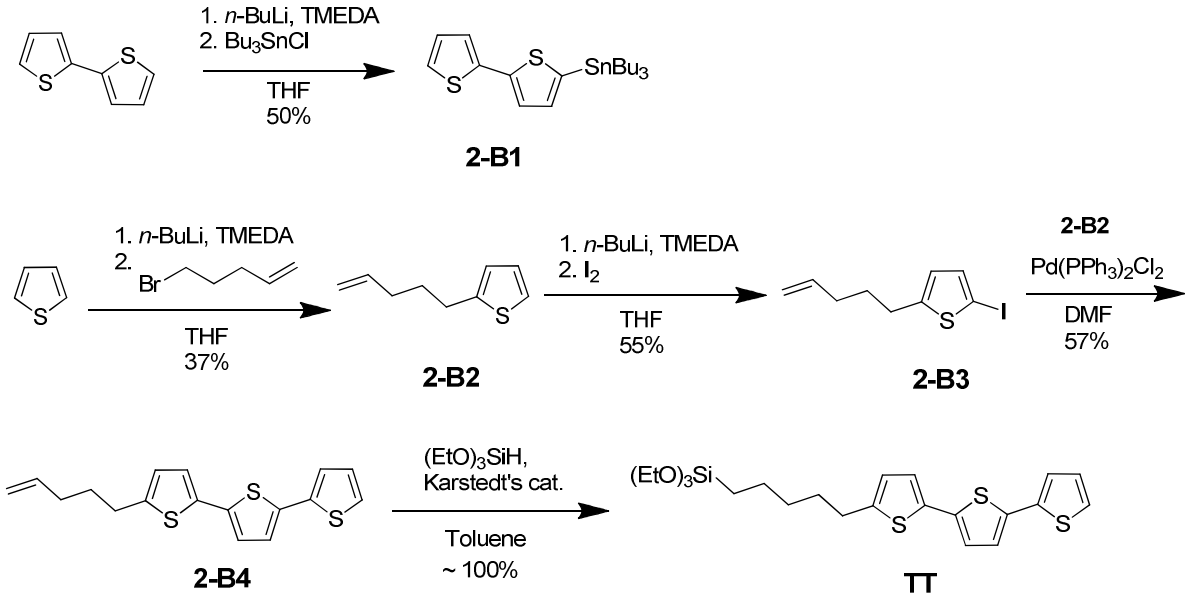

2-Iodo-5-(pent-4-en-1-yl)thiophene (2-B3). This compound was prepared following the procedure for compound **2-A4**. A reaction of 1.6 g (10.5 mmol) of **2-B2**, 1.47 g (1.9 ml, 12.9 mmol) of TMEDA, *n*-BuLI (7.9 ml of 1.6 M solution in hexanes, 12.6 mmol), and 3.5 g (13.8 mmol) of iodine gave, after distillation on a Kugelrohr apparatus, 1.6 g (55%) of **2-B3** as a yellow oil. ^{1}H NMR ($CDCl_3$) δ 7.04 (d, J = 3.6 Hz, 1H), 6.47 (dd, J_1 = 3.6, J_2 = 0.9 Hz, 1H), 5.90 – 5.60 (m, 1H), 5.14 – 4.83 (m, 2H), 2.80 (t, J = 7.7 Hz, 2H), 2.11 (q, J = 6.7 Hz, 2H), 1.73 (t, J = 7.5 Hz, 2H).

5-(Pent-4-en-1-yl)-2,2′:5′,2′′-terthiophene (2-B4). This compound was prepared following the procedure for compound **2-A5**. A reaction of 1.6 g (5.8 mmol) of **2-B3**, 3.14 g (6.9 mmol) of **2-B1**, and 0.20 g (0.29 mmol) of $Pd(PPh_3)_2Cl_2$ in 8 ml of DMF afforded the crude product which was purified by column chromatography on silica gel (eluent CH_2Cl_2 – hexane 1:4), and further

purified by recrystallization from hexane to yield 1.04 g (57%) of **2-B4** as a yellow solid, mp 47-51 °C. ^{1}H NMR ($CDCl_3$) δ 7.20 (dd, J_1 = 5.1 Hz, J_2 = 1.1 Hz, 1H), 7.16 (dd, J_1 = 3.6 Hz, J_2 = 1.0 Hz, 1H), 7.09 – 6.92 (m, 4H), 6.69 (d, J = 3.6 Hz, 1H), 5.95 – 5.70 (m, 1H), 5.14 – 4.90 (m, 2H), 2.81 (t, J = 7.5 Hz, 2H), 2.15 (q, J = 7.0 Hz, 2H), 1.79 (p, J = 7.7 Hz, 2H). HRMS *m/e* 317.0485 $(M+H)^+$ (calcd for $C_{17}H_{17}S_3$ 317.0487).

5-(5-Triethoxysilylpent-1-yl)-2,2′:5′,2″:5″,2‴-terthiophene (TT). This compound was prepared following the procedure for compound **TEDT**. Thus, the precursor **2-B4** (32 mg, 0.10 mmol) was quantitatively converted to **TT** (yellow solid), which can be stored in refrigerator as a 1 mM solution in toluene. ^{1}H NMR (acetone-D_6) δ 7.42 (d, J = 4.7 Hz, 1H), 7.28 (d, J = 2.9 Hz, 1H), 7.19 (d, J = 3.7 Hz, 1H), 7.16 – 7.02 (m, 3H), 6.80 (d, J = 3.1 Hz, 1H), 3.80 (q, J = 7.0 Hz, 6H), 2.93 – 2.75 (m, 2H), 1.79 -1.62 (m, 2H), 1.58 – 1.35 (m, 4H), 1.18 (t, J = 7.0 Hz, 9H), 0.70 – 0.50 (m, 2H).

5.2.2 Synthesis of Precursors in Chapter 3.

Scheme 5.3. Synthesis of **3-1** and **3-2.**

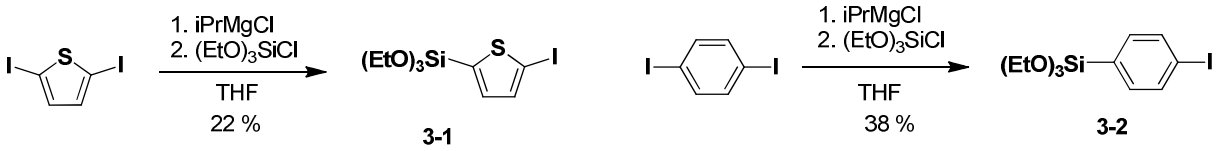

Triethoxy(5-iodothiophen-2-yl)silane (3-1). A solution of iPrMgCl (1 ml of 2.0 M solution in THF, 2.0 mmol) was added dropwise to a stirred solution of 0.67 g (2.0 mmol) of 2,5-diiodothiophene in 3 ml of THF at 0 °C. The reaction mixture was stirred for 1.5 h at the same temperature and then the temperature was lowered to -78 °C. A solution of 0.34 g (0.43 ml, 2.2 mmol) of chlorotriethoxysilane in THF was added dropwise. The resulting solution was allowed to warm to room temperature overnight, concentrated in vacuo, and precipitated with hexane. The solid precipitate was filtered and filtrate was concentrated in vacuo to afford the crude

product which was purified by chromatography on silica gel (eluent $CHCl_3$, R_f 0.59), and yielded 0.16 g (22%) of **3-1** as a brown colored oil. ^{1}H NMR ($CDCl_3$) δ 7.31 (d, J = 4 Hz, 1H), 7.13 (d, J = 4 Hz, 1H), 3.87 (q, J = 8 Hz, 6H), 1.24 (t, J = 8, 9H).

Triethoxy(4-iodophenyl)silane (3-2). This compound was prepared following the literature procedure.[4] A reaction of 0.66 g (2.0 mmol) of 1,4-diiodobenzene, 1 ml (2.0 mmol) of 2.0 M solution of iPrMgCl in THF, and 0.34 g (0.43 ml, 2.2 mmol) of chlorotriethoxysilane in 5 ml of THF afforded the crude product which was purified by column chromatography on silica gel (eluent $CHCl_3$, R_f 0.60), and yielded 0.28 g (38%) of product as a yellow oil. The characterization data were in a good agreement with the literature data ^{1}H NMR ($CDCl_3$) δ 7.73 (d, J = 8 Hz, 2H), 7.39 (d, J = 8 Hz, 1H), 3.85 (q, J = 8 Hz, 6H), 1.24 (t, J = 8 Hz, 9H).

Scheme 5.4. Synthesis of **3-3.**

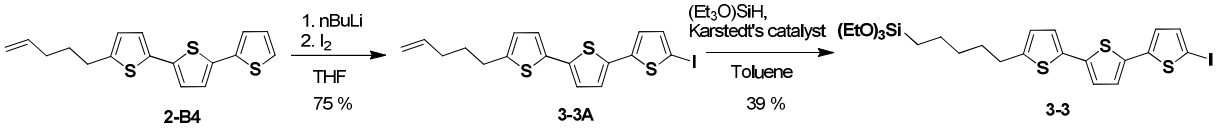

5-iodo-5''-(pent-4-en-1-yl)-2,2':5',2''-terthiophene (3-3A). A solution of *n*-BuLi (1.2 ml of 1.6 M solution in hexanes, 1.9 mmol) was added dropwise to a stirred at -78 °C solution of 0.2 g (0.63 mmol) of previously prepared **2-B4** and 0.22 g (0.28 ml, 1.9 mmol) of TMEDA in 10 ml of THF. The resulting mixture was stirred for 3 h at the same temperature and then allowed to warm to room temperature and stirred at this temperature for 10 min. Then the temperature was decreased to -78 °C, and a solution of 0.5 g (1.95 mmol) of I_2 in 3 ml of THF was added dropwise. The reaction mixture was allowed to warm to room temperature overnignt. Then it was poured into conc. $Na_2S_2O_3$ solution, extracted with CH_2Cl_2, washed with water and brine, and dried over Na_2SO_4. Conventration in vacuo gave a crude product which was purified by column chromatography on silica gel (eluent $CHCl_3$ – hexane 1:6), and a fraction with R_f 0.56 afforded

0.21 g (75%) of **3-3A** as a yellow solid, mp 99 - 106 °C. ^{1}H NMR ($CDCl_3$) δ 7.15 (d, *J* = 3.8 Hz, 1H), 7.13 – 6.94 (m, 3H), 6.82 (d, *J* = 3.8 Hz, 1H), 6.69 (d, *J* = 3.6 Hz, 1H), 5.90 – 5.75 (m, 1H), 5.16 – 4.98 (m, 2H), 2.80 (t, *J* = 7.6 Hz, 2H), 2.14 (q, *J* = 7.1 Hz, 2H).

Triethoxy(5-(5''-iodo-[2,2':5',2''-terthiophen]-5-yl)pentyl)silane (3-3) A solution of 100 mg (0.226 mmol) of **3-3A** and 0.2 ml of Platinum(0)-1,3-divinyl-1,1,3,3-tetramethyl-disiloxane complex (Karstedt's catalyst, 0.1 M solution in poly(dimethylsiloxane)) in 3 ml of toluene was stirred for 10 min at room temperature, followed by addition of 2.7 g (3 ml, 16 mmol) of triethoxysilane. The reaction mixture was stirred for 2 days at room temperature, and concentrated in vacuo. Purification by column chromatography on silica gel (eluent $CHCl_3$) afforded 54 mg (39 %) of **3-3** as a brown oil. ^{1}H NMR (acetone-D_6) δ 7.14 (d, *J* = 3.7 Hz, 1H), 7.00 – 6.90 (m, 3H), 6.80 (d, *J* = 3.8 Hz, 1H), 6.67 (d, *J* = 3.4 Hz, 1H), 3.82 (q, *J* = 7.0 Hz, 6H), 2.79 (t, *J* = 7.4 Hz, 2H), 1.72 – 1.66 (m, 2H), 1.65 – 1.30 (m, 4H), 1.23 (t, *J* = 7.0 Hz, 9H), 0.65 (t, *J* = 6.0 Hz, 2H).

5.2.3 Synthesis of Monomers and Precursors in Chapter 4.

5,5'-diiodo-2,2'-bithiophene (4-1). This product was prepared following the modified literature procedure.[5] A reaction mixture of 4.0 g (24 mmol) of bithiophene, 13.5 g (60 mmol) of NIS, and 4 ml of acetic acid in 360 ml of methanol was stirred for 2 hours at room temperature. The precipitate was filtered and washed with copious amount of cold methanol to yield 9.23 g (92 %) of **4-1** as a green solid. The characterization data were in a good agreement with the literature data.[5] ^{1}H NMR ($CDCl_3$) δ 7.15 (d, *J* = 3.8 Hz, 2H), 6.78 (d, *J* = 3.8 Hz, 2H).

5,5'-bis((trimethylsilyl)ethynyl)-2,2'-bithiophene (4-2) was prepared following the modified literature procedure.[5] A solution of 1.0 g (2.4 mmol) of **4-1**, 0.56 g (0.81 ml, 5.8 mmol) of trimethylsilylacetylene, 0.138 g (0.12 mmol) of $Pd(PPh_3)_4$, and 46 mg (0.24 mmol) of CuI in 10 ml of 7 : 3 mixture of toluene and diisopropylamine was stirred at room temperature in a

sealed flask for 2 days. After concentration in vacuo, the crude product was purified by column chromatography on silica gel (eluent CH_2Cl_2 – hexane 1:4, R_f 0.30) to give 0.85 g (99 %) of **4-2** as a yellow solid. The characterization data were in a good agreement with the literature data.[5] ^{1}H NMR ($CDCl_3$) δ 7.11 (d, J = 3.8 Hz, 2H), 7.00 (d, J = 3.8 Hz, 2H), 0.25 (s, 18H).

Scheme 5.5. Synthesis of monomer **4-1**, **4-2**, and **4-3.**

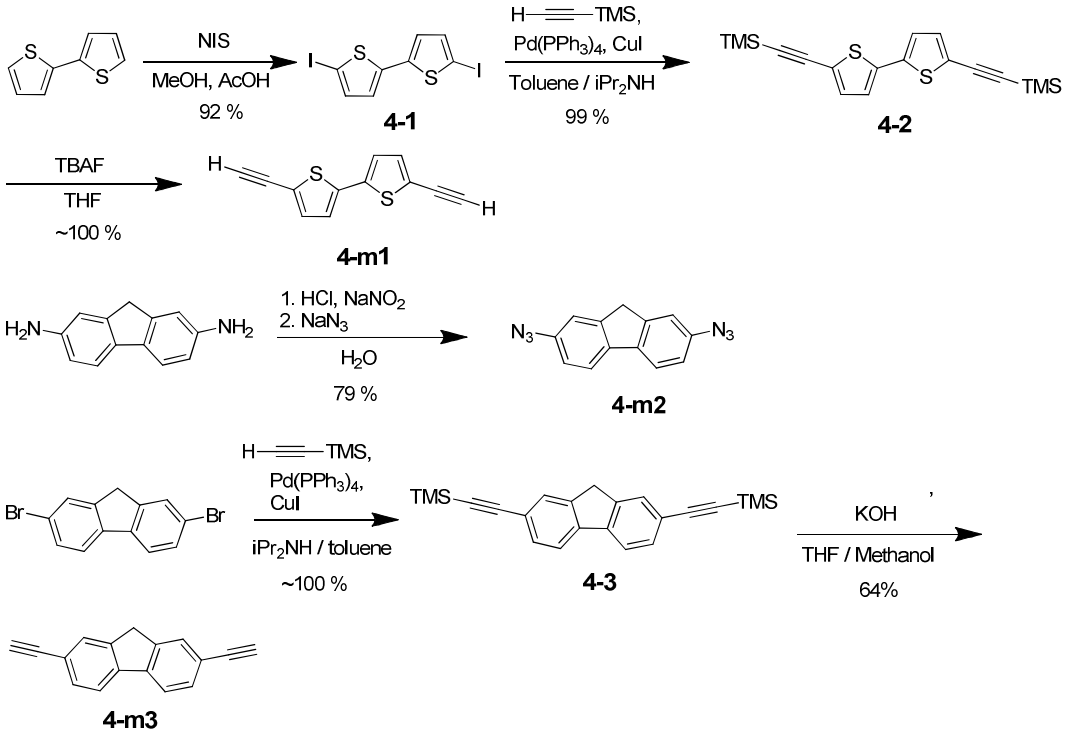

5,5'-diethynyl-2,2'-bithiophene (4-m1) was prepared following the modified literature procedure.[5] To a stirred solution of 0.7 g (1.95 mmol) of **4-2** in 10 ml of THF, a solution of KOH (0.65 g, 11.7 mmol) in 5 ml of methanol was added. After stirring for 1 hour at room temperature, the mixture was poured into water, extracted with $CHCl_3$, washed with water and brine, and dried over Na_2SO_4. Concentration in vacuo gave a crude product, which was purified by flash column chromatography on silica gel (eluent CH_2Cl_2 – hexane 1:4, R_f 0.30) to give quantitative yield (0.43 g) of **4-m1** as a brown solid. The characterization data were in a good agreement with

the literature data.[5] ^{1}H NMR ($CDCl_3$) δ 7.18 (d, J = 3.8 Hz, 2H), 7.04 (d, J = 3.8 Hz, 2H), 3.41 (s, 2H).

2,7-diazido-9H-fluorene (4-m2) was synthesized through modified literature procedure.[6] A solution of 0.2 g (1 mmol) of 9H-fluorene-2,7-diamine, 0.2 g (3 mmol) of $NaNO_2$, 2 ml of HCl in 6 ml of D.I. water was stirred at 0 °C for 2 hours. Then temperature was increased to room temperature, and 0.2 g (3 mmol) of NaN_3 in 2 ml of D.I. water was added dropwise. After stirring for additional 1 hour at the same temperature, the mixture was poured into water, extracted with CH_2Cl_2, washed with water, and dried over Na_2SO_4. Concentration in vacuo gave a crude product, which was purified by column chromatography on Florisil (eluent ethyl acetate – hexane 1:10, R_f 0.20) to give 0.17 g (79 %) of **4-m2** as a brown solid. The characterization data were in a good agreement with the literature data.[6] ^{1}H NMR ($CDCl_3$) δ 7.67 (d, J = 8.2 Hz, 2H), 7.19 (s, 2H), 7.03 (d of d, J_1 = 8.2 Hz, J_1 = 2 Hz. 2H).

2,7-bis((trimethylsilyl)ethynyl)-9H-fluorene (4-3). This compound was prepared following the procedure for compound **4-2**. A reaction of 2.0 g (6.3 mmol) of 2,7-dibromo-9H-fluorene, 2.2 ml (15.1 mmol) of ethynyltrimethylsilane, 0.138 g (0.12 mmol) of $Pd(PPh_3)_4$, and 46 mg (0.24 mmol) of CuI in 20 ml of 7 : 3 mixture of toluene and diisopropylamine afforded the crude product which was purified by column chromatography on silica gel (eluent $CHCl_3$ – hexane 2:1, R_f 0.89) to produce quantitative yield (2.3 g) of **4-3** as a white solid, mp 139 - 141 °C. ^{1}H NMR ($CDCl_3$) δ 7.69 (s, 2H), 7.65 (d, J = 5.9 Hz, 2H), 7.48 (d, J = 7.8 Hz, 2H), 0.27 (s, 18H).

2,7-diethynyl-9H-fluorene (4-m3). This compound was prepared following the procedure for compound **4-m1**. A reaction of 1.00 g (2.79 mmol) of **4-3** in 20 ml of THF, and 0.93 g (16.76 mmol) of KOH in 15 ml of methanol afforded the crude product which was purified by flash column chromatography on silica gel (eluent $CHCl_3$ – hexane 2:1, R_f 0.90) to yield 0.38 g

(64 %) of **4-m3** as a white solid, mp 133 - 135 °C. ^{1}H NMR ($CDCl_3$) δ 7.73 (s, 2H), 7.69 (d, *J* = 7.5 Hz, 2H), 7.52 (d, *J* = 7.8 Hz, 2H), 3.12 (s, 2H).

1-(Trimethylsilyl)-2-(4-(10-undecenyloxy)phenyl)acetylene (4-6) was synthesized following the literature procedures.[7]

Scheme 5.6. Synthetic route for **4-P1** and **4-P2.**

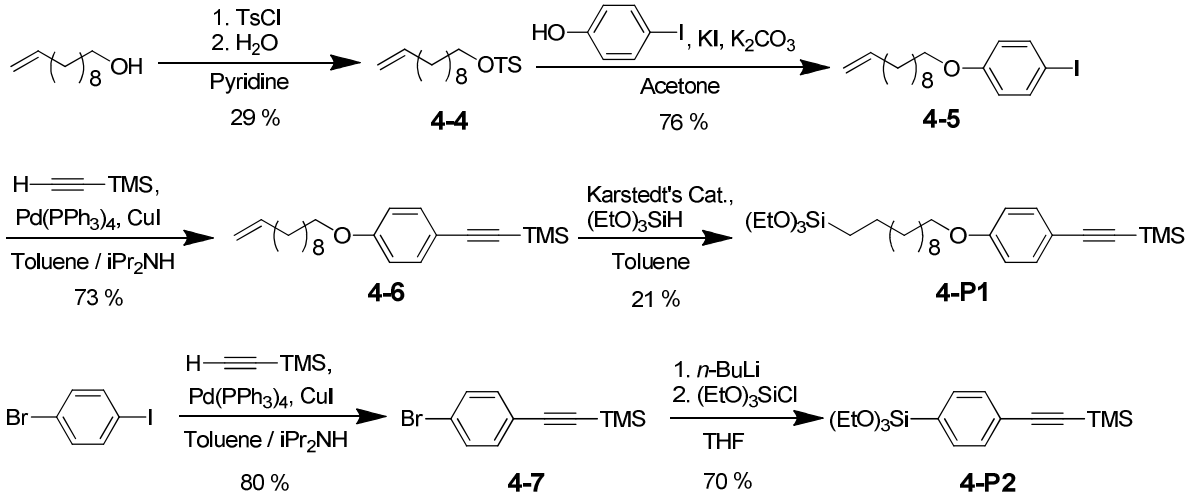

Triethoxy(11-(4-((trimethylsilyl)ethynyl)phenoxy)undecyl)silane (4-P1). This compound was prepared following the procedure for compound **3-3**. A reaction of 0.50 g (1.46 mmol) of **4-6**, 1.68 g (1.88 ml, 6.9 mmol) of triethoxysilane, and 1.5 ml of 0.1 M solution of Karstedt's catalyst in 10 ml of toluene afforded the crude product which was purified by column chromatography on silica gel (eluent $CHCl_3$) to yield 0.16 g (21%) of **4-P1** as a yellow oil. ^{1}H NMR ($CDCl_3$) δ 7.39 (d, *J* = 6.8 Hz, 2H), 6.81 (d, *J* = 8.8 Hz, 2H), 3.94 (t, *J* = 6.6 Hz, 2H), 3.82 (q, *J* = 7.0 Hz, 6H), 1.76 (p, *J* = 6.6 Hz, 2H), 1.54 – 1.24 (m, 25H), 0.63 (t, *J* = 5.8 Hz, 2H), 0.23 (s, 9H).

((4-Bromophenyl)ethynyl)trimethylsilane (4-7). This compound was prepared following the procedure for compound **4-2**. A reaction of 10.0 g (35.4 mmol) of 1-bromo-4-iodobenzene, 6 ml (42.4 mmol) of ethynyltrimethylsilane, 0.456 g (0.65 mmol) of $Pd(PPh_3)_4$, and 38 mg (0.2 mmol)

of CuI in 150 ml of 7 : 3 mixture of toluene and diisopropylamine afforded the crude product which was purified by column chromatography on silica gel (eluent hexane, R_f 0.50) to yield 7.7 g (86 %) of **4-7** as a white solid, mp 51 - 53 °C. ^{1}H NMR ($CDCl_3$) δ 7.72 (d, J = 8.4 Hz, 2H), 7.31 (d, J = 8.4 Hz, 2H), 0.24 (s, 18H).

Triethoxy(4-((trimethylsilyl)ethynyl)phenyl)silane (4-P2) A solution of *n*-BuLi (1.25 ml of 1.6 M solution in hexanes, 2 mmol) was added dropwise to a stirred at -78 °C solution of 0.51g (2.0 mmol) of **4-7** in 7 ml of THF. The reaction mixture was stirred for 3 h at the same temperature, followed by dropwise addition of 0.43 ml (2.2 mmol) of $(EtO)_3SiCl$. The resulting solution was stirred at -78 °C for 1 h. After allowing to warm to room temperature, the reaction mixture was concentrated in vacuo, and purified by column chromatography on silica gel (eluent $CHCl_3$, R_f 0.46) to yield 48 mg (7 %) of **4-P2** as a yellow oil. ^{1}H NMR ($CDCl_3$) δ 7.60 (d, J = 8.1 Hz, 2H), 7.46 (d, J = 8.1 Hz, 2H), 3.85 (q, J = 7.0 Hz, 6H), 1.23 (t, J = 7.0 Hz, 9H), 0.25 (s, 18H).

Scheme 5.7. Synthetic pathway for soluble polymer **4-R1.**

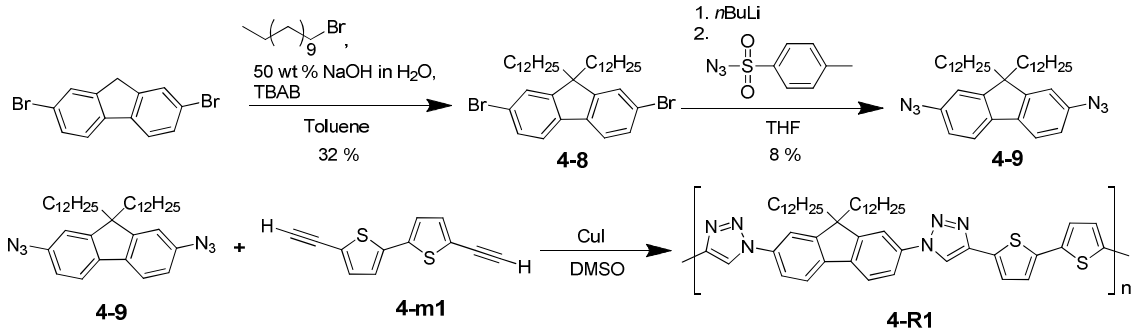

2,7-diazido-9,9-didodecyl-9H-fluorene (4-9) was prepared following the literature procedures.[8]

Soluble reference polymer (4-R1). A mixture of 16.8 mg (0.03 mmol) of **4-9**, 6.4 mg (0.03 mmol) of **4-m1**, and 0.5 mg (0.003 mmol) of CuI in 3 ml of DMSO was stirred for 2 days at 50 °C. To remove the DMSO, reaction mixture was precipitated into water, and precipitate was washed with

copious amount of methanol. The crude precipitated polymer was redissolved in THF and precipitated into acetone; the precipitate was separated, and dried in vacuo. This afforded 3.0 mg (13 %) of **4-R1** as a dark brown solid material.

5.3 Surface-initiated *in situ* Polymerizations.

5.3.1 Activation of Substrates.

Preparation of ITO-glass substrates. Rectangular ITO-covered glass slides (approx. 1.1×2.5 cm) were ultrasonicated in CH_2Cl_2 for 20 min, followed by rinsing with acetone and deionized water. The pre-cleaned slides were subjected to an RCA-type cleaning procedure by keeping in a water – 30% H_2O_2 – 30% aqueous NH_3 (5:1:1) mixture at 70°C for 1 hour. The substrates were then rinsed with copious amount of deionized water and dried in N_2 flow at room temperature for 4 h, and then activated using O_2 plasma for 10 min.

Activation of Quartz substrates. Rectangular quartz slides (approx. 1.1×2.5 cm^2) were ultrasonicated sequentially for 10 min in $CHCl_3$, methanol, and deionized water. The pre-cleaned slides were placed into a Piranha solution (a mixture of conc. H_2SO_4 and 30 % H_2O_2 (7:3)) and ultrasonicated for 30 min. After rinsing with copious amount of deionized water, substrates were dried in N_2 flow at room temperature for 4 h, and then activated using O_2 plasma for 10 min.

Cleaning of Si (111) wafer. Pieces of boron-doped polished wafers of Si(111) were cut into 1 × 1 cm^2 squares and placed in Piranha solution. Next, silicon substrates were rinsed with copious amount of deionized water and dried in ambient air.

5.3.2 Preparation of Surface-immobilized Organic Conducting Polymer Thin Films.

5.3.2.1 Electrochemically Deposited Thin films and Related Materials in Chapter 2.

Immobilization of electroactive initiator on solid substrates. Freshly-cleaned ITO slides were immersed into a 1 mM solution of initiator (**TEDT** or **TT**) in toluene and kept at 60 °C under argon atmosphere for 3 days. After cooling to room temperature, the slides were rinsed

with copious amount of toluene and ultrasonicated in toluene for three 20 min periods, every time with a fresh portion of toluene. This was followed by rinsing with CH_2Cl_2, acetone, and MeOH and drying in N_2 flow for 30 min.

Preparation and electrochemical characterization of ITO/Initiator/PEDOT sample. Electrodeposition of PEDOT was accomplished by a single scan in CV mode through the voltage range between -0.75 and 1.0 V using an ITO substrate modified with a monolayer of initiator as a working electrode in a 10 mM solution of bisEDOT in 0.1 M Bu_4NPF_6 in CH_2Cl_2, at the scanning range of 0.1 V/s. The sample was rinsed with copious amount of CH_2Cl_2 and ultrasonicated in CH_2Cl_2 for three 20 min periods, every time with a fresh portion of the solvent, followed by drying in N_2 flow. The substrate was placed in a monomer-free electrolyte for CV characterization that included 10 successive scans through the voltage range between -0.75 and 1.0 V at the scanning rate of 0.1 V/s. At the end of the last scan, the sample was left at the standby potential of -1.0 V to ensure leaving the polymer in an electrochemically undoped state. The sample was washed with copious amount of CH_2Cl_2 and dried in N_2 flow. An **ITO/PEDOT** sample was prepared in the same conditions, but using an unmodified ITO-glass substrate as a working electrode. Due to instability, this sample was not ultrasonicated after the electrodeposition, but simply rinsed with CH_2Cl_2.

Preparation and electrochemical characterization of ITO/Initiator/PEDOT/PT sample. Electrodeposition of PT was accomplished by three successive scans in the CV mode through the voltage range between -0.5 and 1.5 V using an **ITO/Initiator/PEDOT** sample as a working electrode in a 10 mM solution of bithiophene in 0.1 M Bu_4NPF_6 in CH_2Cl_2, at the scanning range of 0.1 V/s. The sample was rinsed with copious amount of CH_2Cl_2 and ultrasonicated in CH_2Cl_2 for three 20 min periods, every time with a fresh portion of the solvent, followed by drying in N_2 flow. The substrate was placed in a monomer-free electrolyte for CV characterization that

included 10 successive scans through the voltage range between -0.75 and 1.75 V at the scanning rate of 0.1 V/s. At the end of the last scan, the sample was left at the standby potential of -1.0 V to ensure leaving the polymer in an electrochemically undoped state. The sample was washed with copious amount of CH_2Cl_2 and dried in N_2 flow. An **ITO/TT/PT** sample was prepared exactly in the same conditions, but using an ITO-glass substrate modified with a monolayer of **TT** as a working electrode. An **ITO/PEDOT/PT** sample was prepared in the same conditions, but using an **ITO/PEDOT** substrate as a working electrode, and excluding the ultrasonication steps due to the sample's low stability.

ITO/PEDOT/PSS/spin-coated P3HT was prepared following a modified literature procedure.[6] PEDOT/PSS solution was filtered through 0.2 um filter and spin-coated on clean ITO suface at 5,000 rpm for 3 min. Spin-coated PEDOT/PSS films were annealed in N_2 at 120 °C for 1h. Regioregular P3HT solution (4 mg ml^{-1} in toluene) was spin-coated on PEDOT/PSS at 1,000 rpm for 2 min. The sample was dried in vacuo (0.01 mmHg) overnight.

ITO/TEDT/PEDOT/spin-coated P3HT. Using **ITO/TEDT/PEDOT** coated substrate, which was prepared through usual pathway, regioregular P3HT solution (4 mg ml^{-1} in toluene) was spin-coated at 1,000 rpm for 2 min. The sample was dried in vacuo (0.01 mmHg) overnight.

ITO/TEDT/spin-coated P3HT. Regioregular P3HT solution (4 mg ml^{-1} in toluene) was spin-coated on **TEDT** modified ITO slide at 1,000 rpm for 2 min. The sample was dried in vacuo (0.01 mmHg) overnight.

5.3.2.2 Surface-immobilized Thin Films Prepared by *in situ* Kumada Polycondensation in Chapter 3.

Polymerization initiator (3-I1). A portion of 44 mg (0.05 mmol) of $Ni(dppp)_2$ (prepared as described in literature[7]) was added into a solution of 9.0 mg (0.025 mmol) of triethoxy(5-iodothiophen-2-yl)silane **3-1** in 10 ml of toluene. The reaction mixture was stirred at 40 °C for

overnight, and the resulting solution (nominal concentration of **3-I1** was 2.5 mM) was used for the surface immobilization without further purification.

Scheme 5.8 Preparation of polymerization initiator.

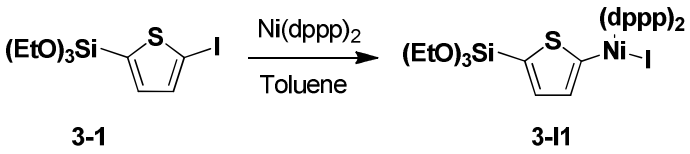

3-1 **3-I1**

Preparation of surface-immobilized initiator. Activated quartz slides were immersed into a solution of polymerization catalytic initiator **3-I1** in toluene and kept at 60 °C for 3 days followed by gentle rinsing with anhydrous toluene. Due to air sensitive nature of compounds involved, all procedures were carried out inside a glovebox.

Surface-bound initiator prepared by *in situ* activation. Quartz slides were immersed into a 10 mM solution of one of the precursors **3-1** – **3-3** in toluene for 3 days at 60 °C. The slides were ultrasonicated in $CHCl_3$ (2 x 10 min) followed by drying under N_2 flow for 4 h. In order to prepare surface-bound initiator, precursor-immobilized quartz slides were activated by immersing into 5 mM solution of $Ni(dppp)_2$ in toluene at 40°C for 2 days inside a glovebox. Subsequent thorough rinsing with anhydrous toluene afforded surface-immobilized initiator monolayer.

Surface-initiated *in situ* polymerization with regeneration of Ni(II) catalytic center (a typical procedure).

Substrates modified with initiator monolayer were immersed into a 0.1 M solution of a Grignard monomer ((5-bromothiophen-2-yl)magnesium chloride) in THF (prepared from 0.24 g (1.0 mmol) of 2,5-dibromothiophene and 0.5 ml of 2.0 M solution of iPrMgCl (1.0 mmol)). The reaction mixture was gently stirred for 16 hours at 40 °C, and the substrates were rinsed with anhydrous toluene. Then the PT covered substrates were immersed into a 5 mM solution of

$Ni(dppp)_2$ in toluene for 2 days. After residual $Ni(dppp)_2$ were removed by washing with anhydrous toluene three times, Ni(II) catalytic center regenerated thin films were again immersed into a 0.1 M solution of Grignard monomer in THF upon gentle stirring for 16 h at 40 °C. The procedure of regeneration and polymerization was repeated for 2 more times. At the end, the reactive Ni(II) centers were quenched by placing the substrates into methanol and ultrasonicating for 10 min. The resulted PT thin films were further cleaned by ultrasonication in $CHCl_3$ (2 x 10 min).

Deposition of surface-immobilized OTS mask on Si(111). Monodisperse latex mesospheres (300 nm diameter) were washed with deionized water to remove surfactants by centrifugation. A small volume (300 µL) of aqueous latex suspension (1 wt%) was centrifuged at 14000 rpm for 15 min, and the supernatant was decanted. The pellet of latex was resuspended in 300 µL of deionized water. A drop of the latex suspension (30 µL) was deposited on the freshly cleaned substrate and dried in air for 2 h. During the drying step, as water was evaporating, the monodisperse latex spheres formed crystalline layers on the substrate, which provided a lithographic mask for patterning organosilanes. Next, a 2x2 cm^2 block of polydimethylsiloxane (**PDMS**) was prepared for patterning octadecyltrichlorosilane (**OTS**). A 30 µL volume of a 30% v/v solution of OTS in bicyclohexyl was deposited on the surface of the PDMS block and then dried quickly with a stream of nitrogen. The "inked" PDMS block was placed on top of the masked silicon substrate. The areas of contact between the latex mesospheres and substrate were protected from deposition of OTS. After 1 h, the PDMS block was removed from the sample and the surface was rinsed with deionized water. The mask of latex particles was removed completely by rinsing with ethanol and deionized water several times, using sonication. After removal of the latex mask, a layer of OTS persisted on the surface to define periodic circular pores of uncovered substrate for further chemical steps.

Surface-immobilized nano-patterned columnar PT thin films (columnar arrays) were manufactured by following the procedure outlined on page 104 (surface-initiated *in situ* polymerization with regeneration) for continuous PT thin films, but with using an OTS-patterned Si(111) substrate.

5.3.2.3 Manufacturing of Surface-bound Thin Films by Stepwise *in situ* Polymerization in Chapter 4.

Preparation of surface-immobilized initiator. Activated substrates were immersed into a 10mM solution of initiator (**4-P1** or **4-P2**) in toluene and kept at 60°C for 3 days. To obtain optimal result, immobilization was performed inside a glovebox. After ultrasonication (2 times for 10 min) in $CHCl_3$, samples were dried under N_2 flow for 2 hours.

Surface-immobilized 1,2,3-triazole incorporating conducting polymer thin films. Substrates modified with monolayer of initiators were immersed into a 10 mM solution of diacetylene monomer **4-m1** (or **4-m3**) and 9 mg (0.05 mmol) of CuI in 50 ml of DMSO. After click reaction was performed by heating at 40 °C for 1 hour with gentle stirring, the slides were rinsed twice with copious amount of $CHCl_3$ followed by 10 min ultrasonication in $CHCl_3$. Diazido-functionalized monomer, **4-m2**, was immobilized through the same procedure. Repeated sequential CuAAC steps with alternating monomers gave surface-immobilized 1,2,3-triazole incorporating copolymer (or homopolymer) on the solid substrate.

5.4 Electrochemical and AFM Measurements.

5.4.1 Electrochemical Measurements.

These were performed using an Autolab PGSTAT 302 potentiostat from Eco Chemie. All experiments were carried out using a three-electrode system with either a Pt button electrode (diameter 2 mm, CH Instruments, Inc.) or a precursor-immobilized ITO-covered glass working electrode, a $Ag/AgNO_3$ nonaqueous reference electrode, and a Pt gauze counter electrode. The

reference electrode was checked against a ferrocene standard before and after each experiment was performed. All experiments were carried out in 0.1 M Bu_4NPF_6 solution in CH_2Cl_2 (Chapter 2) or CH_3CN (Chapter 3 and 4) as the supporting electrolyte.

5.4.2 Atomic Force Microscopy in Chapter 2.

Topography and current-sensing AFM (CS-AFM) images were acquired with an Agilent 5500 (PicoPlus) system with PicoScan v5.3 acquisition software. Silicon nitride tips with an average force constant of 0.5 N m^{-1} were used for contact mode AFM in air (MSCT-AUHW, Veeco Instruments, Inc.). To minimize tip-surface adhesion, the probes were coated with octadecyltrichlorosilane. Current-sensing AFM was used to map the sample conductance while operating in contact mode. A dc bias (-4 V) was applied to the ITO substrate of the devices. The tips used for CS-AFM were highly doped silicon probes with a Ti/Pt coating that have an average force constant of 0.2 N m^{-1} (ANSCM- PC, Nanoscience Instruments, Inc.). To measure the film thickness, an area of the surface was nanoshaved. The details of this procedure are given in the Experimental section. Surface roughness factors were estimated from AFM data with Scanning Probe Image Processor (version 3.2.2.0) software (Image Metrology A/S).

5.4.3 Atomic Force Microscopy in Chapter 3 and 4.

Samples were characterized with an Agilent 5500 atomic force microscope (AFM) equipped with Picoscan v5.3.3 software (Agilent Technologies, Chandler, AZ). Images were acquired using contact mode in ambient conditions. Oxide-sharpened silicon nitride cantilevers with a force constant of 0.5 N/m were used for imaging and nanoshaving experiments (Veeco Probes, Camarillo, CA). Digital images were processed with Gwyddion open source software (version 2.9), which is supported by the Czech Metrology Institute.[8]

5.5 References

(1) Mohanakrishnan, A. K.; Hucke, A.; Lyon, M. A.; Lakshmikantham, M. V.; Cava, M. P., Functionalization of 3,4-ethylenedioxythiophene, *Tetrahedron* **1999**, *55*, 11745-11754.

(2) Zhu, S. S.; Swager, T. M., Conducting Polymetallorotaxanes: Metal Ion Mediated Enhancements in Conductivity and Charge Localization, *J. Am. Chem. Soc* **1997**, *119*, 12568-12577.

(3) Fuerstner, A.; Grabowski, J.; Lehmann, C. W.; Kataoka, T.; Nagai, K., Synthesis and Biological Evaluation of Nonylprodigiosin and Macrocyclic Prodigiosin Analogues, *ChemBioChem* **2001**, *2*, 60-68.

(4) Maegawa, Y.; Nagano, T.; Yabuno, T.; Nakagawa, H.; Shimada, T., Preparation of functionalized aryl(diallyl)ethoxysilanes and their palladium-catalyzed coupling reactions giving sol-gel precursors, *Tetrahedron* **2007**, *63*, 11467-11474.

(5) Cardolaccia, T.; Funston, A. M.; Kose, M. E.; Keller, J. M.; Miller, J. R.; Schanze, K. S., Radical Ion States of Platinum Acetylide Oligomers, *J. Phys. Chem. B* **2007**, *111*, 10871-10880.

(6) Nimura, S.; Kikuchi, O.; Ohana, T.; Yabe, A.; Kondo, S.; Kaise, M., Effects of Additional Linkers in Biphenyl-4,4‘-dinitrene on the Low-Lying Singlet–Triplet Energy Gap and Zero-Field Splitting, *J. Phys. Chem. A* **1997**, *101*, 2083-2088.

(7) Acharya, J. R.; Zhang, H.; Li, X.; Nesterov, E. E., Chemically Controlled Amplified Ratiometric Fluorescence in Surface-Immobilized End-Capped Oligo(p-phenylene ethynylene)s, *J. Am. Chem. Soc.* **2009**, *131*, 880-881.

(8) van Steenis, D.; David, O. R. P.; van Strijdonck, G. P. F.; van Maarseveen, J. H.; Reek, J. N. H., Click-chemistry as an efficient synthetic tool for the preparation of novel conjugated polymers, *Chem. Commun.* **2005**, 4333-4335.

(9) Wong, W. Y.; Wang, X. Z.; He, Z.; Djurisic, A. B.; Yip, C. T.; Cheung, K. Y.; Wang, H.; Mak, C. S. K.; Chan, W. K., Metallated conjugated polymers as a new avenue towards high-efficiency polymer solar cells, *Nature Mat., Published online* **2007**, *13*.

(10) Corain, B.; Bressan, M.; Rigo, P., The behaviour of nickel(0) diphosphine complexes towards unsaturated organic compounds, *J. Organomet. Chem.* **1971**, *28*, 133-136.

(11) Gwyddion, 2.9 ed.; Czech Metrology Institute: http://gwyddion.net/, 2010.

APPENDIX I : PERMISSIONS

AMERICAN CHEMICAL SOCIETY LICENSE
TERMS AND CONDITIONS

Mar 29, 2011

This is a License Agreement between Euiyong Hwang ("You") and American Chemical Society ("American Chemical Society") provided by Copyright Clearance Center ("CCC"). The license consists of your order details, the terms and conditions provided by American Chemical Society, and the payment terms and conditions.

All payments must be made in full to CCC. For payment instructions, please see information listed at the bottom of this form.

License Number	2621700418693
License Date	Mar 03, 2011
Licensed content publisher	American Chemical Society
Licensed content publication	Langmuir
Licensed content title	Self-Assembled Monolayer Initiated Electropolymerization: A Route to Thin-Film Materials with Enhanced Photovoltaic Performance
Licensed content author	Euiyong Hwang et al.
Licensed content date	Sep 1, 2008
Volume number	24
Issue number	17
Type of Use	Thesis/Dissertation
Requestor type	Not specified
Format	Print
Portion	Full article
Number of languages	1
Languages	English
Author of this ACS article	Yes
Title of the thesis / dissertation	SURFACE-INITIATED POLYMERIZATION AS A NOVEL STRATEGY TOWARDS ORGANIC SEMICONDUCTING THIN FILM
Expected completion date	Aug 2011
Estimated size(pages)	100
Billing Type	Invoice
Billing Address	272 Choppin hall Baton Rouge, LA 70803 United States
Total	0.00 USD

APPENDIX II : NMR SPECTRAL DATA

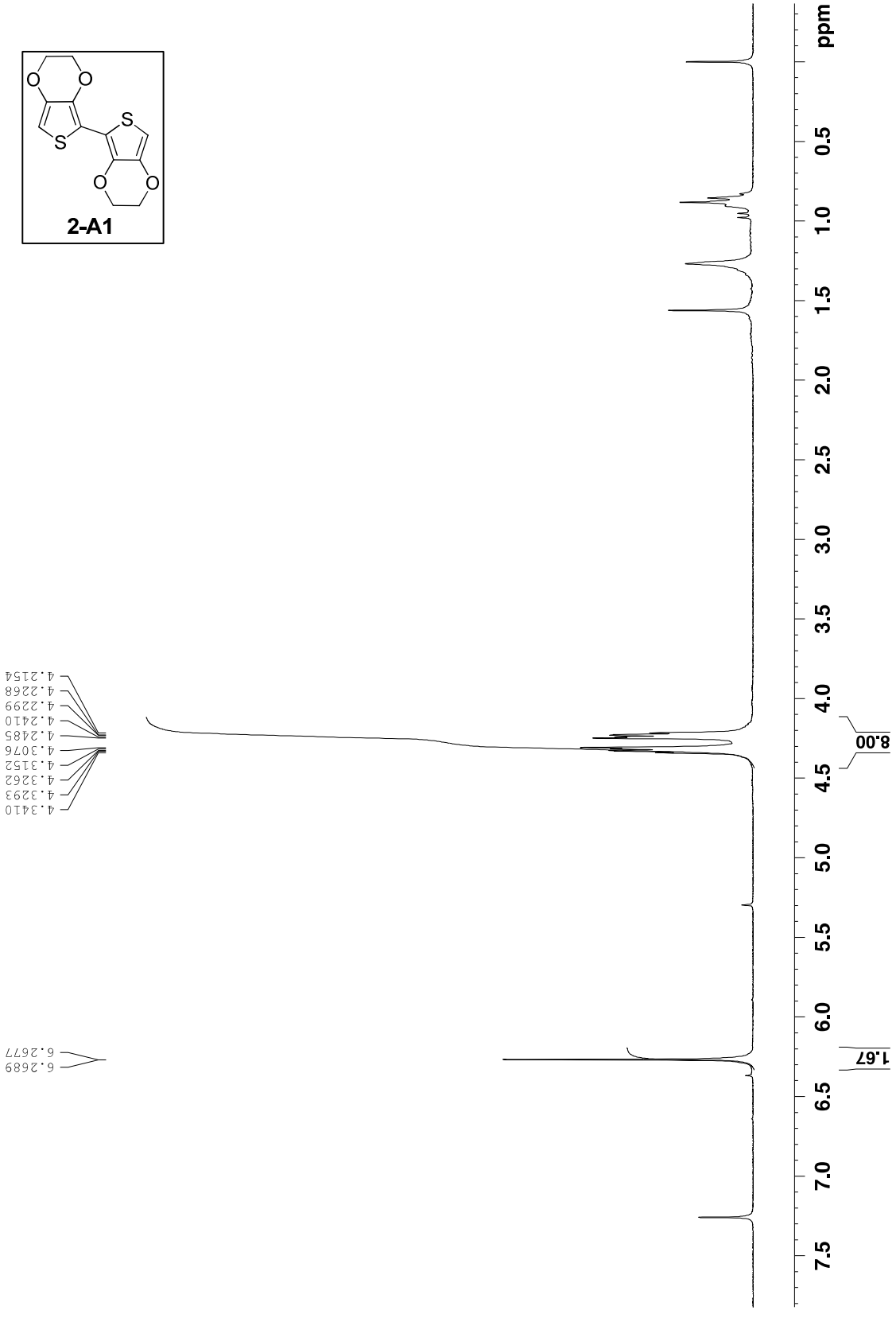

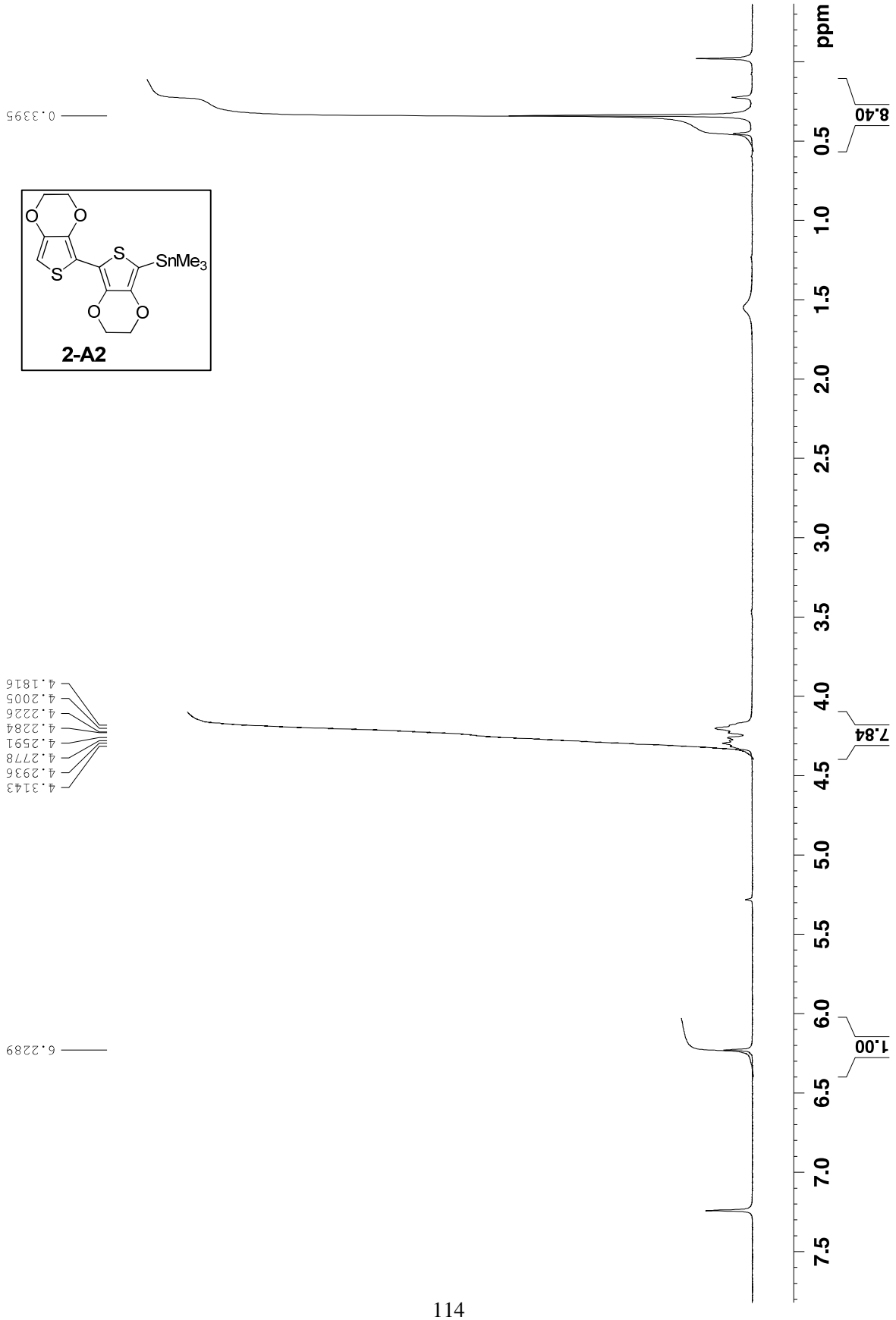
0.3395
6.2289
4.3143
4.2936
4.2778
4.2591
4.2284
4.2226
4.2005
4.1816
SnMe3
2-A2
8.40
7.84
1.00
ppm

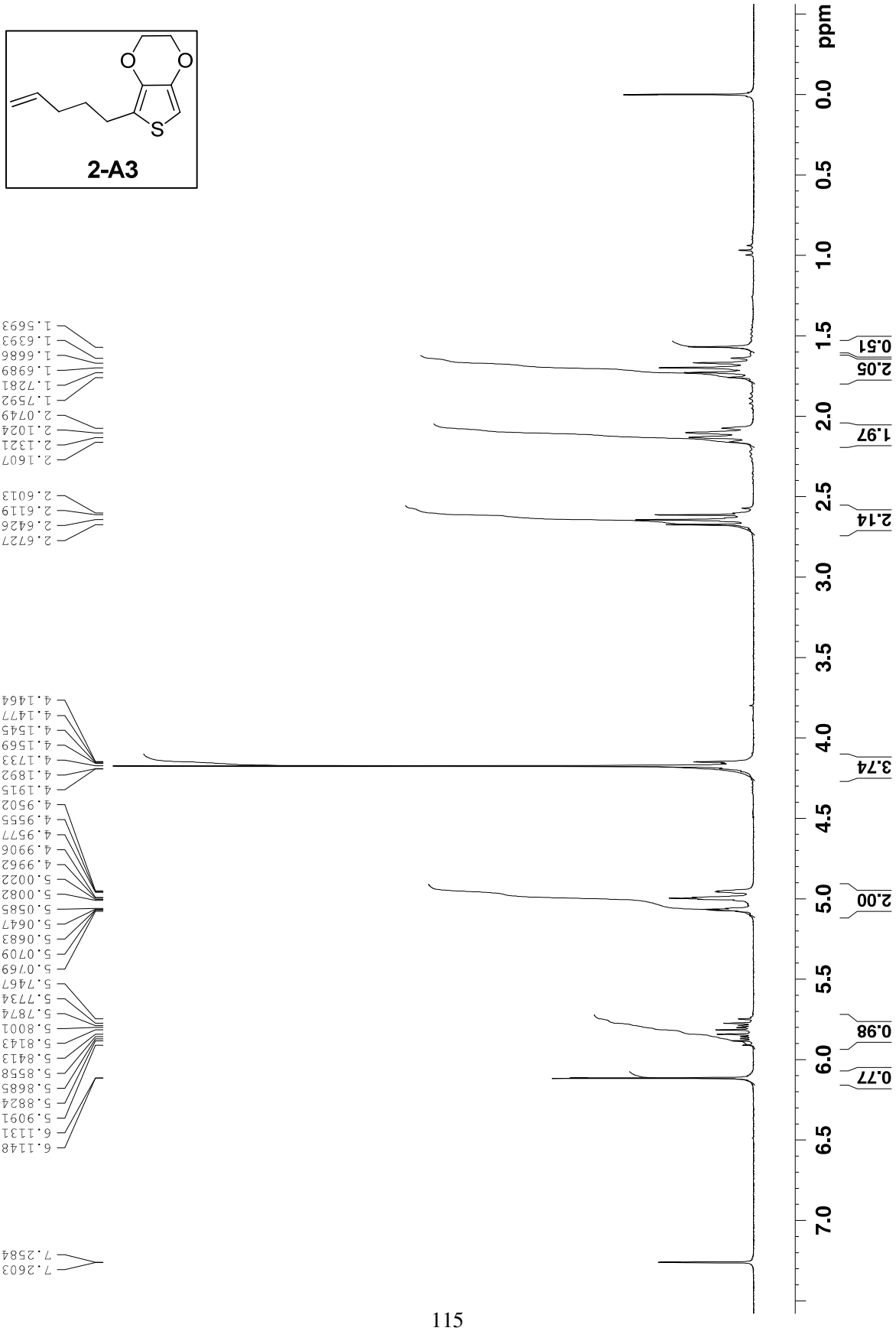
2-A3
O
O
S
ppm
0.0
0.5
1.0
1.5
2.0
2.5
3.0
3.5
4.0
4.5
5.0
5.5
6.0
6.5
7.0
0.51
2.05
1.97
2.14
3.74
2.00
0.98
0.77
1.5693
1.6393
1.6686
1.6989
1.7281
1.7592
2.0749
2.1024
2.1321
2.1607
2.6013
2.6119
2.6426
2.6727
4.1464
4.1477
4.1545
4.1569
4.1733
4.1892
4.1915
4.9502
4.9555
4.9577
4.9906
4.9962
5.0022
5.0082
5.0585
5.0647
5.0683
5.0709
5.0769
5.7467
5.7734
5.7874
5.8001
5.8143
5.8413
5.8558
5.8685
5.8824
5.9091
6.1131
6.1148
7.2603
7.2584

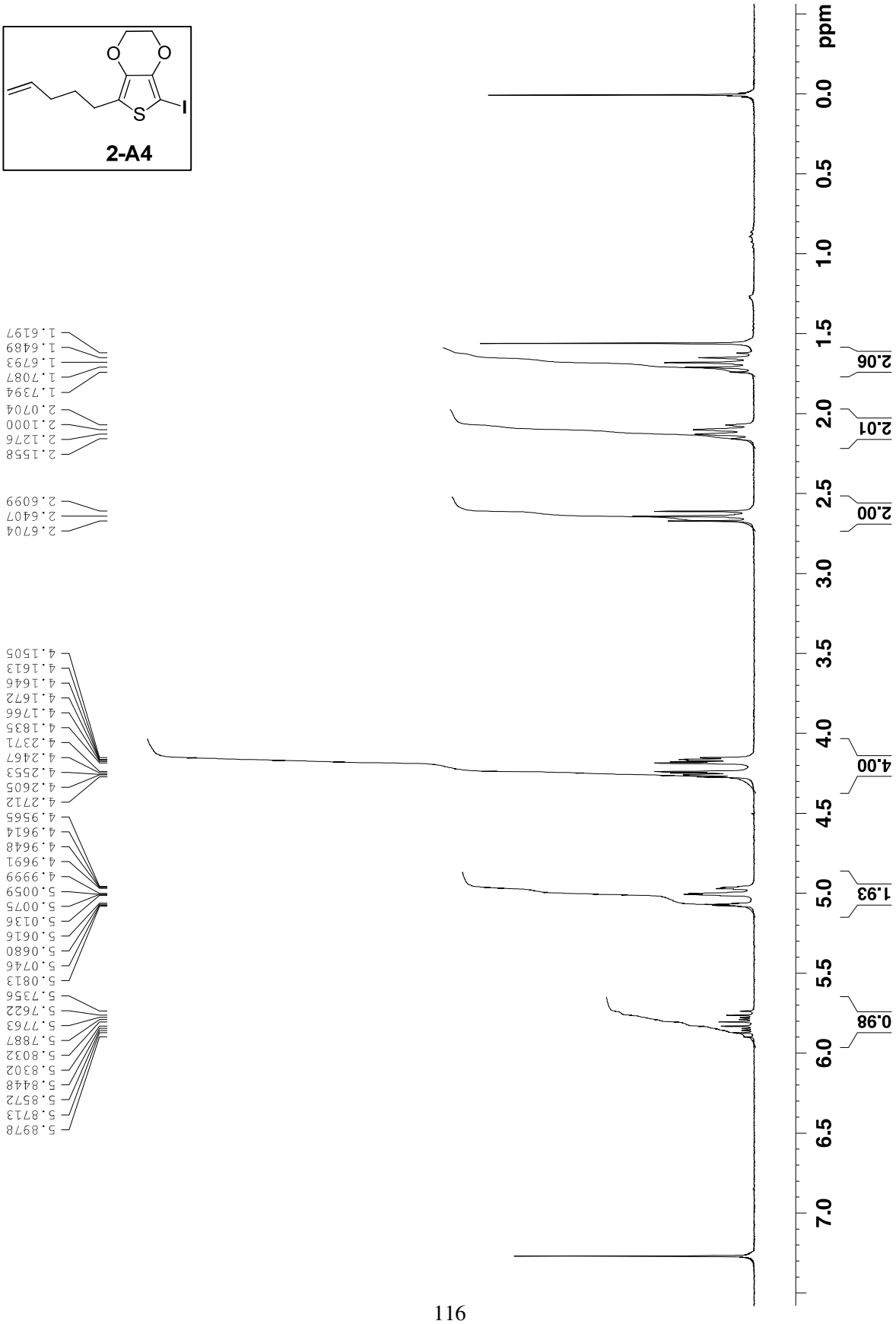
O
O
S
I
2-A4
ppm
0.0
0.5
1.0
1.5
2.0
2.5
3.0
3.5
4.0
4.5
5.0
5.5
6.0
6.5
7.0
2.06
2.01
2.00
4.00
1.93
0.98
1.6197
1.6489
1.6793
1.7087
1.7394
2.0704
2.1000
2.1276
2.1558
2.6099
2.6407
2.6704
4.1505
4.1613
4.1646
4.1672
4.1766
4.1835
4.2371
4.2467
4.2553
4.2605
4.2712
4.9565
4.9614
4.9648
4.9691
4.9999
5.0059
5.0075
5.0136
5.0616
5.0680
5.0746
5.0813
5.7356
5.7622
5.7763
5.7887
5.8032
5.8302
5.8448
5.8572
5.8713
5.8978

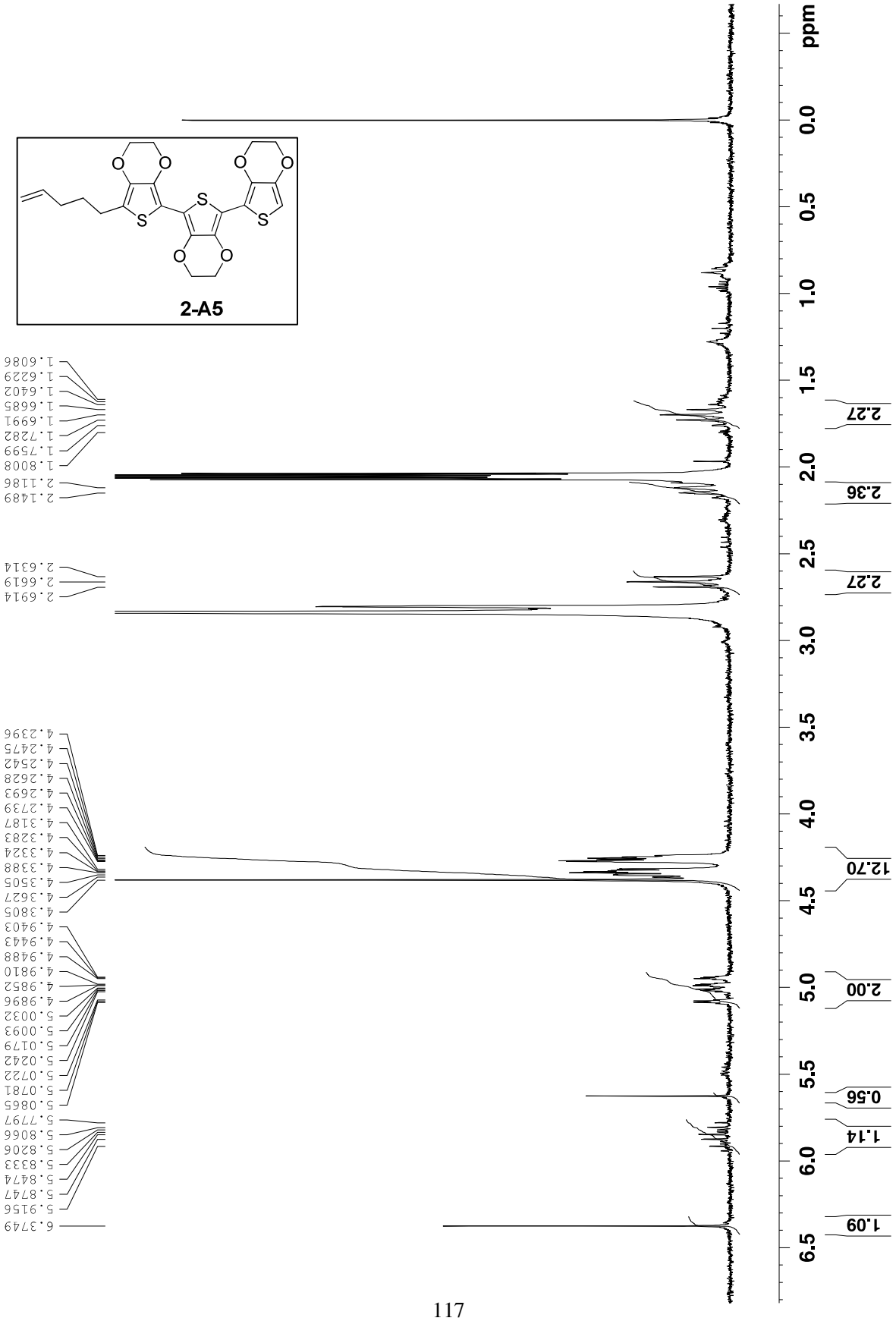
2-A5
ppm
0.0
0.5
1.0
1.5
2.0
2.5
3.0
3.5
4.0
4.5
5.0
5.5
6.0
6.5
2.27
2.36
2.27
12.70
2.00
0.56
1.14
1.09
1.6086
1.6229
1.6402
1.6685
1.6991
1.7282
1.7599
1.8008
2.1186
2.1489
2.6314
2.6619
2.6914
4.2396
4.2475
4.2542
4.2628
4.2693
4.2739
4.3187
4.3283
4.3324
4.3388
4.3505
4.3627
4.3805
4.9403
4.9443
4.9488
4.9810
4.9852
4.9896
5.0032
5.0093
5.0179
5.0242
5.0722
5.0781
5.0865
5.7797
5.8066
5.8206
5.8333
5.8474
5.8747
5.9156
6.3749

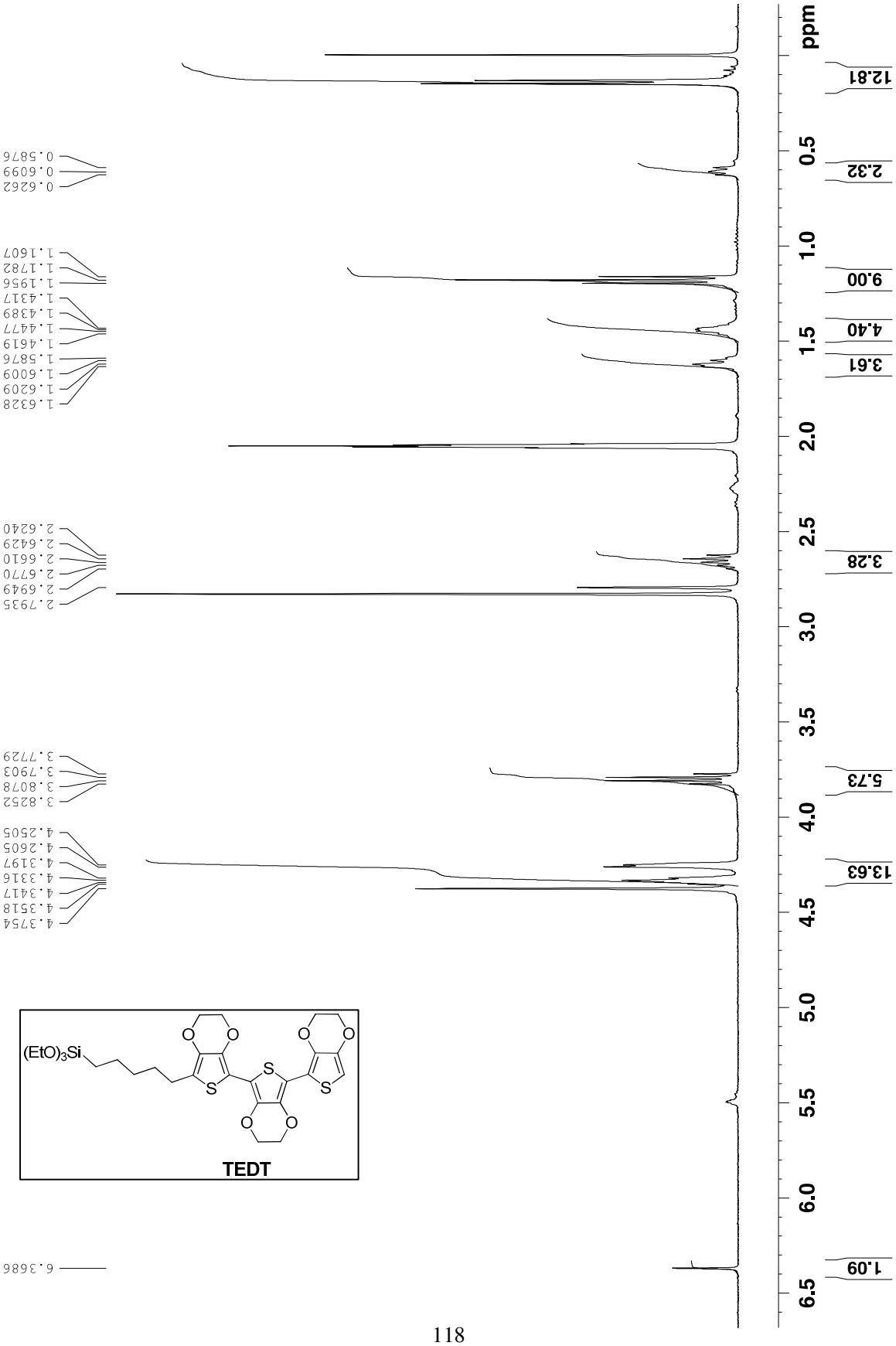
ppm
12.81
2.32
9.00
4.40
3.61
3.28
5.73
13.63
1.09
0.5876
0.6099
0.6262
1.1607
1.1782
1.1956
1.4317
1.4389
1.4477
1.4619
1.5876
1.6009
1.6209
1.6328
2.6240
2.6429
2.6610
2.6770
2.6949
2.7935
3.7729
3.7903
3.8078
3.8252
4.2505
4.2605
4.3197
4.3316
4.3417
4.3518
4.3754
6.3686
(EtO)3Si
S
O
TEDT

0.0011
0.8741
0.9032
0.9320
1.0836
1.1146
1.1479
1.2750
1.3031
1.3317
1.3614
1.3909
1.4197
1.5186
1.5324
1.5422
1.5520
1.5819
1.6146
1.6406
6.9817
6.9975
6.9992
7.0163
7.0532
7.0655
7.1655
7.1787
7.1860
7.2504
7.2850
7.2975
ppm
0.5
1.0
1.5
2.0
2.5
3.0
3.5
4.0
4.5
5.0
5.5
6.0
6.5
7.0
7.5
9.34
0.78
5.29
0.74
6.59
5.59
0.62
1.76
1.57
1.00
S
S
SnBu3
2-B1

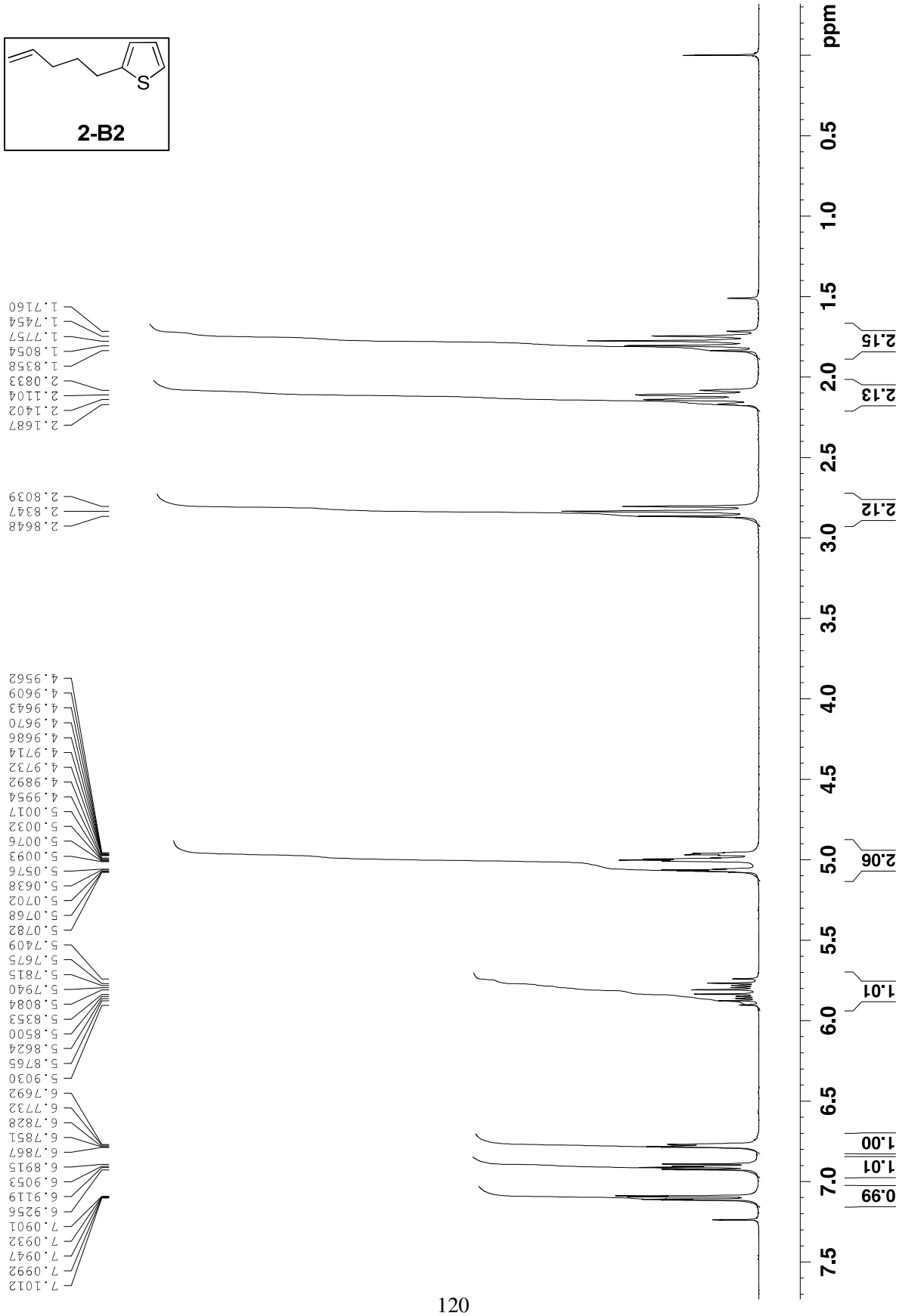
S
2-B2
ppm
0.5
1.0
1.5
2.0
2.5
3.0
3.5
4.0
4.5
5.0
5.5
6.0
6.5
7.0
7.5
2.15
2.13
2.12
2.06
1.01
1.00
1.01
0.99
1.7160
1.7454
1.7757
1.8054
1.8358
2.0833
2.1104
2.1402
2.1687
2.8039
2.8347
2.8648
4.9562
4.9609
4.9643
4.9670
4.9686
4.9714
4.9732
4.9892
4.9954
5.0017
5.0032
5.0076
5.0093
5.0576
5.0638
5.0702
5.0768
5.0782
5.7409
5.7675
5.7815
5.7940
5.8084
5.8353
5.8500
5.8624
5.8765
5.9030
6.7692
6.7732
6.7828
6.7851
6.7867
6.8915
6.9053
6.9119
6.9256
7.0901
7.0932
7.0947
7.0992
7.1012

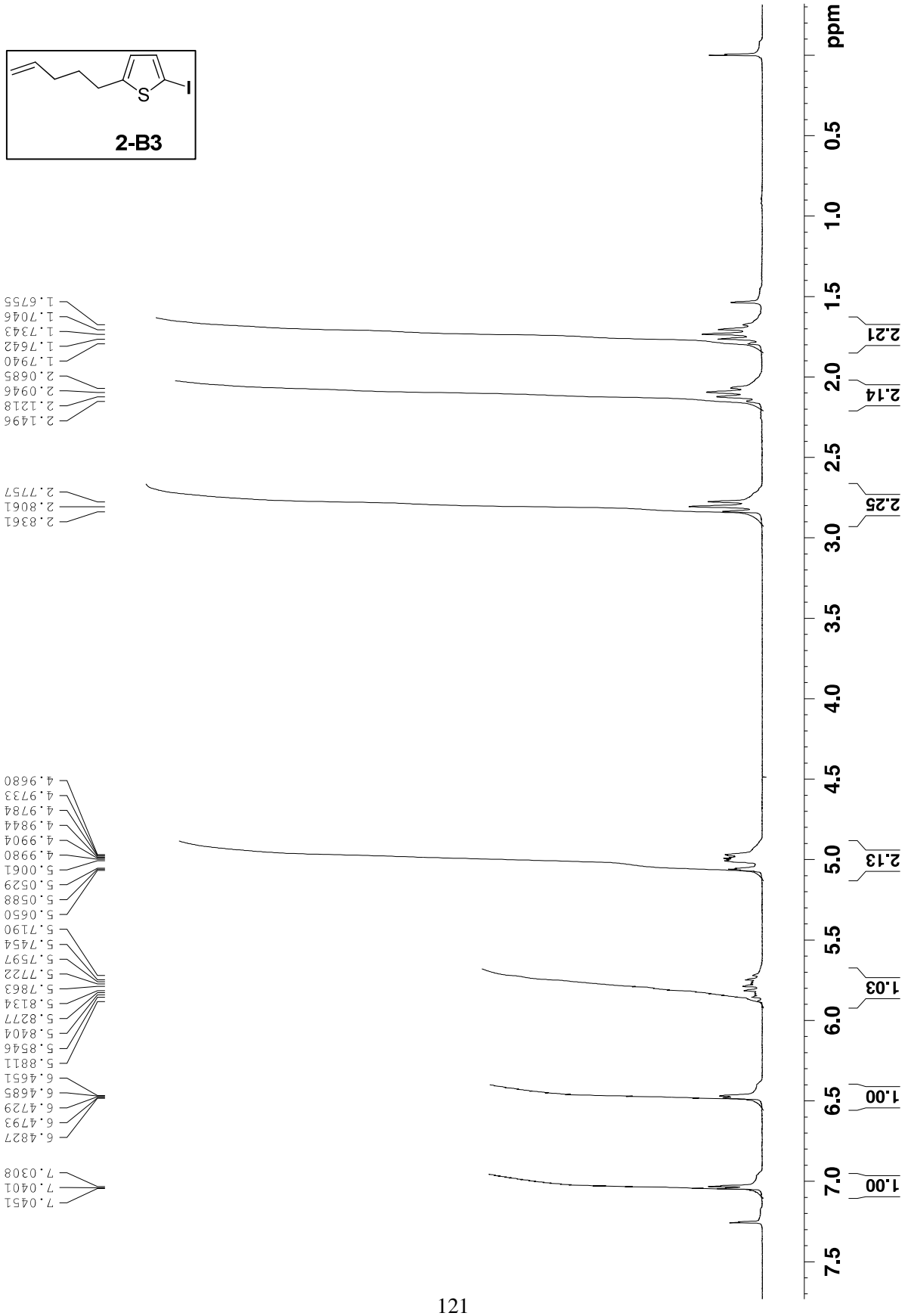
S
I
2-B3
1.6755
1.7046
1.7343
1.7642
1.7940
2.0685
2.0946
2.1218
2.1496
2.7757
2.8061
2.8361
4.9680
4.9733
4.9784
4.9844
4.9904
4.9980
5.0061
5.0529
5.0588
5.0650
5.7190
5.7454
5.7597
5.7722
5.7863
5.8134
5.8277
5.8404
5.8546
5.8811
6.4651
6.4685
6.4729
6.4793
6.4827
7.0308
7.0401
7.0451
ppm
0.5
1.0
1.5
2.0
2.5
3.0
3.5
4.0
4.5
5.0
5.5
6.0
6.5
7.0
7.5
2.21
2.14
2.25
2.13
1.03
1.00
1.00

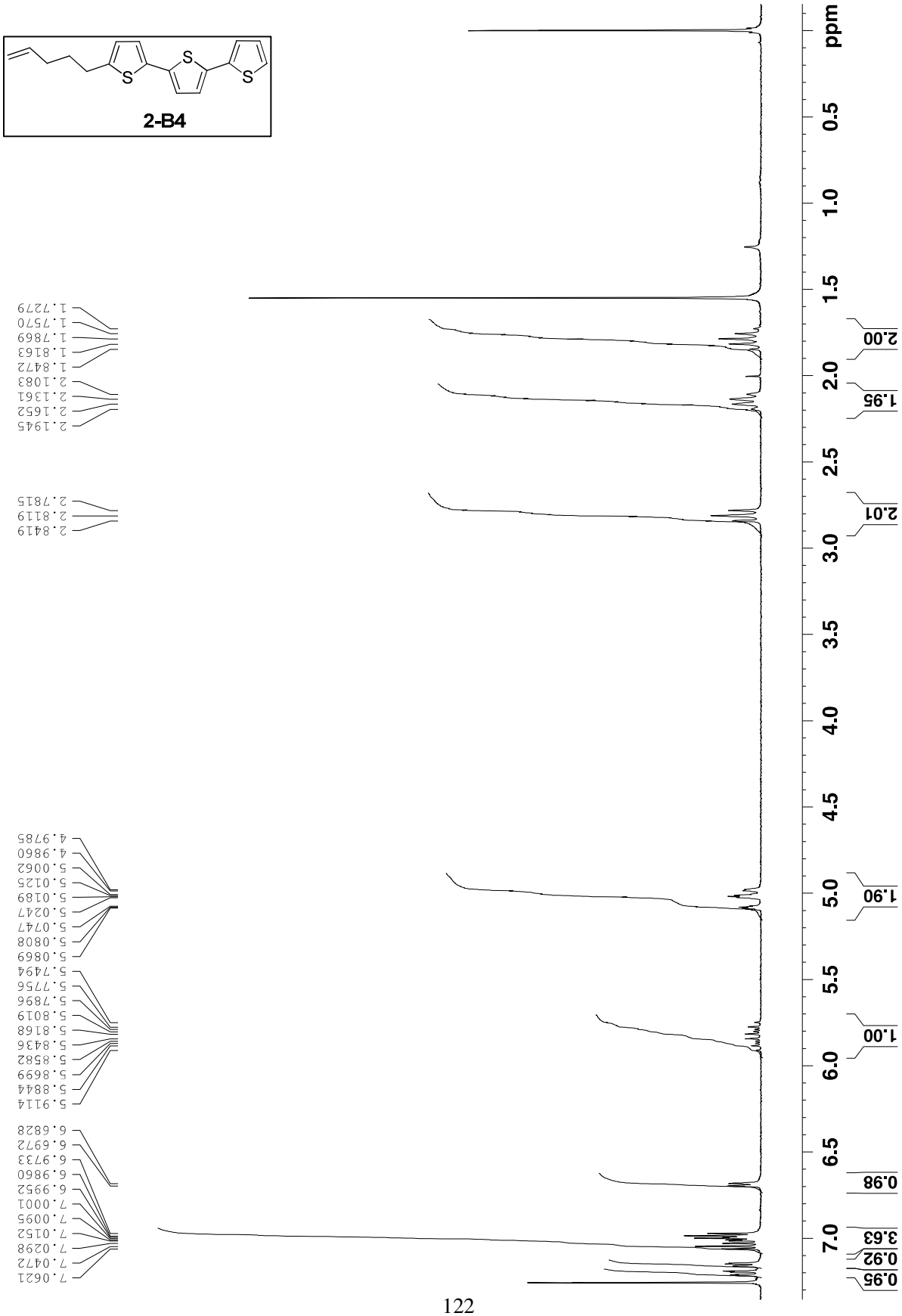
2-B4
S
S
S
ppm
0.5
1.0
1.5
2.0
2.5
3.0
3.5
4.0
4.5
5.0
5.5
6.0
6.5
7.0
0.95
0.92
3.63
0.98
1.00
1.90
2.01
1.95
2.00
7.0621
7.0472
7.0298
7.0152
7.0095
7.0001
6.9952
6.9860
6.9733
6.9672
6.6828
5.9114
5.8844
5.8699
5.8582
5.8436
5.8168
5.8019
5.7896
5.7756
5.7494
5.0869
5.0808
5.0747
5.0247
5.0189
5.0125
5.0062
4.9860
4.9785
2.8419
2.8119
2.7815
2.1945
2.1652
2.1361
2.1083
1.8472
1.8163
1.7869
1.7570
1.7279

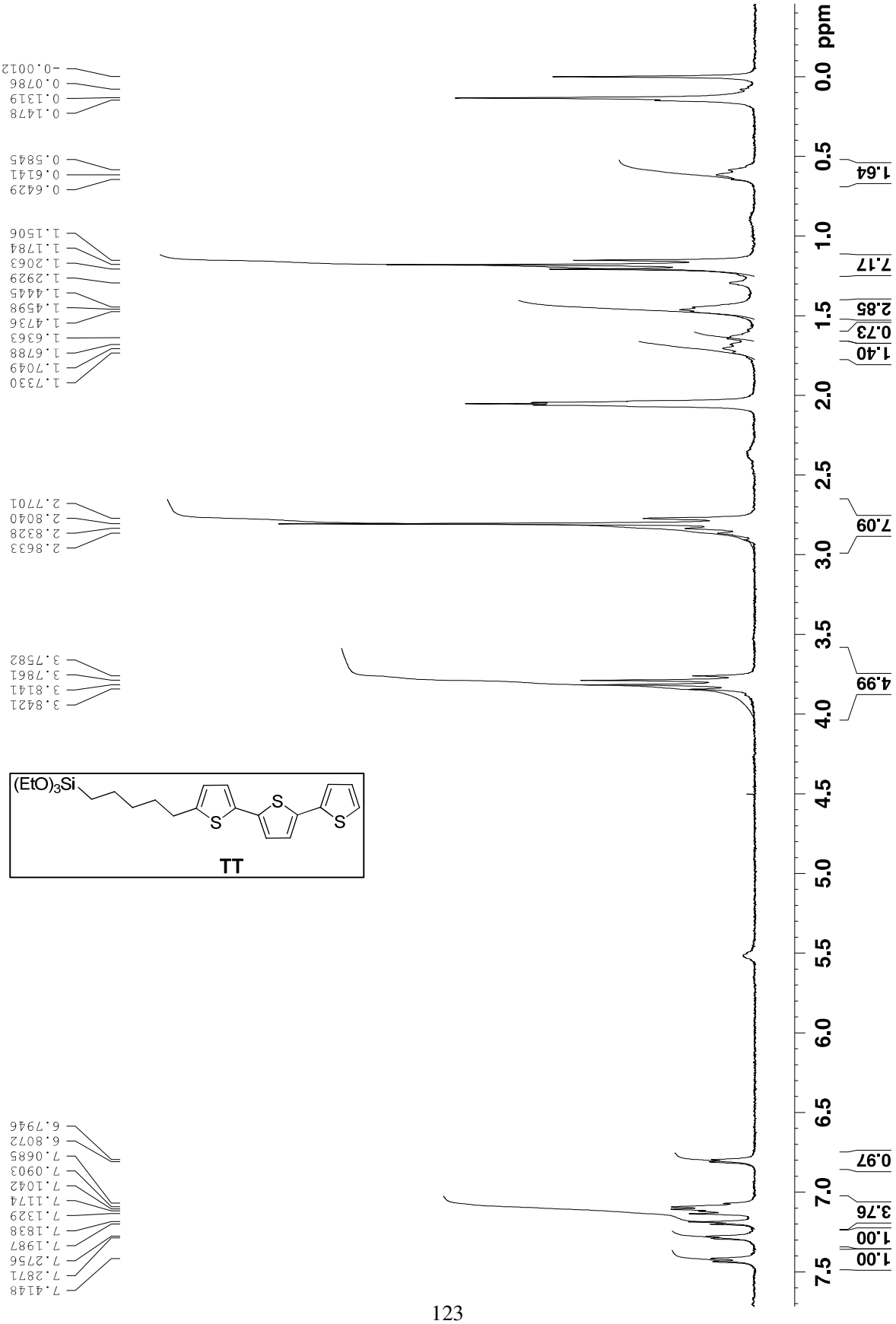
(EtO)3Si
S
S
S
TT
7.4148
7.2871
7.2756
7.1987
7.1838
7.1329
7.1174
7.1042
7.0903
7.0685
6.8072
6.7946
3.8421
3.8141
3.7861
3.7582
2.8633
2.8328
2.8040
2.7701
1.7330
1.7049
1.6788
1.6363
1.4736
1.4598
1.4445
1.2929
1.2063
1.1784
1.1506
0.6429
0.6141
0.5845
0.1478
0.1319
0.0786
-0.0012
0.0 ppm
0.5
1.0
1.5
2.0
2.5
3.0
3.5
4.0
4.5
5.0
5.5
6.0
6.5
7.0
7.5
1.64
7.17
2.85
0.73
1.40
7.09
4.99
0.97
3.76
1.00
1.00

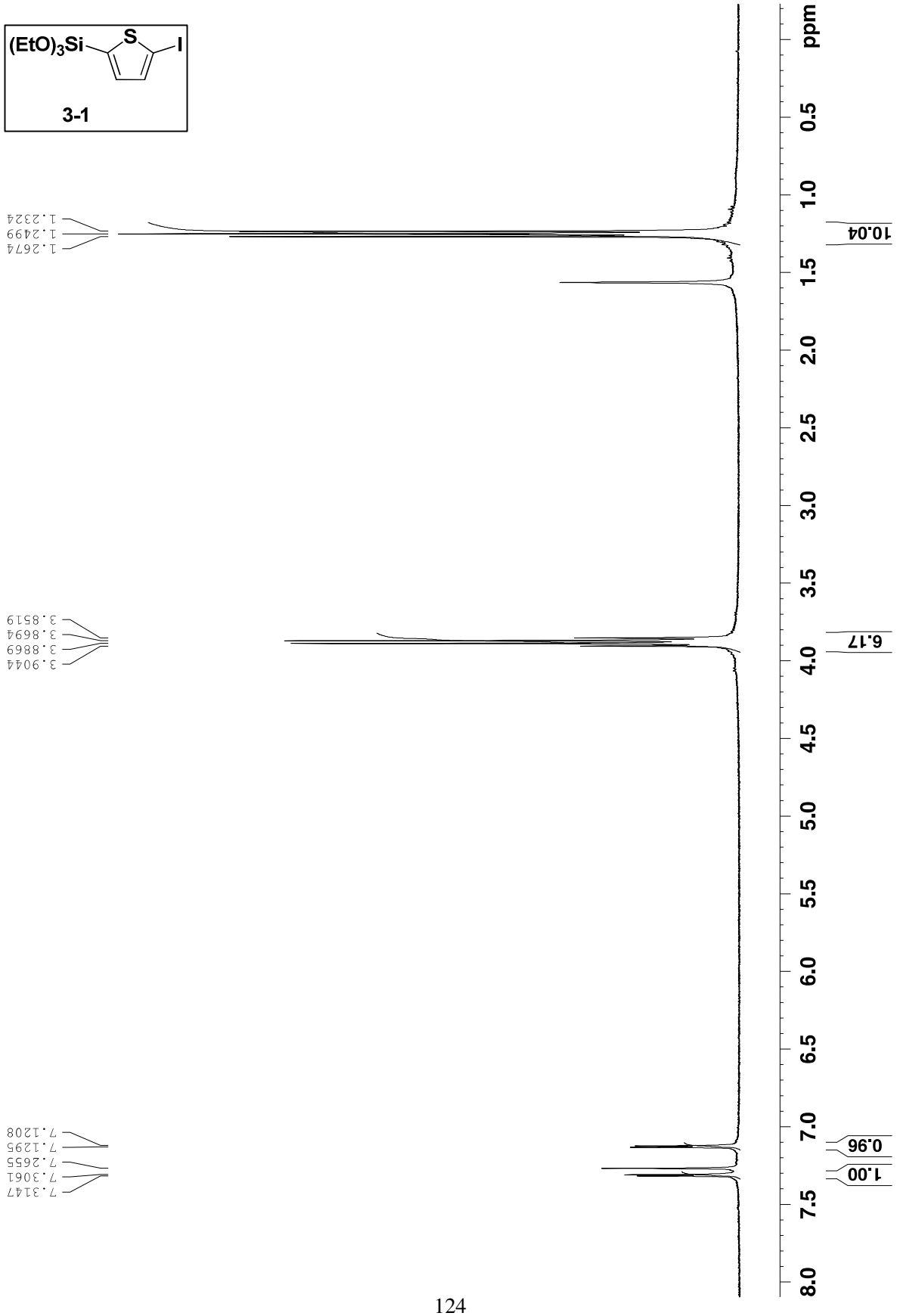
(EtO)3Si
S
I
3-1
1.2324
1.2499
1.2674
3.8519
3.8694
3.8869
3.9044
7.1208
7.1295
7.2655
7.3061
7.3147
10.04
6.17
0.96
1.00
ppm
0.5
1.0
1.5
2.0
2.5
3.0
3.5
4.0
4.5
5.0
5.5
6.0
6.5
7.0
7.5
8.0

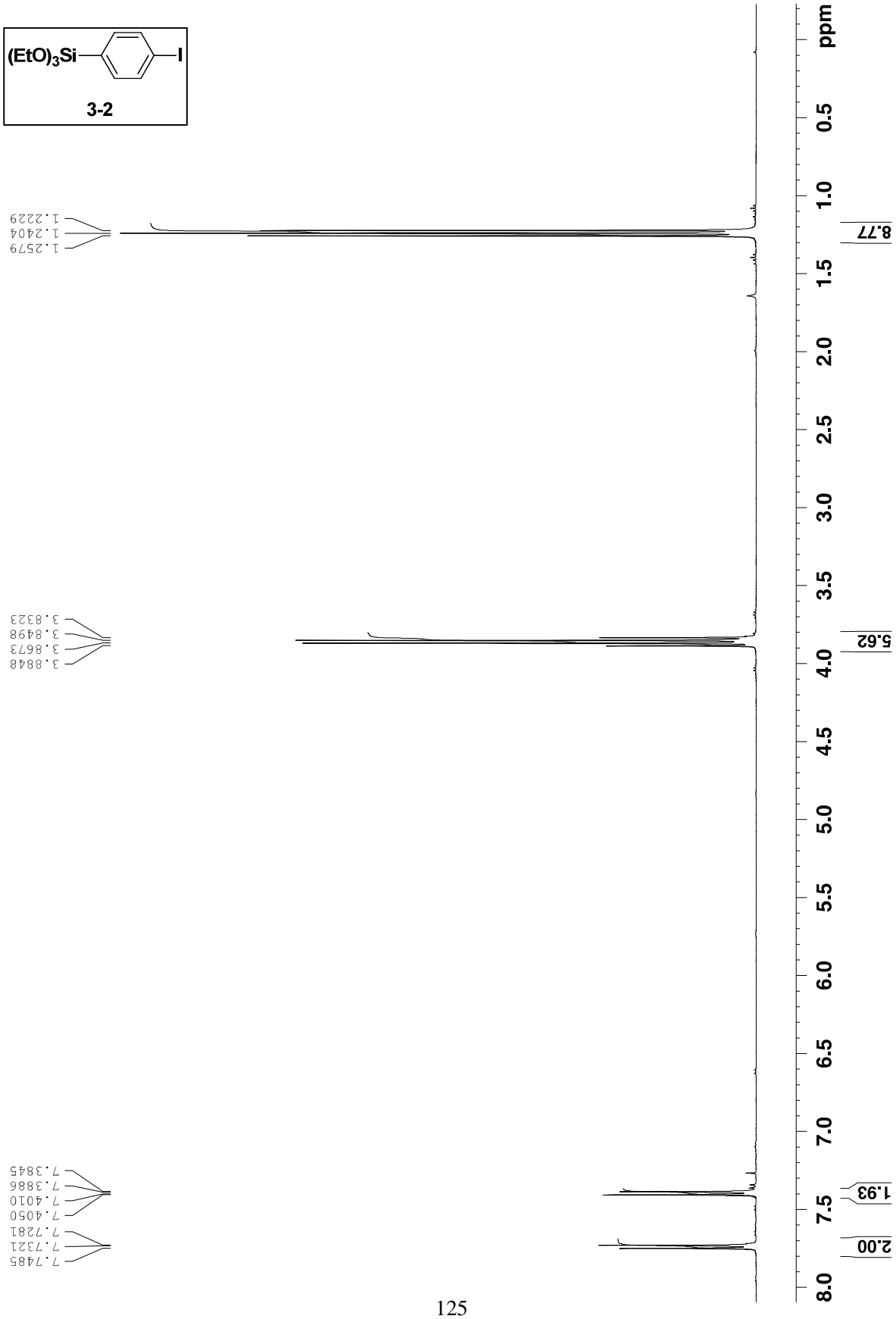
(EtO)3Si
I
3-2
1.2579
1.2404
1.2229
3.8848
3.8673
3.8498
3.8323
7.7485
7.7321
7.7281
7.4050
7.4010
7.3886
7.3845
8.77
5.62
1.93
2.00
ppm

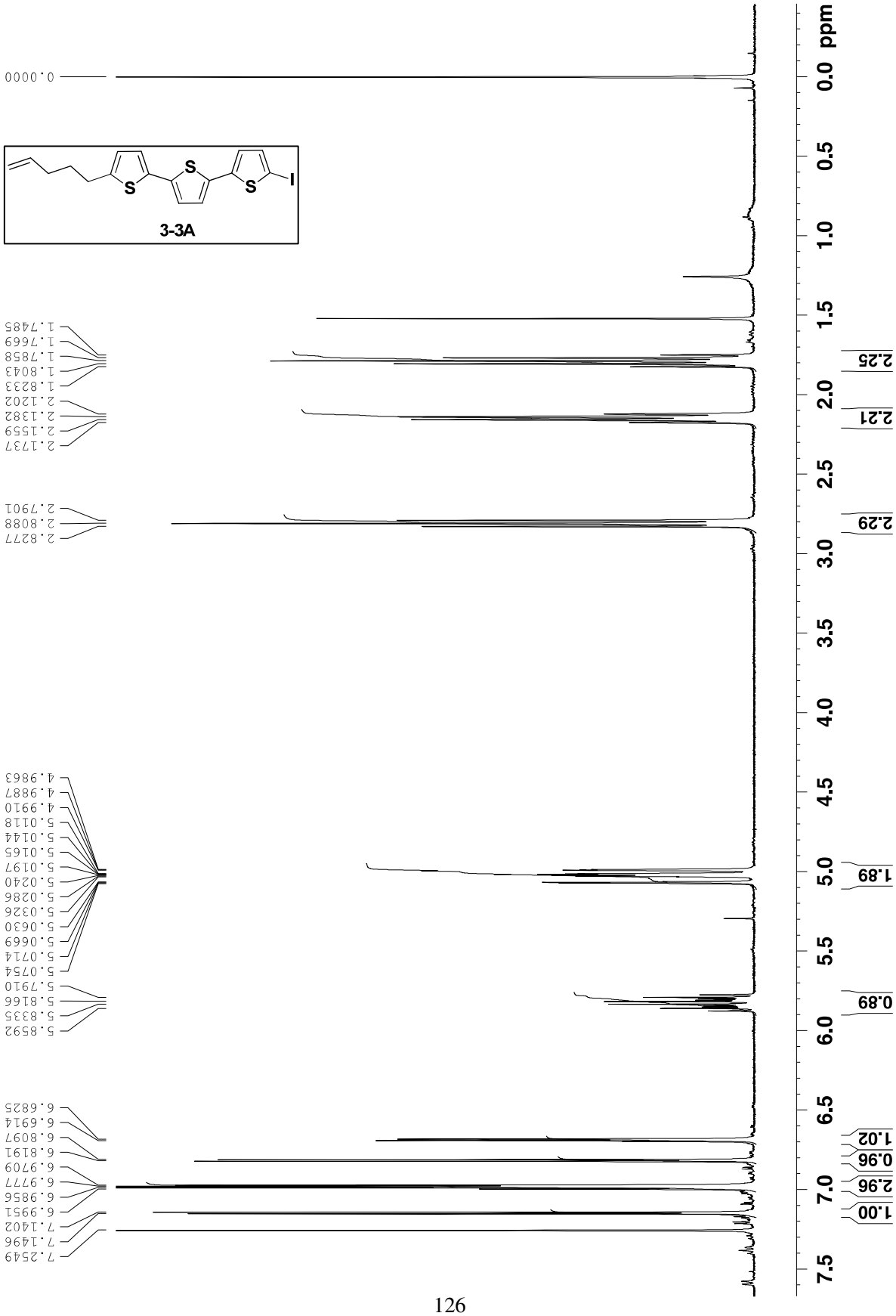
0.0000
3-3A
1.7485
1.7669
1.7858
1.8043
1.8233
2.1202
2.1382
2.1559
2.1737
2.7901
2.8088
2.8277
4.9863
4.9887
4.9910
5.0118
5.0144
5.0165
5.0197
5.0240
5.0286
5.0326
5.0630
5.0669
5.0714
5.0754
5.7910
5.8166
5.8335
5.8592
6.6825
6.6914
6.8097
6.8191
6.9709
6.9777
6.9856
6.9951
7.1402
7.1496
7.2549
ppm
0.0
0.5
1.0
1.5
2.0
2.5
3.0
3.5
4.0
4.5
5.0
5.5
6.0
6.5
7.0
7.5
2.25
2.21
2.29
1.89
0.89
1.02
0.96
2.96
1.00

7.2611
7.1488
7.1339
6.9782
6.9636
6.8181
6.8031
6.6834
6.6698
3.8639
3.8360
3.8081
3.7803
2.8177
2.7883
2.7585
1.7174
1.6903
1.6637
1.4485
1.4338
1.2611
1.2332
1.2053
0.6792
0.6550
0.6196
0.5700
0.82
0.93
2.40
0.96
6.00
1.88
2.16
3.91
9.52
2.07
7.5
7.0
6.5
6.0
5.5
5.0
4.5
4.0
3.5
3.0
2.5
2.0
1.5
1.0
0.5
0.0 ppm
(EtO)3Si
S
S
S
I
3-3

0.0000
1.5403
6.7782
6.7876
7.1408
7.1502
7.2595
2.00
2.00
7.5
7.0
6.5
6.0
5.5
5.0
4.5
4.0
3.5
3.0
2.5
2.0
1.5
1.0
0.5
0.0
ppm

I
S
S
I

4-1

0.2494
TMS
S
S
TMS
4-2
7.1152
7.1056
7.0001
6.9905
18.06
2.00
2.01
7.5
7.0
6.5
6.0
5.5
5.0
4.5
4.0
3.5
3.0
2.5
2.0
1.5
1.0
0.5
0.0
ppm

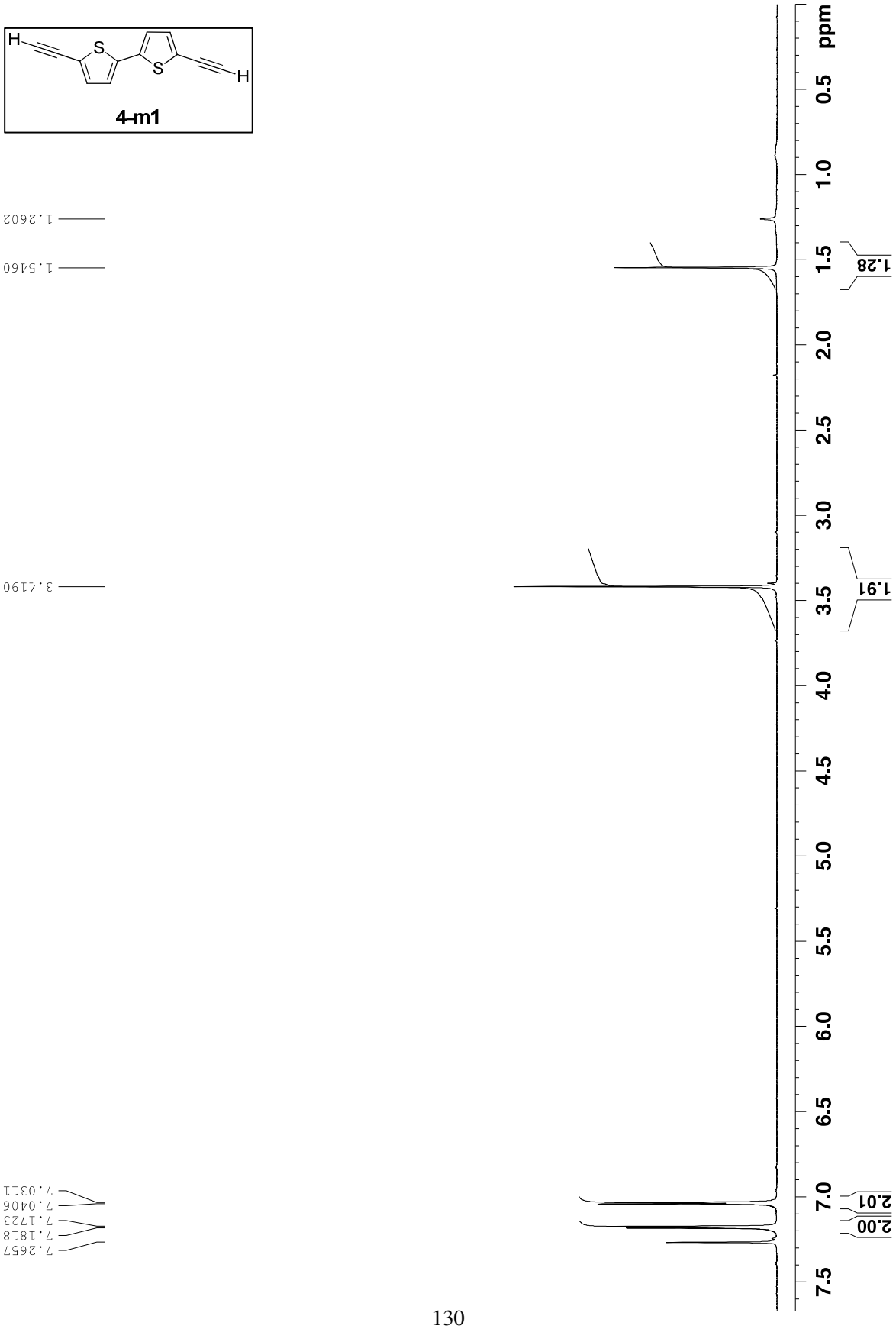
H
S
S
H
4-m1
1.2602
1.5460
3.4190
7.2657
7.1818
7.1723
7.0406
7.0311
ppm
0.5
1.0
1.5
2.0
2.5
3.0
3.5
4.0
4.5
5.0
5.5
6.0
6.5
7.0
7.5
1.28
1.91
2.00
2.01

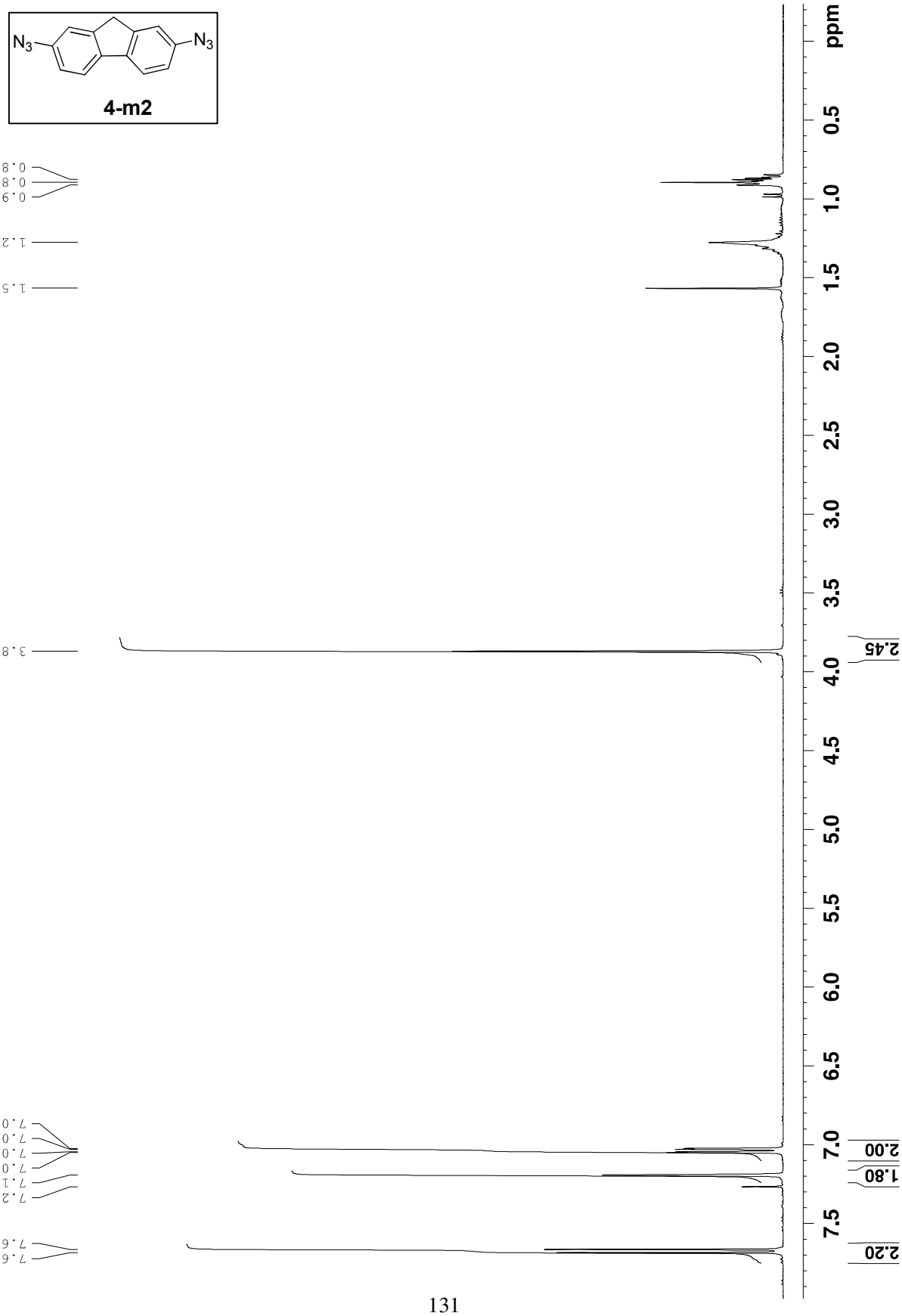
N3
N3
4-m2
ppm
0.5
1.0
1.5
2.0
2.5
3.0
3.5
4.0
4.5
5.0
5.5
6.0
6.5
7.0
7.5
2.45
2.00
1.80
2.20

0.2652
TMS
TMS
4-3
7.6920
7.6601
7.6366
7.5048
7.4737
7.2573
ppm
17.59
3.84
2.00

4-m3
7.7340
7.7024
7.6721
7.5424
7.5113
7.2584
3.1504
4.14
2.00
1.63
7.5
7.0
6.5
6.0
5.5
5.0
4.5
4.0
3.5
3.0
2.5
2.0
1.5
1.0
0.5
ppm

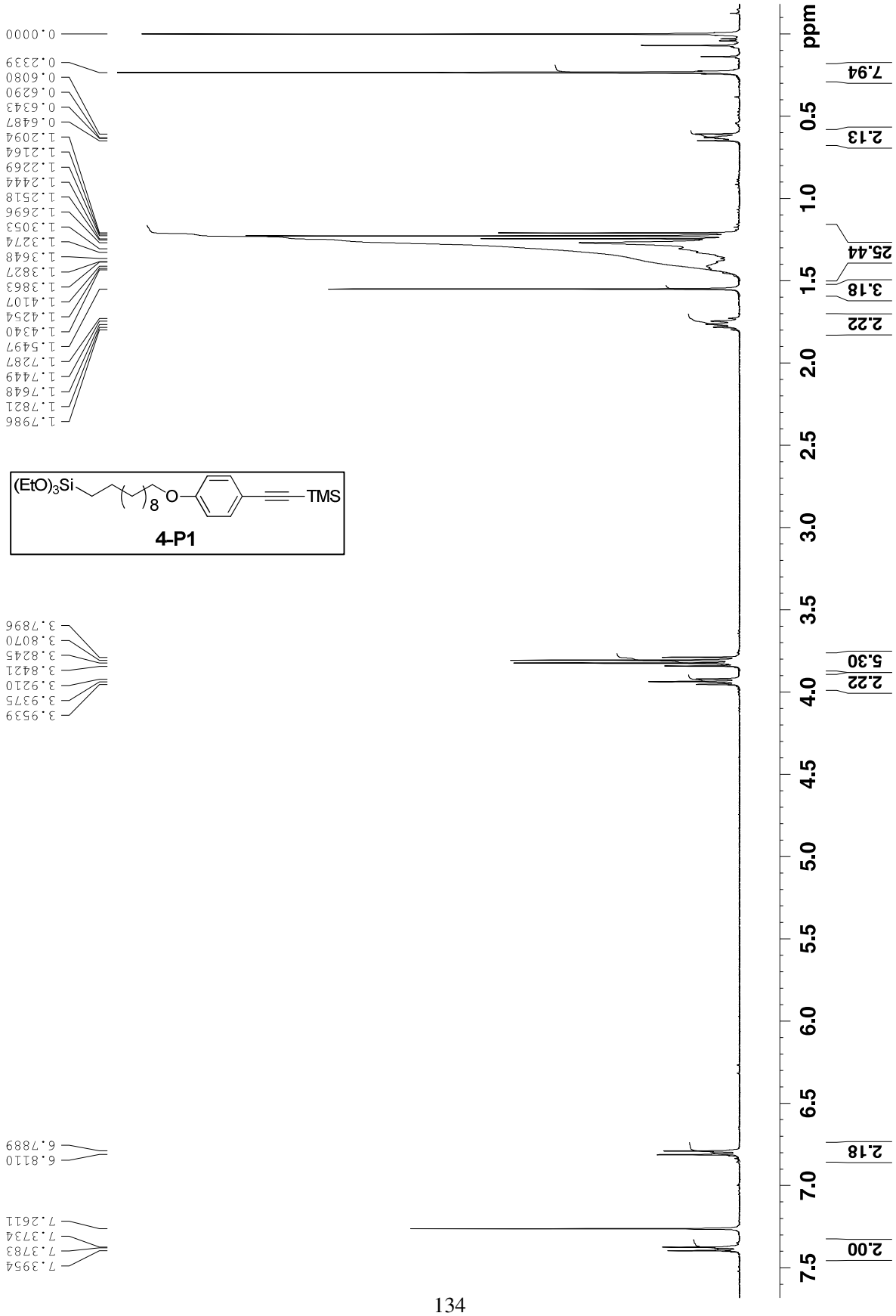
0.0000
0.2339
0.6080
0.6290
0.6343
0.6487
1.2094
1.2164
1.2269
1.2444
1.2518
1.2696
1.3053
1.3274
1.3648
1.3827
1.3863
1.4107
1.4254
1.4340
1.5497
1.7287
1.7449
1.7648
1.7821
1.7986
3.7896
3.8070
3.8245
3.8421
3.9210
3.9375
3.9539
6.7889
6.8110
7.2611
7.3734
7.3783
7.3954
(EtO)3Si
8
O
TMS
4-P1
ppm
0.5
1.0
1.5
2.0
2.5
3.0
3.5
4.0
4.5
5.0
5.5
6.0
6.5
7.0
7.5
7.94
2.13
25.44
3.18
2.22
5.30
2.22
2.18
2.00

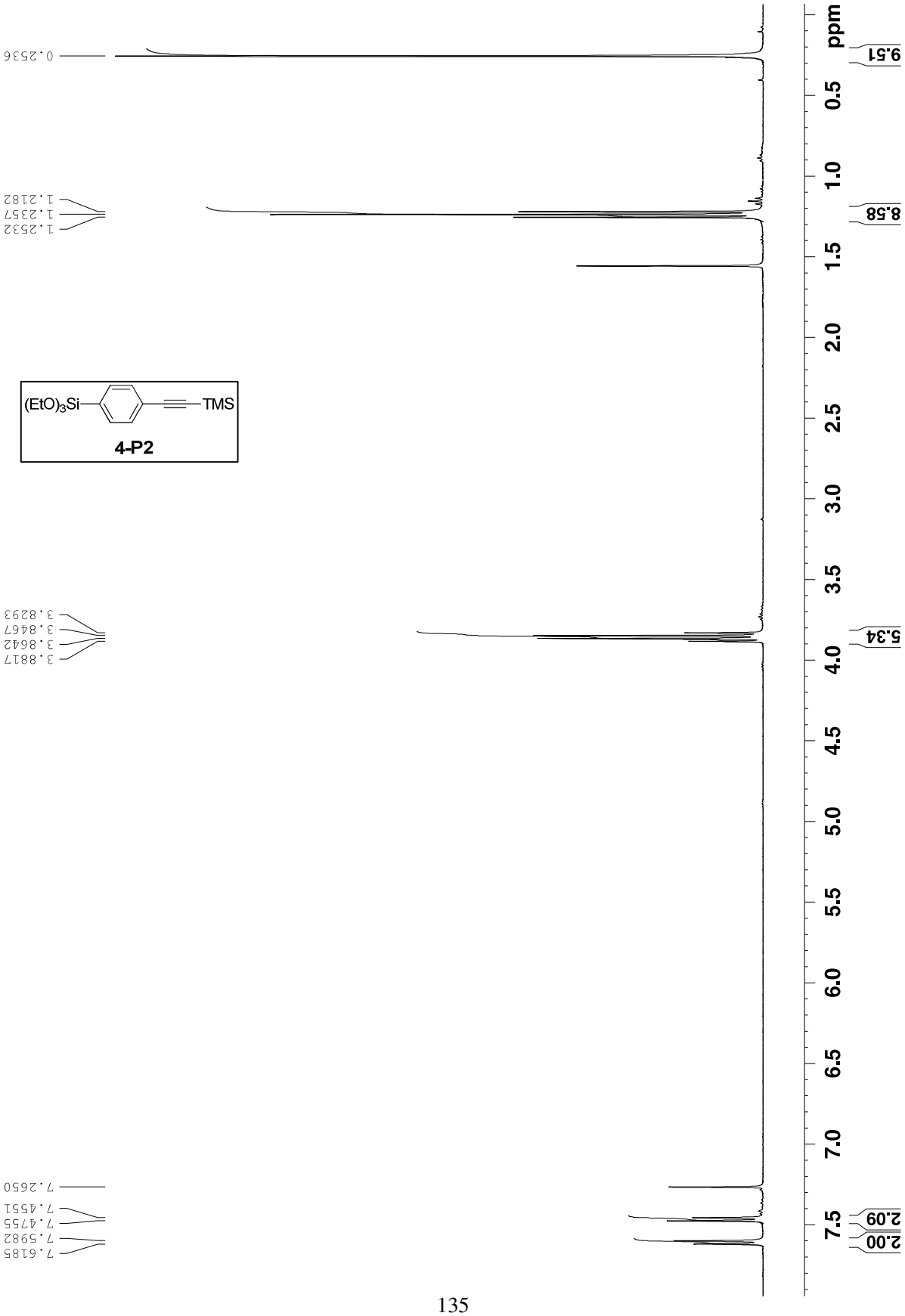
0.2536
1.2182
1.2357
1.2532
3.8293
3.8467
3.8642
3.8817
7.2650
7.4551
7.4755
7.5982
7.6185
(EtO)3Si
TMS
4-P2
ppm
0.5
1.0
1.5
2.0
2.5
3.0
3.5
4.0
4.5
5.0
5.5
6.0
6.5
7.0
7.5
9.51
8.58
5.34
2.09
2.00

(dppp)2
S
Ni
I
9.99
33.67
4.00
0.71
ppm
45
40
35
30
25
20
15
10
5
0
-5

VITA

Euiyong Hwang was born on December 20, 1976 in Seoul, Korea. After he received a Bachelor of Science in Chemistry from Chung-Ang University, Seoul, Korea, in February 2002, he started his research experience at an organic synthesis lab in the Department of Chemistry at Chung-Ang University, Seoul, Korea. In February 2004, he received his Master of Science in Chemistry with the thesis: "Halogenation of benzylic alcohols and conversion of benzylic acids into thioesters." With enthusiasm for organic chemistry, he enrolled as a graduate student in the Department of Chemistry at Louisiana State University, Baton Rouge, Louisiana, in August 2005. Currently, he is cultivating knowledge of organic semiconducting materials based on conjugated polymer under the supervision of Professor Evgueni E. Nesterov.

Euiyong Hwang is a candidate for the Doctor of Philosophy in organic chemistry which will be awarded in August 2011 with the thesis: "Surface-initiated polymerization as a novel strategy towards organic semiconducting polymer thin films."